STUDY OF A BATCH SOLAR WATER HEATER WITH INTEGRATED COLLECTOR STORAGE SYSTEM AND COMPOUND PARABOLIC REFLECTOR

Submitted in fulfilment of the requirements for the Degree of

DOCTOR OF PHILOSOPHY

IN

MECHANICAL ENGINEERING

Submitted By

JAJI VARGHESE
(2K12/PHDME/01)

Under the Supervision of

PROF. SAMSHER
(Professor)

Dr. MANJUNATH K.
(Associate Professor)

Department of Mechanical Engineering
Delhi Technological University
(Formerly Delhi College of Engineering)
Bawana Road, Delhi- 110042, INDIA.

December 2017

CERTIFICATE

This is to certify that the thesis entitled **"Study of a batch solar water heater with integrated collector storage system and compound parabolic reflector"** being submitted by Jaji Varghese to the Department of Mechanical Engineering, Delhi Technological University, Delhi for the award of the degree of **Doctor of Philosophy** is a bonafide record of original research work carried out by him. He has worked under our guidance and supervision and has fulfilled the requirements for the submission of this thesis, which has reached the requisite standard. The results contained in this thesis have not been submitted, in part or full, to any other University or Institute for the award of any degree or diploma.

PROF. SAMSHER
(Professor)
Department of Mechanical, Production
& Industrial and Automobile Engineering,
Delhi Technological University,
Delhi-110042,
INDIA

DR. MANJUNATH K.
(Associate Professor)
Department of Mechanical Engineering
Ch. Brahm Prakash Govt. Engg. College
(Govt. of NCT of Delhi)
Jaffarpur, Delhi-110073,
INDIA

ACKNOWLEDGEMENT

I am deeply indebted to my supervisors Dr. Samsher and Dr. Manjunath K. who supported, encouraged and provided valuable insights that saw the successful fruition of my work. I owe my sincere thanks to them for their patient and painstaking attention to details, often putting aside their own pressing commitments. I consider myself very fortunate to work under them, not just for their guidance and expertise to complete my dissertation but also to help me evolve as a better researcher.

I am very much grateful to the Directorate of Technical Education, Delhi, faculty members of my Department, especially Sh. S.C Jain (HOD), Mechanical Engg. Department at Aryabhat Institute of Technology, Delhi, for providing me the platform to pursue my research work. I owe special thanks to my colleagues Dr. Kumar Rakesh Ranjan and Mr. Bharat Sanga who provided valuable suggestions on books and literature which enriched and enhanced the level of my research. My sincere thanks to Mr. Naushad Ahmad Ansari (Asst. Professor) and Mr. H.K Verma, Department of Mechanical Engineering, Delhi Technological University, (D.T.U) for helping me in the instrumentation of Test rig. My thanks also to Mr. Mohammad Zunaid (Asst. Prof.) and Mr. K. Srinivas (Asst. Prof.) at D.T.U for offering me the necessary and timely advice. I offer my heartfelt thanks to my friends Dr. G. Narasimhulu, Mrs. Sunita .G, Dr. M. S Rao, Dr. Gajanan Awari, Mr. Rakesh Verma, and Mr. Jitender Yadav, who supported and motivated me at times of mental fatigue. I would also place on record my thanks to Chief Editors and anonymous reviewers of International Journals who published my work, whose timely and scholarly reviews helped me in bringing the best out of this research.

Last but not the least, my humble reverence to my mother Saramma Varghese who instilled in me the attitude to work, my in-laws, Late Mr. N.G Thomas and Mrs. Annamma Thomas who stood by

me, my sisters Mrs. Susan and Mrs. Jessy, my brother Dr. Saji Varghese, my very close pals Abey & Mini, family members and friends who lent me the emotional support to get going. My special thanks is reserved to my wife Jessy who took the family responsibility and bore the brunt of my neglect with cheerful disposition. I express my affection to my daughter Neha who also helped me in computational work and son Joel for bearing with me in my preoccupied work.

I thank God Almighty that I could accomplish this task and pray with utmost humility that my work add to the corpus of knowledge in the field and contribute to the betterment of society.

Dated: (Jaji Varghese)

Roll No: 2k12/PHD/ME01

ABSTRACT

A batch heater is an integrated collector storage unit wherein the absorber serves the dual purpose of a collector and storage unit. The present experimental work is an integration of the older concept of batch water heating with the modern trends in solar water heating technologies i.e. incorporating a concentrator in the design. The concentrator used here is the Compound Parabolic Concentrator (CPC) which is a non-imaging device having wider acceptance angle. It requires only occasional tracking and thus can be best suited for household purposes. The concentrator i.e. the reflector, in this case, is supported on a wooden cradle which comprises the two parabolas of the compound parabolic concentrator. While Batch Solar Water Heater (BSWH) facilitates easy installation, operation, and maintenance besides providing cost reduction it operates at much lower daily collection efficiencies as compared to separate storage tank facilities. The focus of the study is therefore to obtain good heat retention and better long time performance estimates and in accordance, changes have been made in the design in addition to the use of CPC concentrator. In the present work, experimental studies have been carried out and mean collector efficiency is computed on the model with an air gap introduced in the side walls (arms of the CPC). Unlike conventional systems with a large number of smaller diameter tubes, here is a single larger diameter drum which serves both as an absorber and storage unit positioned at the focus of CPC. The system works on thermosyphon principle, unlike conventionally forced circulation domestic water heating systems. The system as a whole operates at a lower temperature which reduces the overall convective and radiative losses and increases useful heat gain. The parametric study of the theoretical design by EES hovering before and after solar noon is in good agreement with experimental results with the thermal efficiency of the collector as high as 38% obtained and with water temperatures varying from 40^{o}C to 60^{o}C depending upon the time of the year. The key aspect is its heat retention capability which can prolong high temperatures attained for longer hours after

dusk. This model shows better performance compared to a similar model designed and developed but without an air gap. Heat loss tests performed on the collector on a 24-hour cycle period showed good long time performance estimates. Collector characterization parameters are obtained by performing thermal performance tests on the collector, under conditions meeting ASHRAE specifications for outdoor tests. The response time of collector computed and performance characteristic curve plotted to predict system response under any given conditions of solar insolation and ambient temperature. The economic figures of merit of the model are also obtained by f-chart design method and using EES software. The proposed model has low initial cost and better long time thermal performance estimates. The annual solar fraction for the model is 0.55 and the payback period is two years. Comparative studies with similar models show its competency based on collector efficiency and economic viability.

Highlights

- Passive system employed in comparison to the conventional active systems for household applications.
- Introduction of a concentrator in domestic solar water heating system.
- No usage of Transparent insulation material (TIM) or Phase change material (PCM), heat retention obtained by introducing an air gap, without adding to the cost of collector.
- Better adaptability for metro cities like Delhi, where roof space is a major constraint for installation of flat plate collectors.
- Economically viable

Keywords: household, batch water heater, compound parabolic, solar water heater, air gap, economic analysis.

TABLE OF CONTENTS

LIST OF FIGURES

LIST OF TABLES

NOMENCLATURE AND ABBREVIATIONS

A_p Aperture surface area in m^2

A_{ap} Effective area of absorber (drum) in m^2

BSWH Batch solar water heater

c_{pw} Specific heat of water in J/Kg-K

C Concentration Ratio

CP Collector performance parameter

CPC Compound parabolic concentrator

DSWH Direct solar water heater

D_o Outside diameter of drum in m

f − Monthly solar fraction

$F_R U_l$ Heat loss factor

$F'\eta_o$ Optical efficiency factor

F'' Flow factor

F_R Heat removal factor

G_m Mean solar radiation for the time interval in W/m^2

G (t) Solar radiation intensity in W/m^2

H Height of solar water heater in m

$\overline{H}_T$ − Monthly average daily radiation incident on collector surface per unit area in J/m^2

h_w Wind heat transfer coefficient in W/m^2-K

h_i Heatt transfer coefficient of air in air gap in W/m^2-K

ICS Integrated collector solar heater

I_T Solar insolation on tilted plane in W/m^2

I_b Beam radiation in W/m^2

I_d Diffuse radiation in W/m^2

K Thermal conductivity in W/m-K

L Length of collector in m / Thickness of insulation in m

L Monthly heating load in GJ

MLR Multi-linear regression

m Average number of reflections

m_w Mass of water in storage cum absorber drum in Kg

ṁ Mass flow rate of water in Kg/sec

N Days in month

PCM Phase change material

Q_a The solar energy intercepted by the aperture surface in J

Q_{wd} Amount of heat quantity of stored water in J

q_u Useful heat gain in W

R Thermal resistance in m^2-k/W

S Flux absorbed in W/m^2

SF Annual solar fraction

SPSS Statistical package for social sciences

S_{max} Day length in hrs.

TIM Transparent insulation material

T_{pm} Mean plate (drum) temperature in ^oC

$T_{ref} -$ Reference temperature (60^oC in our case)

$\overline{T}_a -$ Monthly average ambient temperature

T_{a1}, Ta_2, Ta_3, Ta_4 Thermocouple probes inserted in air gap

T_{d1}, T_{d2}, T_{d3}, T_{d4} Thermocouple probes located on drum

T_{g1}, T_{g2} Thermocouple probes located on glass surface

T_{w1}, T_{w2} Thermocouple probes inserted inside drum

T_w Thermocouple probe for measuring outside wall temperature

T_i Initial temperature of water in ºC at the time of charging 11:00 am

T_f Mean final temperature of water at 3:00 pm in ºC

t_i Time of start of experiment

t_f Time at the finish of experiment

Δt The time interval between start and finish of experiment in seconds

U_f Front loss coefficient W/m^2-K

U_b Bottom loss coefficient W/m^2-K

U_s Side loss coefficient W/m^2- K

U_t Top loss coeffient in W/m^2- K

U_l Overall loss coefficient in W/m^2- K

W Aperture in m

Greek letters

δ Declination angle

ΔT Temperature difference between collector and ambient in ºC

ρ_e Effective reflectivity

ε_p Emissivity of absorber surface for long wave radiation

ε_c Emissivity of cover for long wave radiation

ω Hour angle

θ_a Half acceptance angle

ρ Reflectivity of SS mirror finish

α_v Solar swing angle

$(\lambda\alpha)_b$ Transmissivity-absorbivity product for beam radiation

$(\lambda\alpha)_d$ Transmissivity-absorbivity product for diffuse radiation

$\overline{\tau\alpha}-$ Monthly average transmittance – absorptance product

δT Temperature difference between drum and ambient in ◦C

σ Stefan Boltzmann constant $W/m^2\text{-}K^4$

η_{it} Instantaneous thermal efficiency

η_c Collector efficiency

$\Delta t-$ Total number of seconds per month

X− Dimensionless variable

Y− Dimensionless variable

Subscripts

a air gap

b bottom of collector

f front face of collector

p plywood

r rear face of collector

s sides of collector

t top or aperture surface

thf Thermal resistance of front face

thr Thermal resistance of rear face

thb	Thermal resistance of bottom face
ths	Thermal resistance of side face
w	glass wool

CHAPTER 1.0

INTRODUCTION

Solar energy usage for power generation and thermal applications is a well-accepted concept. The thermal application of solar energy includes solar distillation, solar dryer, solar heating and ventilation, solar cookers and solar water heating systems. The most commonly used is the solar water heating systems. Solar water heating technology is one of the well-accepted technologies in the world. In India solar hot water system are being utilized in industrial, commercial as well as domestic sectors. Few countries bank on solar water heating systems (SWHS) to meet their domestic hot water needs, instead prefer to use fuel or electric/gas geysers. The reason for this is that the former having relatively high initial investment and performance marred by poor maintenance and the latter having low initial cost. The Government of India, through Ministry of New and Renewable Energy (MNRE), (Source: www.mnre.gov.in, May 2016) provides soft loans/capital subsidy for installation of solar water heating systems, through banks/financial institutions at an interest rate of 2% – 5% to various categories of users. Seventy-six percent of the surveyed SWH owner households owned a car and thus it can be concluded that a majority of the households owning SWH fall under the rich and striver categories as per affluence layers distribution based on household income (Veeraboina and Ratnam [2012]; Chandrashekar and Kandpal [2004]). The target population should be the middle class which still strive on the use of electric geysers, the most common water-heating device in the households. Thermosiphon solar water heating systems offer significant protection to the environment and should be employed whenever possible in order to achieve a sustainable future (Kalogirou [2009]).The potential of solar water heating in India is slowly growing with a market potential of approximately 500 crores (website: www.mnre.gov.in). This is due to the growing awareness amongst the consumers of the energy, money-saving benefits and environmentally friendly aspects of solar

water heaters. The growth of LPG gas water heater market is hampered by low diffusion of piped gas networks. Also, electric shortages and frequent outages are major constraints for electric water heaters, especially in Tier II and Tier III towns in India. Government subsidies in solar supplemented by better infrastructure in rural India are propelling the growth of solar water heaters. Solar water heaters (SWH) are an integral part of the recently announced Jawaharlal Nehru National Solar Mission (JNNSM) of Government of India which targets to have 20 million m^2 (Gross area) of Solar Water. (Phase III capacity addition 2017 – 22). (Source: Solar Energy Corporation of India, website: www.seci.co.in, May 2016).

With such a positive environment, the need of the hour is to motivate users to go solar by providing solar water heater which is economically viable, efficient with good heat retention capability and hassle-free in operation.

1.1 History

The history of solar water heating can be traced back to a Swiss naturalist, De Saussure, who in the year 1767, made a prototype of a solar water heater and called it a 'Hot Box' as it was capable of aiding in cooking and producing hot water. But the first commercial Solar Water Heater (SWH), an integral storage system was patented in the US, by Clarence M. Kemp in 1890. In 1909, William Bailey improved upon the Kemp's SWH system by segregating it into two major parts, the solar thermal collector for collecting solar radiation and a separate well-insulated storage tank to store the hot water. The SWH became a commercial product in the early 1960's. A typical SWH uses an absorber area of 3-4 m^2 with a capacity of 150-180 liters per day storage tank. One of the popular types of systems is the forced circulation water heating system. Except for the solar collectors, other auxiliary items such as the storage tank incorporated with piping, pump, and differential thermostat are usually kept indoors. The Production of SWH is now in packaged form and

developed into a considerable business in the 21st century. In countries such as China, Australia, Germany, Greece, Israel, USA and including India, the manufacturing of SWH's have become an industrial sector.

Today solar water heater system uses the flat plate and tubular solar collectors. Flat-plate collectors are widely used to obtain low-grade heat. (Hottel and Woertz [1942]; Bliss [1959]; Morse [1961]; Garg [1975]) have made extensive studies on these type of collectors. Depending upon the capacity, these collectors are connected in a series-parallel combination. For smaller capacity up to 100-200 liters per day (LPD), the water heaters are installed working on thermosyphon principle, while large capacity systems make use of electrically operated pumps. The hot water is stored in a properly insulated tank for use in the night, early morning or any time of the day/night. Domestic collectors for house purposes, available in the market are of two types, the Flat plate collectors (FPC) and the Evacuated tube collectors as shown in Fig.1.1, Page No. 4. Simple design makes FPC's more in common usage but it requires large exposed aperture area. The solar radiation that falls on the face of the collector is absorbed by blackened metallic absorber sheets and with built-in channels or riser tubes to carry water. The absorbed radiant heat is transferred to the flowing water. The water that heats up is then pumped and stored in a well-insulated separate storage tank which is connected to the utilities. The entire enclosure of the absorber unit is housed in a well-insulated metal box with normally two top glass covers. Capacities in multiples of 100 liters per day are available in the market.

The other collector is the evacuated tube collector (ETC) based solar water heaters, which are less expensive than FPC system. This collector consists of double layer evacuated borosilicate glass tubes having a selective coating on the outer surfaces of inner tubes to absorb solar radiation. The life of these collectors is comparatively less than FPC's. These systems are available in any size i.e.

50, 75, 100, 125, 150 LPD etc. The efficiency of collector to convert solar radiation into thermal energy depends upon several meteorological and design parameters such as:

(i) Solar radiation geometry (Please refer Appendix A), Page No. 157.

(ii) Absorption coefficient of the collector surface for incident solar radiation.

(iii) Emissivity of the collector surface for large wavelength.

(iv) Heat losses due to conduction, convection and radiation.

(v) Design parameters such as Heat removal factor F_R, collection efficiency factor F' and stagnation temperature.

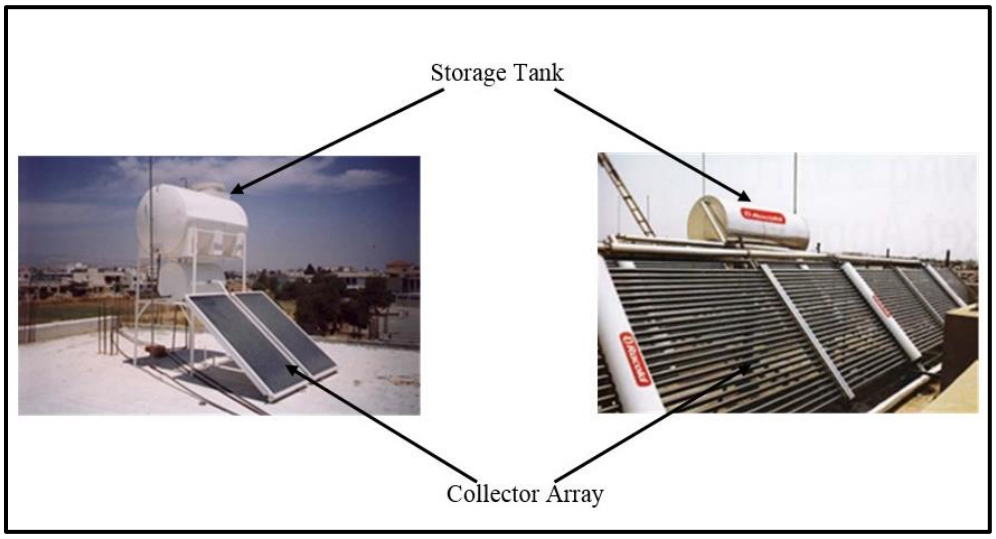

(a) **(b)**

Fig. 1.1

Fig 1.1 Conventional solar water heater (a) Flat plate collector

(b) Evacuated tube collector

1.2 Basic Components

The flat plate collector is the simplest and most commonly used means to convert the sun's radiation into the useful heat.

The basic elements of a conventional liquid flat-plate collector are (i) the absorber, (ii) the tubes fixed to the absorber plate through which the liquid to be heated flows, (iii) the transparent covers, and (iv) the storage tank.

The tubes which are made of metals like copper, aluminium, galvanized iron, and steel are soldered, brazed or clamped to the bottom (in some cases, to the top) of the absorber plate with the pitch ranging from 5 to 15 mm. In India, because of the shortage of copper, collectors have been made from metals like aluminium and steel. However, gradually, steel is being favored more because aluminium collectors require specially treated water in order to avoid corrosion. The absorber plate is made from metal sheet 1 to 2 mm in thickness. The header pipes, which lead the water in and out of the collector and distribute it to the tubes, are made of the same metal as the tubes and are of slightly larger diameters. Glass is the most favored material for the transparent covers. Thicknesses of 3 or 4 mm are commonly used. The usual practice is to have 1 or 2 covers with spacing ranging from 1.5 cm to 3 cm. The insulation on the bottom and sides is usually mineral wool or glass wool and has a thickness ranging from 5 to 8 cm. The whole assembly is contained within a sheet metal container which is tilted at a suitable angle. The face areas of most commercially available collectors range from $1m^2$ to 2 m^2 with the length (along with the sloping direction) being usually larger than the width. In case of natural circulation systems (Passive systems), the hot water withdrawn from the top of the tank is automatically replaced by cold water at bottom of the tank. Such systems are restricted to smaller capacities ranging from 100 to 200 liters with the delivery temperature of hot water in the moderate range. For larger capacities, large

arrays of the flat plate collectors are used and forced circulation maintained with a circulating water pump operated by an on-off controller to sense temperature difference between hot water drawn at exit and system temperature and an auxiliary heater as shown in Fig 1.2.

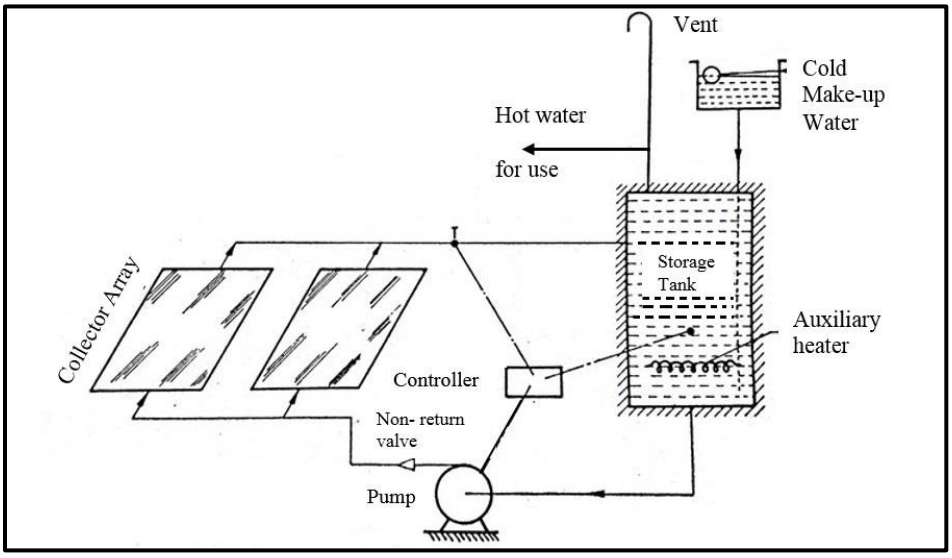

Fig. 1.2 Schematic diagram of a forced circulation solar water heater

1.3 Concept of batch type solar water heaters

The early design consists of well-insulated weather-tight enclosures, with one or more tanks tilted at an angle approximately equal to the geographic latitude of the site. The south wall of the enclosure is fitted with transparent glass covers for allowing maximum solar insolation to fall on the absorber tank. The word 'batch' stems from the fact that the sun shines directly on the tank and heats up the water and stores a batch of hot water within the tank itself. There is no separate storage tank. Unlike conventional active solar heating systems, it is simple in design, as batch heaters need no pumps, differential thermostats, or other externally powered devices. The tank is supported in an insulated wooden box, and connected to the supply line with valves installed so that one can fill and drain the system as needed. The entire setup is supported by a concrete wall structure or even

kept underground to minimize the thermal losses. These batch heaters also referred to as built-in storage heaters are mostly used as passive heaters. Built-in storage-type solar water heaters are designed with a view toward reducing costs. Such units were widely used in Japan (Tanishita [1970]) and are recommended for low-income communities in South Africa (Richards et al. [l967]. However, such systems suffer from heavy energy losses during nights or periods of insufficient radiation. Several methods have been used to reduce these losses, such as using a movable insulation cover at night, using an insulated baffle plate, or using phase changing material inside the tank. Another way to reduce heat losses from the top is to use highly transparent insulation at the top. Numerous studies have been performed on the built-in- storage type solar water heaters. Chinnappa and Gnanalingam [1973] have tested a built-in-storage solar water heater which consists of a square coil of 7.5 cm diameter pipe, 13.5 m in length, in a wooden box with heat insulation at the bottom and two glass covers. Garg [1975] has studied a built-in-storage type solar water heater with a capacity of 90 1itres and made up of a 112 x 80 x 10 cm rectangular tank which performs the dual function of absorbing heat and storing the heated water. The prototype tested at Jodhpur, India, is shown in Fig. 1.3.

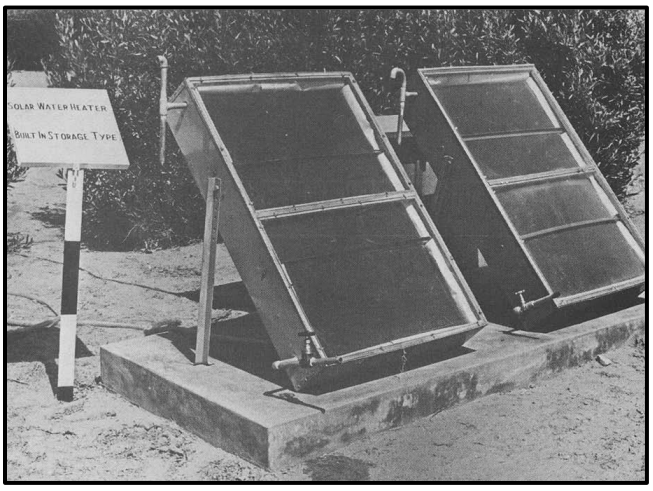

Fig.1.3 Simple box type batch solar water heater (Garg [1975])

With this heater sufficient hot water could be obtained in the morning if the heater was covered overnight with an insulation blanket or if the hot water is stored in an insulated tank.

Chauhan and Kadambi [1976] have tested a built-in storage solar water heater with a capacity of 70 1itres and made up of a 140 x 90 x 5.5 cm rectangular tank. They have ascertained the collection efficiency under natural convection conditions to be around 50% - 53% for a rise in water temperature of 50ºC - 57ºC. Sokolov and Vaxman [1983] have analysed the thermal performance of an integral compact solar water heater numerically and compared results with experimental data. They have investigated two proposed solar water heaters which have a rectangular shaped tank and a triangular shaped one respectively. Sodha et al. [1983] have analysed the thermal performance of several built-in-storage water heaters connected in series. The history and the technological advances made in integrated collector storage solar water heaters (ICSSWH) have been dealt in detail by (Smyth et al. [2006] and Suman et al. [2015]).

1.4 Principle of compound parabolic concentrator (CPC)

The introduction of a concentrator in a domestic solar water heating system is not yet commercialized but research studies have been carried out and model validation done with the symmetrical and asymmetrical type of reflectors. To increase the optical efficiency extensive study on the domestic use of solar water heaters with stationary concentrating reflectors has been performed by Tripanagnostopoulos and Yianoulis [2006], presenting a new concept on ICS systems.

The concept of CPC was introduced by Winston [1984] also referred to as the father of non-imaging optics. The basic shape of the compound parabolic concentrator (CPC) is illustrated in Fig.1.4, Page No. 9. The reflector comprises of two mirror segments with different focal points

which derives the name compound parabolic. As seen in the figure, the focal point for parabola *A* lies on parabola B, whereas the focal point of parabola *B* lies on parabola A. 25% - 30% of the total radiation is diffuse component and with concentrating collectors, on thick cloudy day, the useful energy gain can be zero, as it is incapable to capture diffuse radiation. The advantage of CPC is its capability to accept even diffuse radiation. It has a reasonable concentration ratio of 2 – 3, but has wider acceptance angle and therefore requires minimal or almost no tracking requirement throughout the year.

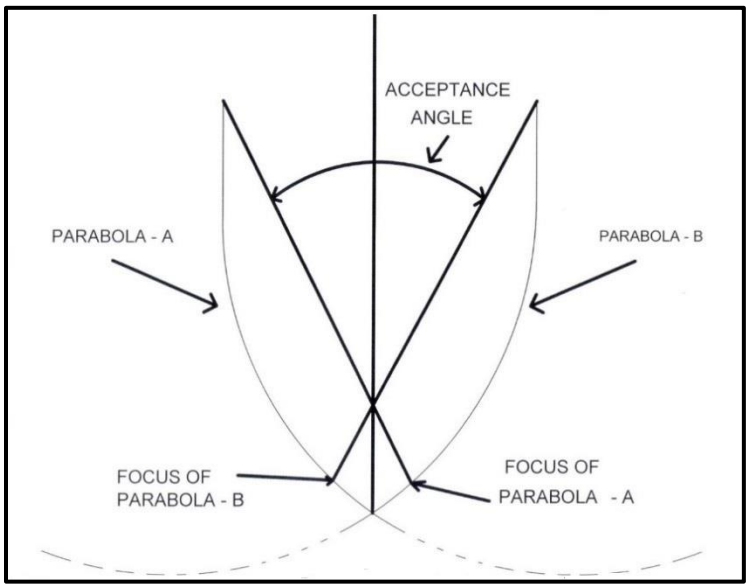

Fig. 1.4 Basic profile of CPC

1.5 Need for present work

In India, inspite of the efforts made by MNES, IREDA and other Government of India and Private agencies the concept of Solar Water Heating for domestic purposes is not widely accepted. Even the global status report published by REN21 (2010), depicting the average annual growth rates of renewable energy capacity, (2005-2010), the growth in the solar water heating system is at standstill, (Year 2005- 16% & Year 2010 also 16%) whereas there has been substantial growth in

concentrated solar power (25% to 77%) and solar photovoltaic (49% to 72%). The reasons being high first-time capital and installation cost, although operating cost is negligible. It requires close monitoring as operating cost increases with poor up keeping and maintenance. However, the factors like advancements in design and materials like the use of TIM, PCM etc. have especially contributed in the increase in the global use of domestic solar water heaters, during the last ten years (Colangelo et al. [2016]; Gautam et al. [2017]). The present work is an integration of the older concept of batch water heating with the modern trends in solar water heating technologies i.e. incorporating a concentrator in the design. So the design in principle is a BSWH with a concentrator. The concentrator, in this case, is a CPC reflector supported in a wooden cradle, backed with glass wool insulation. The SWH is designed to cater the need of a family of four members. The cylindrical storage tank painted black is positioned at the focus of CPC so as to absorb maximum solar radiation. Since the focus of the study is for households although the use of TIM, PCM can enhance system efficiency but also adds to the cost, alternatively an air gap is introduced in the arms of CPC to enhance system performance. The use of CPC reflector reduces the thermal mass of system compared to an FPC and hence transient effects are also small. Also, the wider acceptance angle requires minimal tracking and thus user-friendly in operation. A solar water heater of the built-in-storage type also referred as Integrated collector storage (ICS) system i.e. incorporating the storage volume and collector in a single unit is thus one attractive alternative to direct solar water heater systems (DSWH's). The elimination of a vertical storage tank in the compact unit could markedly reduce the cost of the solar water heater and may well remove aesthetic objections to rooftop installations.

1.6 Organization of the thesis

The presentation of the thesis is structured in the following sequence.

Chapter 1 dealt with the basic aspects of solar water heating systems, its history, and background and its evolution to the present day packaged form in the commercial market. It also covers the need and scope of present work.

Chapter 2 reviews the issues related to performance enhancement techniques for solar water heater (SWH) systems and technological advances made in integrated collector storage (ICS) solar water heaters in particular both in design and choice of materials used. The review is presented by revisiting the related reported works. Subsequently, the gap in the existing research is identified and reported.

Chapter 3 includes the details of experimental test rig, instrumentation, and its installation.

Chapter 4 briefs about the experimental procedure adopted and the analytical method of evaluating the performance parameters of the system, model studies and performance evaluation and validation.

Chapter 5 is devoted to presenting the results of the present investigations. In view of examining the validity of numerical results comparisons between numerical and experimental results obtained in the present work and also reported in the literature are obtained. The results are presented in the form of characteristics curves and numerical parameters that influences collector performance. The logical reasons for the obtained results are comprehensively discussed at appropriate places. It also deals with the economic feasibility of the collector in the long run that makes it compatible with conventional systems. The analysis makes use of the f-chart and life cycle cost savings method.

Chapter 6 is summary of the work, includes conclusions and scope for future work.

References and appendix are placed after chapter 6.

CHAPTER 2.0
LITERATURE REVIEW

In this chapter, review of published literature on related similar works are presented. Besides providing an overview, with this review, an attempt has been made to draw comparisons of the work by different authors and highlight their unique contributions. Based on the pool of information gathered, the research gaps are identified which culminated in the output of the present work. In the following sub-sections, integrated collector solar water heaters are reviewed and classified in terms of their energy collection and storage principles, with a discussion on the designs and modifications in recent years.

2.1 Batch solar water heating systems (BSWH)

The benefits of installing a renewable energy system include both energy savings and the decrease in environment pollution (Diakoulaki et al. [2001]). Solar water heating systems for households include both active systems and passive systems. The active systems require circulating pump and controls and are more efficient compared to passive systems (Kalogirou, [2004]). However passive systems are less expensive due to the absence of pump and controls. They are more reliable and lasts longer. Batch solar water heating systems (BSWH's) can be categorized into integrated collector storage passive systems. The word integrated stems from the fact that there is no separate storage tank in this collector unit, the absorber serves the dual purpose of a collector and storage also referred as integrated collector storage (ICS) systems.

The first BSWH collector system was demonstrated in the late 18th century in the southwest of the USA which reportedly produced sufficient hot water on clear days (Smyth et al. [2006]). The system was very simple in design consisting of a metal tank placed within a wooden box and the top part of the box was covered by a glass cover. Further, Walker [1903] proposed that the tank to

be installed in the focal zone of a concentrating mirror so as to enhance the system performance. The concept was further improved by introducing cylindrical vessels (a combined collector and storage tank), which is still used in many commercial designs (Tanishita [1970]). Later on, many researchers have shown their interests in this area and designed, developed and analyzed many improved ICS systems in different parts of the world. Unlike conventional flat plate/evacuated tube collectors, the design is uncomplicated because batch heaters need no pumps, blowers, differential thermostats, or other externally powered devices. It is naturally circulated type operating under overhead tank pressure. The tank/drum is supported in an insulated wooden box, and connected to the supply line with valves installed so that one can fill and drain the system as needed. The performance of a solar water heating system depends upon many factors like system size, load flow rates, heat losses and auxiliary input.

Measurements and performance predictions of domestic hot water systems were carried out by (Fanney and Klein [1983]; Garg and Rani [1982]). They concluded that use of an insulating baffle plate inside the storage tank improved the performance of the system significantly during daytime as well as for night time operation. Parkash et al. [1985] have integrated a baffle plate in an ICS solar water heater in order to control the heat losses. Expectedly, the baffle plate in the system reduced the heat losses effectively. Kaptan and Kilic [1996] have also investigated the performance of a built-in-storage type solar water heater made of five pipes (each of length 1.8 m and diameter of 12 cm) with a baffle plate in each pipe. A simpler batch solar water heater was investigated by Akuffo and Jackson [1998] in Ghana. The integrated storage-collector unit was a rectangular galvanized steel box with a total storage capacity of 90L. Kaushik et al. [1994] worked on a batch solar water heater with triangular cross-section and found that the system resulted in higher solar gain and leading to a higher water temperature at different flow rates in the winter

season. A similar system was studied by Mousa and Bilal [2002] except the rectangular integrated storage-collector unit incorporated with fins to improve thermal performance and structural stability. The unit was made of stainless steel sheets painted matte black, with four stainless steel fins. When compared to a finless (plain) model, the finned integrated system was found to be more efficient. Alvarez et al. [2016] proposed a corrugated thermal collector using the corrugated parallel approach. The novelty of this design allows the fluid to present a larger contact surface with absorber plate which is higher than sandwich type collectors, and a better performance observed with the parallel corrugated collectors. Ziapour and Aghamiri [2014] proposed a baffle plate storage unit divided into two trapezoids storage volumes. With a higher degree of stratification obtained by this design, this model presented higher efficiencies compared to previous rectangular and triangular type storage unit. A 3D CFD model was developed and studied with storage tank equipped with radial fins for different depths of extended surfaces by Chaabane et al. [2014] also supplemented this fact.

Another integrated storage-collector design was investigated by Mohamad [2013] with the use of a thermal diode and to prevent reverse circulation at night time. Mohamad found that the thermal diode yielded 10% improvement in maintaining the water temperature overnight when compared to a control prototype with no diode. Faiman et al. [2001] used a mechanical valve to prevent reverse thermosiphon flow at night, thereby reducing nighttime loss. A triangular built-in storage water heater was developed by Kaushik et al. [2012] to study how geometrical parameter influences the solar water heater characteristics. To obtain a higher operating temperature for longer time, Kumar and Rosen [2010] modified the plane rectangular absorber surface with corrugated surface thereby having more area exposed to solar radiation although they found the system efficiency reduced marginally. To broaden the usefulness of integrated collector storage

system especially for overnight applications Kumar and Rosen [2011] investigated on storage tank with an extended storage unit resulting in an enhanced performance of 5 %. Souliotis et al. [2009] combined artificial neural network and TRNSYS to predict the annual thermal performance of an ICS system.

2.2 Heat loss and techniques for thermal protection

Contrary to FPC 's, thermal protection of the storage tank cannot be made in ICS systems, as it has to be exposed to solar radiation. Opaque thermal insulation can be made only on the non-illuminated parts. These systems, therefore, present higher thermal losses during the night or during periods of low sunshine hours. Many techniques have been evolved to have good heat retention (Sadhishkumar and Balusamy [2014]).

2.2.1 Use of Transparent insulation Material (TIM)

In recent years improvement in thermal performance is envisaged by use of transparent insulation material (TIM) to suppress heat loss coefficient. TIM glazing typically consists of glass or plastic capillaries or honeycomb structures sandwiched between two glass panes. These systems diffuse light well while reducing glare and shadowing (Lien et al. [1997]). The use of TIM lowers the heat loss coefficient in the systems and eventually reduces the thermal losses from the cover while allowing solar radiation to hit the absorber. Nayak et al. [1982] have investigated the effect of different insulation thicknesses, placed on (top and bottom) of the water in the tank of a built-in storage solar water heater. Different insulating materials including transparent insulation material (TIM) have extensively been used in the ICS systems (Kaushika et al. [2003]; Ortabasi et al. [1983]). The earliest references relate to both theoretical and experimental work on the use of TIM as aperture covers for flat-plate solar collectors dealt by (Hollands [1965]; Tabor [1969]; Symons

[1984]; Hollands and Iynkaran [1985]; Schmidt and Goetzberger, [1990]; Nordgaard and Beckman [1992]). Basic components are a south facing TIM cover, which transmits solar energy reducing convection and radiation losses to the atmosphere, and a black solar absorbing surface to transfer absorbed energy to the working fluid which is water in this case. Cobble [1964] and Cobble et al. [1966], suggested the use of a transparent slab of methyl methacrylate (MMA) as transparent insulation material used in a solar heat trap. These systems are designed to heat air or water when irradiated by the sun. Samuel and Wijeysundera [1981] made similar studies with multilayer thermal trap collector, which consists of slabs of semitransparent materials of finite thickness with air gaps between them.

To minimize the nocturnal heat losses Shridhar and Reddy [2007] designed and developed a modified cuboid solar integrated-collector-storage (ICS) system with TIM. Well documented application of transparent insulation materials in flat plate solar collectors has been dealt by (Kaushika and Sumathy [2003]; Wong et al. [2007]). Chaurasia and John Twidell [2001] carried out studies to measure overall loss coefficient with simple glass glazing and with the use of transparent insulation material (TIM). The absorber-parallel configuration is simple and useful for application in passive solar water heaters. The effect of using TIM and varying its configuration within the collector has been studied by Reddy and Kaushika [1999].

2.2.2 Use of Phase Change Material (PCM) and selective coating on absorber

Thermal energy storage (TES) is defined as the temporary holding of thermal energy in the form of hot or cold substances for later utilization. TES systems have the potential for increasing the effective use of thermal energy, particularly by bridging the period between periods when energy is harvested and periods when it is needed. That is, TES is helpful for balancing between the supply and demand of thermal energy (Abedin and Rosen [2011]; Dincer and Rosen [2011]). Latent TES

type systems store energy in PCM, with the thermal energy stored when the material changes phase, usually from a solid to liquid, most commonly used is paraffin wax and salt hydrates. A review on PCM's and the types of materials as thermal energy storage and their applications has been dealt in detail by (Sharma et al. [2007]; Cabeza et al. [2011]). The introduction of phase change materials (PCMs) to utilize the latent heat stored in it during the melting process is one of the most repeatedly proposed techniques in solar water heating systems (Chen et al. [2010]). The higher heat storage capacity in the form of latent heat and isothermal behaviour during the melting process of PCM successfully extends the operational period of domestic solar water heaters (Mazman [2009]; De Beijer [1998]). The PCM stores extra thermal energy in the form of latent heat during the daytime by changing its phase and releases this thermal energy to heat the water when it is extracted from the system to meet the demands of hot water in the night or during the overcast sky conditions. Cold water enters into the system extracts stored latent heat from the PCM and changes the phase of the PCM. The PCM-integrated solar collector can also eliminate the need for conventional storage tanks thus reducing the cost and space. PCM and simple black paint or selective coating can be categorized as elements for thermal energy storage.

Performance studies made on a natural circulation solar water heater with heat exchanger by Sodha et al. [1979,1983], consisting of an insulated rectangular collector/ storage tank, showed good night time heat preservation when its top surface was suitably blackened and glazed. Abdul Jabbar Khalifa et al. [2013] suggested DSWH's system with a back layer of phase change material (PCM), which yielded increase in plate temperature and better heat storage during off-sunshine hours. Hailliot.et al. [2012] evaluated the potential of compressed expanded natural graphite (CENG) and phase change material (PCM) composites to improve the performance of solar domestic hot water (SDHW) systems. Going a bit unconventional Kalogirou et al. [2005] suggested colouring the

absorber in order to maximize absorption of the solar spectrum, instead of the typical black colour. To study the effect on thermal performance by introducing PCM in the collector, a 3D CFD model was developed by Monia Chabaaane et al. [2014], showed a decrease in nocturnal heat loss. Due to the low thermal conductivity and high viscosity of PCM, heat transfer in the PCM module is repressed. Xue [2016] carried out an experimental investigation on direct exposure PCM to that of evacuated tube solar water heaters. Gianluca et al. [2015] developed a low-temperature SWH based on slurry PCM. Relative studies on the basis of the type of collector unit and the type of storage i.e. sensible or latent were done by Shukla et al. [2009]. Ghoneim [2005] made a comparison between different sized latent heat storage vessels and sensible heat storage in a water tank with different degree of stratification. The storage vessel consists of a number of closed cylindrical pipes filled with the phase change medium, surrounded by heat transfer fluid. Boy et al. [1987] and Rabin et al. [1995], proposed an integrated collector storage systems based on a salt hydrate phase change materials as an appliance for providing hot water instantaneously, where salt hydrate PCM was encapsulated in a specially corrugated fin heat exchanger, which however increased the cost of the system. Tayeb [1993] developed a system for domestic hot water using Na2SO4.10H2O as a PCM and compared it with the simulation model that gives the optimum flow rate of the inlet water supply required to maintain the constant-temperature water at the outlet.

2.2.3 Improved performance by better stratification

Stratification increases the performance of solar systems. Stratification is affected by several factors, which have been investigated by different authors. The location and geometry of tank are important to maintain temperature stratification in the storage tank of a solar water heater. Mixing is the major cause of loss of stratification, with significant mixing losses occurring during lengthy storing periods (Duffie and Beckman [1974]). Souza et al. [2014] developed a new ICS with a

partially heated cavity with a plate parallel to the front wall of the cavity that separates the upward and downward flow reduces mixing effect within the storage and improves stratification. Mohsen and Akash [2002] have tested a box type ICS solar water heater with single glazing and observed a temperature rise by 30^{o}C in the tank water. Further, Mohsen et al. [2009] have reported a similar type of system, suitable for supplying hot water for 24 hrs. The thermal performance of the system has been assessed for three different tank depths (i.e. 5, 10 and 15 cm) with single and double glazing. For a 10 cm tank's depth, the system has yielded the hot water at a higher temperature, up to 68^{o}C, than the other depths. Also, the system with double glazing exhibits higher potency of retaining the water temperature high in the night.

Ecevit et al. [1989] have proposed a triangular ICS solar water heater. The design has enhanced the heat transfer between the absorber surface and the water, and also exhibited better overall performance compared to a rectangular design. The triangular cross-section also helps in getting higher solar gain and better natural convection and eventually a higher water temperature. Kaushik et al. [1994] have compared the performance of a triangular system with the rectangular design of the system. Both systems were tested experimentally under identical operating conditions. The triangular system performed more efficiently and had lower night heat losses. Cruz et al. [2002] have studied the performance of a trapezoidal-shaped solar water heater, with an optimal collector tilted at 45^{o}. The trapezoidal cross-section has induced thermal stratification in the stored water and provided sufficient energy storage to meet typical daily hot-water demands. The system yielded energy savings between 30% - 70 % and hot water at 31^{o}C for a radiation value of 600 W/m^{2}.

The vertical tanks exhibit a high degree of stratification. However vertical tanks increase the height of a solar system rendering it less aesthetic. Consequently, horizontal tanks have still

found application in hot water storage, especially with integrated collector–storage solar water (ICSSW) heaters. A formulation of two and three zone stratification for solar water heating systems have been presented by Misra [1993,1994].Tests on an integrated collector storage-solar heater with two horizontal cylindrical tanks were performed by Madhlopa et al. [2005], to study the effect on thermal stratification with tank interconnection geometry. Carrilleo and Cejudo [2002] used TRNSYS software to study a model, an indirect solar domestic hot water system with horizontal storage and a mantle heat exchanger. Soteris and Christos [2000] did a simple model validation of a SWH consisting of two flat plate collectors using TRNSYS, the tool was used to optimise the design parameters and the annual solar fraction obtained was 79%.

Tank volume to collector area (V_t/A_c) ratio has also an important bearing on system performance for thermosyphon systems. Using TRNSYS simulation program, Sharaih and Lof [1996] obtained optimum values for tank height and volume, which maximizes the annual solar fraction for temperatures ranging from 50^{o}C - 80^{o}C. The positioning of the auxiliary heater within the tank, is also an important parameter thereby providing good thermal stratification. Shariah and Lof [1997] made studies on the effects of an auxiliary heater on the annual performance of thermosyphon solar water heater simulated under variable operating conditions. The optimal performance of a thermosyphon system depends upon the operating parameters and design parameters which are interlinked with each other and varying one affect the other. Abunabbi and Loveday, [2002] used a modified TRNSYS model that takes into account changes in the collector and tank performance characteristics, while on changing some design parameters. Study on parabolic trough collectors (PTC) was done by Tzivanidis et al. [2015], using solidworks software on a simulated model. It is observed that the thermal loss coefficient has very low values ranging from 0.6 W/m^2-K to 1.3 W/m^2-K, which can be explained by use of selective coating and vacuum between absorber and

cover. Smyth et al. [1999, 2003)] proposed an ICS vessel with inner sleeve arrangement which showed improved thermal collection, heat retention capability, and reduces heat loss up to 20 %. A model developed by Ulrike and Simon [2005] to describe thermal stratification after draw-offs showed that it depends upon draw-off-volumes, flow rates, and initial temperature in the storage tank.

2.2.4 Enhanced collector performance by increased optimal efficiency

The success of any solar water heater system is envisaged only if it is capable of delivering hot water when needed and even during non-sunshine hours. The design, therefore, should incorporate these two important criteria, a good solar fraction, and good heat retention. A good solar fraction can be obtained by improved optical efficiency and heat retention by proper insulation and good thermal storage as already discussed. The concentrator designs in the solar collector for low to medium concentrations can be flat or curved, line-axis or line-focus (circular, parabolic or compound parabolic) reflectors, symmetrical or asymmetrical. The introduction of a concentrator in a domestic solar water heating system is not yet commercialized but research studies have been carried out and model validation done with the symmetrical and asymmetrical type of reflectors. Performance study on an ICS with single tube involute reflector was done by Schmidt and Goetzberger [1990]. Such reflector has an acceptance angle of 180°. This means that even diffuse light which is scattered by the transparent insulation material is completely reflected onto the absorber. An annual SF of 0.65 and annual efficiency of 35% was obtained. To increase the optical efficiency extensive study on the domestic use of solar water heaters with stationary concentrating reflectors has been performed by Souliotis et al. [2011; 2013] presenting a new concept on ICS systems. The CPC has been found more suitable for solar thermal applications requiring fluid temperatures over 50^{o}C (Tripanagnostopoulos, [2000]). The high collection efficiency and less

thermal losses make them suitable for high-temperature applications. Therefore, the potential of solar collectors with compound parabolic concentrators has been exploited for the ICS solar water heaters application. The performance of the systems has been assessed and compared in terms of the temperature variation in stored water, mean daily efficiency and heat losses during overcast sky condition and at night (Tripanagnostopoulos [1992]). Helal et al. [2011] designed an ICS solar water heater based on three parabolic sections. The concept of using two storage tanks and based on the combination of asymmetric and symmetric CPC reflectors so as to obtain better water temperature stratification has been done by Tripanagnostopoulos and Souliotis [2002].

The inference drawn from these studies is that solar heaters with symmetric CPC reflectors are of lower cost than with asymmetric CPC reflectors. Also, the positioning of tank becomes cumbersome in asymmetric reflectors. The performance of the system is modeled by a simulation program written in MATLAB programming language and the results compared with the symmetric and asymmetric CPC reflectors of Tripanagnostopoulos model. Senthilkumar and Yasodha [2012], developed a three-dimensional compound parabolic concentrator, with the CPC reflectors fabricated as horizontal segments instead of vertical segments. Surface errors were thus reduced and optical efficiency increased. Smyth et al. [1999] have designed a novel ICS vessel using inner sleeve concept. Thermal buoyancy leads to natural circulation within the vessels during collection periods. A water layer near to the exterior surface is getting heated that leads to step up the hot water and passes through the perforated inner sleeve into the inner store. The results have indicated that the system exhibits higher temperature and better heat retention capability because of the lower value of heat transfer coefficient, Smyth et al. [2001]. Lens walled CPC, a novel design by Yuehong Sua et al. [2012] with large acceptance angle applied to PV applications can be incorporated in the ICS design. Thermal performance of CPC with large acceptance angle has been

studied by Varghese et al. [2007] with the mean daily efficiency of 37% and maximum water temperature 60^0C attained. To increase the optical efficiency different designs of symmetrical and asymmetrical reflectors have been studied. A simple analytic technique for calculating the average number of reflections for radiation passing through a CPC was developed by Rabl [1976] and is used for computing optical losses. In most practical applications, a CPC will be truncated because a large portion of the reflector area can be eliminated without seriously reducing the concentration. An improvement in CPC design has been suggested by Atul Jadhav et.al. [2013], which brings down its height (truncated CPC) without much compromise in concentration ratio. Recent developments in integrated collector storage solar water heater with CPC reflector has been dealt by (Devanarayanan and Kalidasa [2014]; Ramkishore Singh et al. [2016]), suggestive of an alternative to conventional Flat plate collector (FPC) systems.

2.3 Collector characterization

To envisage the collector performance and to make comparative studies with different models, a collector should be characterized by its system performance parameters. Modeling of thermosyphon solar water heating system using TRNYS program and model validation by performing 25 days test was obtained by Kalogirou and Christos [2000]. A new method for measurement of solar time constant was suggested by Hou et al. [2005], apart from the established standards ISO 9806-1 and ASHRAE 93-86. The time constants are dependent on the thermal capacitance of the collector and storage tank, capacitance rate of the circulating liquid, and heat loss coefficients. Munroe [1981] presented a method of determining the time constants of the system from test results on a solar simulator. The study establishes that solar collector is not strictly a first order system. There will always be a thermal lag and corresponding heat loss as the collector comes to its steady operating temperature, due to the heat capacity of collector itself.

A design parameter called the response time is obtained characterizing this transient response of the collector by Wijeysundera [1990]. Patrick and Jacques [1990] made studies to compare the transient behavior of different solar collectors by the calculation of time constant constant τ and predict the thermal performances of solar collectors operating under variable conditions of insolation. An improved procedure to determine the incidence angle modifier is presented and validated against experimental data in evacuated tube solar collectors by Zmabilin and Del [2012]. The thermal quality of a solar collector is characterized by the collector heat loss coefficient U_l and efficiency factor F'. Eisenmann et al. [2004] made studied to obtain correlations between collector efficiency factor and material content of parallel flow flat-plate solar collectors. Case studies done by Tzivanidis et al. [2016] on Parabolic Trough Collector, and developed a numerical model which showed the influence of mass flow rates and storage volumes on the dynamic performance of the system. To determine key parameters that has a greater influence on collector performance, the sensitivity analysis was carried out by Farghally et al. [2014]. In this work to study the dependence of thermal efficiency on the ratio of the temperature difference between collector inlet and ambient relative to global solar radiation was carried out on a PV/T collector.

2.4 Environmental and economic aspects

Solar energy has tremendous potential (Tian and Zao [2013]) to fulfill the world's energy demand that is currently being accomplished by the burning of fossil fuels. The efficient and exhaustive use of solar energy can reduce the intensity of global warming and climate change created by the larger and faster consumption of fossil fuels. In the recent years, various new and innovative technologies and systems have been developed that exploit the solar energy directly or indirectly and protect the environment (Thirugnanasambandam et al. [2010]; Shi and Chew [2012]; Yadav et al. [2013]). However, few of these technologies have some limitations over the technologies

operated by conventional fuels (Saif-Ul-Rehman [1967]; Castro et al. [2013]). The conversion of solar energy by thermal route is highly efficient, more environmentally friendly and economically viable if compared to the other routes of conversion (Koroneous and Nanaki [2012]; Furundzic et al. [2012]; Reddy [1995]). The solar water heater is one of the thermal conversion technologies that convert the solar energy directly into a concentrated form of heat at an appreciable conversion rate (Allen et al. [2010]). It has negligible global warming potential and lower payback period (Shimoda et al. [2010]; Koroneous and Nanaki [2012]). The technology is suitable to provide hot water adequately for both domestic and industrial sectors REN21 [2010] and also contributes to protecting the environment significantly (Purohit and Michaelowa [2008]).

Thermosiphon solar water heating systems offer significant protection to the environment and should be employed whenever possible in order to achieve a sustainable future (Soteris Kalogirou [2009]). Also, the cost-effectiveness studies made by Suri et al. [1998] has shown that conversion of solar energy to thermal form can compete with oil-based thermal energy production. A techno-economic evaluation and an assessment of the potential of solar water heating systems in India, as well as estimating their capacity utilization was undertaken by Chandrasekar and Kandpal [2004]. Evarts and Lukas [2013] estimated accurate hot water consumption information, based on the responses of a survey of 1594 resident occupants, which is handy for system designers and policymakers supporting solar-thermal-incentive programs. An accurate tool for sizing of solar water heating systems is the f-chart method. The f-chart method provides very accurate estimates of the monthly solar fractions for domestic applications but not for higher temperature systems (Braun et al. [1983]). The Lifecycle assessment includes all the life cycle phases as raw material extraction, manufacturing processes, transport, installation, operation, maintenance and end-of-life (dismantling, recycling, and final disposal). A 100 liters capacity SWH system is able to

save about 1500 KWh of electricity annually in the residential sector (Kaushik and Ranjan [2016]), and thus reduces about 1.5 tonnes of CO_2 emission load on the environment. Also, a system working on thermosyphon principle will have lower environmental impacts than evacuated tube designs. A study made by Greening and Azapagic [2014] on the life cycle environmental impacts of the two types of solar thermal systems used for domestic water heating, the flat plate and evacuated tube collectors suggest that the latter has higher environmental impacts due to the greater energy requirements for the production of the evacuated tube collector system. Manufacturing is the main contributor which accounts for (60%) to the environmental impacts. Design and modeling of a novel thermal solar collector for residential building were done by Notton et al. [2014] and high rise apartments in China by Shi et al. [2013]. The performances of this system were calculated for various solar collector configurations as number and position of water pipes and thermal insulation thickness. Three solar fractions are defined and used in the optimization procedure. Due to Government subsidies, Brazil has witnessed an increase in the installation and use of solar water heating systems in low-income housing projects (Giglio et al. [2014]).

Life cycle assessment of a solar thermal collector made by Ardente et al. [2005] also traces the products eco-profile from its state of infancy that synthesizes the main energy and environmental impacts related to the whole product's lifecycle. Lamnatou et al. [2014] carried out life cycle analysis based on embodied energy and embodied carbon methodologies on built-in-solar collectors. To determine key parameters that have a greater influence on collector performance, the sensitivity analysis was carried out by Farghally et.al. [2014]. In this work to study the dependence of thermal efficiency on the ratio of the temperature difference between collector inlet and ambient relative to global solar radiation was carried out on a PV/T collector. A procedure for

estimating the payback period of residential SWH in terms of cost and effective energy savings over conventional heating fuels/electricity was established by Lin et al. [2015], by undertaking a case study in southern Taiwan which can be handy for payback period calculations, especially for domestic solar collectors.

The techno-economic analysis of an integrated storage solar water heater by Smith et al. [2004] compared with SWH installations on domestic dwellings in the UK, showed that the total cost is sufficiently low to give payback periods that can compete with traditional forms of water heating. A simplified method was suggested by Yan et al. [2015] to avoid the mismatch between the solar water delivery with time and hot water demand by optimizing the key parameters of solar water heating systems based on life-cycle energy analysis. Solar economics is the methodology which involves optimal system design and economic evaluation to access solar process in economic terms. The long-term thermal performance can be estimated in terms of design parameters of components and economic evaluation in terms of economic indicators also referred as economic figures of merit like life cycle cost, present worth value, payback period etc. The f-chart method is a design method developed by (Klein et al. [1976]; Buckles and Klein [1980]), are the results of many numerical experiments and simulations correlated in terms of dimensionless variables, which form a basis for further correlations. To determine the optimal collector area as a function of annual load fraction, studies have been made by Barley et al. [1978]. A case study done by Kablan [2004] on the techno-economic analysis of the solar water heating system in Jordan presented policies that promote increased utilization of SWH systems.

2.5 Integration with building design, new trend

Solar thermal technologies have a relatively high conversion efficiency 2 - 4 times higher than PV systems and comparatively shorter payback period (Pinel et al. [2011]). Recently there is a growing trend of integrating solar thermal technologies with building architecture also referred as building integrated (BI) technology over the building added (BA) technology (Mahmut and Safa [2015]). Active solar thermal façade (ASTF) is a new building integrated solar thermal product, which allows integration of a solar thermal collecting device into a building envelope element eg. a wall, window or a roof (Zhang et al. [2015]). Static concentrator configurations are suitable for building integration, as they can be of a considerable size with greater structural strength and thus minimized stability problems, thereby larger concentrator sizes can be accommodated. These systems can be installed in parallel format, requiring no extra space between the collector units and are of flexible operation depending on the solar and climatic conditions, as well as the application energy requirements. New designs of building integrated solar energy systems have been suggested by (Tripanagnostopoulos [2014]; Buker [2015]). Modeling the life-cycle of BI solar thermal systems is a process that is normally integrated with the whole life-cycle assessment of the building. The methods of assessing the impact of the life-cycle comprise the analysis of the input and output of materials, of energy consumption and emissions to the environment of a product over its life-cycle. However, approximately 80% of the data that are needed for a common LCA analysis is already available, so it is not necessary to have the tedious task of collecting all the data via questionnaires, (Lamnatou et al. [2015]).

2.6 From Consumer's point of view

To obtain its wider acceptability in the domestic sector, the need is to improve the water temperature rise during the daily operation and water temperature preservation during the night. Also, it should be economically viable, hassle free in operation and should give a good performance. Recently performance enhancement techniques such as geometrical modifications on the absorber plate, use of solar selective coatings, PCM and Nanofluids have been given a special attention, (Souliotis et al. [2016]; Thirugnanasambandam et al. [2010]).

While BSWH facilitates easy installation, operation and maintenance besides providing cost reduction it operates at much lower daily collection efficiencies as compared to separate storage tank facilities. The focus of the study is therefore to obtain good heat retention and better long time performance estimates and in accordance, changes have been made in the design in addition to the use of CPC concentrator. For a truly stationary CPC, the limit of the useful concentration is about 2, Rabl [1976]. With low concentration ratio, CPC has its greatest advantages in acceptance angle and least disadvantages in cost, as compared to the simple parabolic concentrator. This system utilizes the CPC concept in reflector design, which increases the collection efficiency due to increase in the concentration ratio and also a minimum of tracking required due to increased acceptance angle, (Varghese et al. [2017]).

In this model, to obtain good heat preservation, the thermal resistance is added by providing glass wool insulation on the front, bottom and side panels of the SWH. To minimize the heat losses from the side walls which constitute a major portion of the system compared to its frontal area, an additional thermal resistance is added by introducing an air gap at the arms of CPC. This air in the gap not only offers additional thermal barrier but also serves as a thermal storage. Also the temperature of air between the collector and glass cover offers some effect on inside heat transfer

coeffient, (Shukla et al. [2008, 2002]). To study the effect of air gap on system performance during summer and winter conditions was done using MLR (SPSS) tool. Multi regression analysis is a flexible tool to consider for energy use prediction, (Braun et al. [2014]). Also, heat loss tests have been carried out to compute the values of heat loss factor and optical efficiency factor and performance compared with the ICS systems with symmetric and asymmetric reflectors. The present study does suggest that the use of air gap can be successfully introduced in ICS solar water heaters and enhance its performance with almost no additional cost incurred by providing a simple modification in the design. With the introduction of the air gap, the system is capable of delivering hot water at an average temperature of 45^{o}C to 55^{o}C throughout the day even after dusk and late till 8:00 pm. Working on thermosyphon principle it is environment-friendly and the unique feature is its good long time performance even after dusk. The annual solar fraction for the model is 0.55 and the payback period is two years, (Varghese et al. [2017]).

2.7 Conclusions from the literature review and Research Gaps

In ICS system, the opaque thermal insulation can be provided only on the non-illuminated part. Thus, although ICS system has a simple construction, installation and operation costs are less, is still not widely used as domestic SWH compared to FPC systems as it presents high thermal losses during the night or non-sunshine hours. No matter how well insulated the rear and sides of the collector might be, its solar collecting face would constitute a significant source of nighttime heat loss. The thermal retention and reduction of heat loss have been suggested by the use of baffle plate, use of TIM and PCM.

The use of baffle plate, fins, and corrugated surfaces presents higher characteristic length for convective heat transfer from the storage tank to water, resulting in higher daytime water temperature, however, it results in higher thermal losses during night time operation.

A comparative study of TIM cover systems, (Reddy et al. [1999]) shows that honeycomb systems excel over other systems. TIM covers presently available (e.g. small-celled polycarbonate honeycomb TIM covers), offer good possibilities of their applications where the typical working temperatures are between 50^{o}C - 80°C. However, the measurements of solar transmittance and total heat transport across the TIM devices are available only in assorted samples. These measurements, therefore, fall short in the manufacture of TIM devices of optimum characteristics, with regard to their cost and performance. In stagnation conditions (due to an electricity cut-off, a pump break down) the temperatures inside an optimized TIM collector can reach temperatures around 300^{o}C (absorber temperature). The honeycombs materials available in the market and economically competitive for solar collector applications do not stand such temperatures. Nowadays, this is the most critical technical problem of these kinds of collectors. Therefore, it is necessary to study and design strategies and mechanisms in order to evacuate heat from a solar collector in stagnation conditions, or in order to reduce the solar energy rate incoming into the collector in stagnation conditions. Possible solutions are mechanical shadings and heat evacuation by means of a ventilation channel in the collector maintaining an optimized performance in working conditions. Results suggest that on cold sunny days, no additional heating may be required, yet control strategies are necessary for summer days to minimize overheating. Most common refurbishment problems related to transparent insulation concept is that shading devices are necessary for summer. Also, the major factor associated with the practical realization of the TIM insulated system is the cost-effective manufacturing of the TIM device. Production is very limited with a small market, and it's not yet a regular building product particularly in India.

Phase change material (PCM) based latent heat thermal storage (LHTS) systems offer a challenging option to be employed as an effective energy storage and retrieval device.

Although LHTS systems offer high energy density and transfer energy under isothermal conditions, the poor thermal conductivity (usually 0.1 - 0.6 W/m-K) of PCMs drastically affects the thermal performance of the systems, which in turn limits their practical application, (Zalba et al. [2003]). This necessitates the employment of performance enhancement techniques for LHTS system.

High solar fraction and higher temperatures can be attained by use of reflectors. Most research studies have been carried out and model validation is done with the symmetrical and asymmetrical type of reflectors with involute profile reflector or with three parabolic sections. But the positioning of the tank becomes more cumbersome and compromise has to be done with regard to water temperature stratification and maximum water temperatures. The better option is to choose a reflector with wider acceptance angle to offset the loss of concentration ratio and positioning of the tank on the reflector which would become easier. Also, the design would be easy to fabricate and economically viable. The reflector, in this case, is supported on a wooden cradle which comprises the two parabolas of the CPC. The upper-end points of the collector are parallel to the central plane of symmetry of the collector thus contributes little to the radiation reaching the absorber, and the CPC can be truncated to reduce its height resulting in saving in reflector area but a little sacrifice in performance. Limited truncation affects the acceptance angle very little, but it does change the height-to-aperture ratio, the concentration ratio and the average number of reflections undergone by radiation before it reaches the absorber surface.

Therefore, scope exists to study a novel design which is economically viable, easy to fabricate, facilitate easy installation and capable of meeting the heating loads for households.The proposed model should have low initial cost and better long time thermal performance estimates.

2.8 Scope of present work

With the aim to deliver a model which is an amicable alternative to conventional systems, the following objectives have been framed in the present research work:

(i) Design and fabrication of the compact collector cum storage tank for domestic applications.

(ii) Design and fabrication of CPC reflector to make the integrated system.

(iii) Experimental analysis of the integrated system using standards defined by ASHRAE for performance evaluation.

(iv) Computational study of above integrated system and its validation with experimental results.

CHAPTER 3.0

EXPERIMENTAL SETUP

In this chapter, the details about system design, its fabrication, experimental set up and the instrumentation for conducting the experimental tests are presented.

3.1 Description of system

The BSWH is designed for households, where the drum is sized to cater the needs of a family of four based on the normal consumption pattern. The drum should be able to withstand the overhead line pressure only as there is no separate circulation pump being natural circulation type. The wooden cradle as shown in Fig.3.1, which not only supports the reflectors but it is also an important entity to concentrate the insolation onto the receiver drum.

Fig. 3.1 Wooden Cradle to house absorber

Being part of the CPC concept, the aperture of the cradle should be such that it should have wider acceptance angle so that the SWH requires almost no tracking.

The profile of the parabolic reflector is made in AutoCAD and the printout obtained on a flex at 1:1 scale as shown in Fig. 3.2. The profile is then cut on a sheet metal with the help of a shearing machine. This template (shown in Fig. 3.3) is then used to cut the plywood sheets.

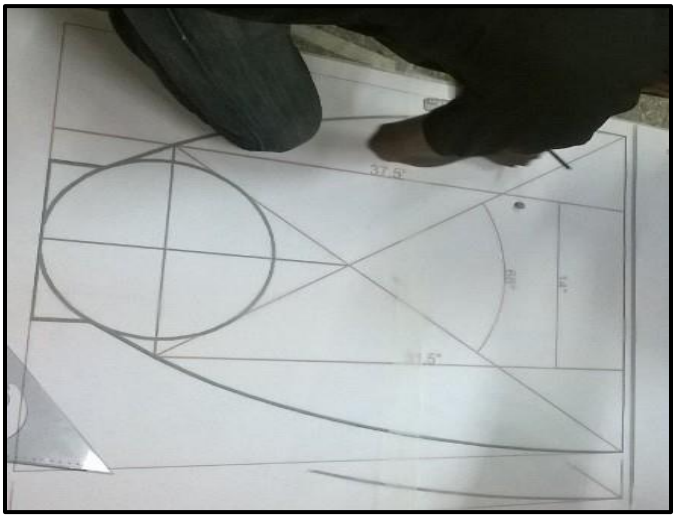

Fig. 3.2 Profile of CPC

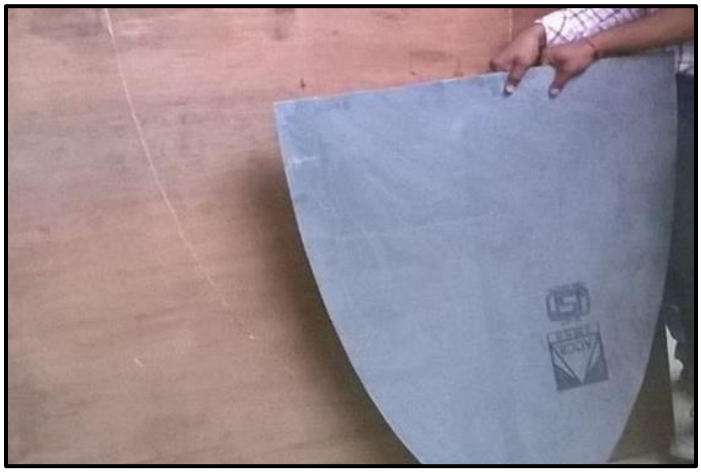

Fig. 3.3 Template of CPC

For the preparation of the wooden cradle, two full sheets (8 ft x 4 ft) phenol bonded plywood are used. For obtaining the CPC profile, the template is superimposed on the plywood and cutting is done. Three such strips are cut and then interconnected by longitudinal strips. The skeleton of the

wooden profile is then backed by supporting frame as shown in Fig. 3.4. The reflector is made of stainless steel sheet of 18 gauge and aligned on the supporting frame as shown in Fig. 3.5. The height of the cradle and its inclination should be such that it should not shadow the drum under any circumstance.

Fig. 3.4 Wooden cradle backed by supporting frame

Fig. 3.5 Aligned with reflector

The drum which is painted black is shown in Fig.3.6. Non- return valve is fitted at the inlet line and air vent/pressure relief valve at the outlet line. It is so positioned on the wooden cradle that its periphery lies on the focus of the parabolic reflector, so as to intercept maximum reflected rays which fall on the focal axis. Since the drum serves the dual purpose of absorber and storage tank, the drum cannot be insulated but thermal resistance is added by providing insulation on the front, bottom and side panels of the SWH.

Fig. 3.6 Absorber cum Storage Drum

The entire assembly is then housed in the wooden cradle (Phenol bonded plywood) and supported with circular clamps as shown in Fig. 3.7. The glass wool insulating material is used between the wooden cradle and stainless steel reflector.The choice of the glass covers, number and thickness can be done only after elaborate experimental analysis. As a thumb rule, one can begin with two glass covers. In the present design to minimize the heat losses from the side walls which constitute a major portion of the system compared to its frontal area, an additional thermal resistance is added by introducing an air gap as also shown in the cut-section, Fig.3.8, Page No. 39, of the arm of CPC. The complete assembly, as shown in Fig.3.9, Page No. 39, is installed on an open terrace, tilted at an angle of 28.58^{o}, the latitude of the location (Delhi).

(a) **(b)**

Fig. 3.7 (a) Positioned at the focus of CPC

(b) Supported by wooden cradle backed with insulation

(a) **(b)**

Fig. 3.8 Sectional view of CPC (a) Inside section of arm of CPC (b) Front view of CPC

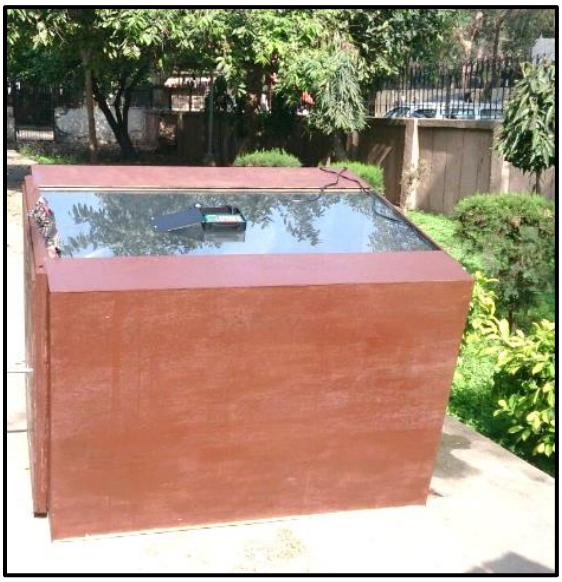

Fig. 3.9 Complete Assembly of BSWH

For prediction of thermal performance of the collector, the experiments were conducted under the clear sky on the open terrace in Aryabhat Institute of Technology, Shakti Nagar, Delhi, as recommended by ASHRAE 93 – 97 and ISO 9458[2] for outdoor tests. The tank was charged at 11:00 hrs. and readings were taken at half hourly interval till 15:00 hrs. The collector is facing due south with collector tilt at an angle of 28.58^{o} equal to the latitude of the location. With no tracking or occasional tracking, it is customary to keep solar tilt equal to the latitude of location to get maximum sunshine hours. The solar insolation falling on the aperture is measured with the help of solar power meter, placed atop the glass cover of the collector, [(Additional temperature included an error (+/- 0.38 W/m^2 / ^{o} C from 25^{o}C)]. For surface temperature measurement of the drum, glass cover and front, bottom and side panels of the collector J-Type thermocouples are used. These thermocouples are suitably mounted and fixed with the help of aluminium tape. The output was obtained from a digital display temperature indicator via a selector switch. A total of thirteen thermocouples were used (with four fixed on drum, four inserted in air gap at arms of CPC, two at different points inside drum for water temperature and two on top of glass surface) and the last thermocouple was kept handy so to measure outer wall temperatures at different locations to obtain the average outer wall temperature. The temperature of inlet and outlet water are measured by a scientific thermometer. The experimental setup is shown in Fig.3.10, Page No. 41.

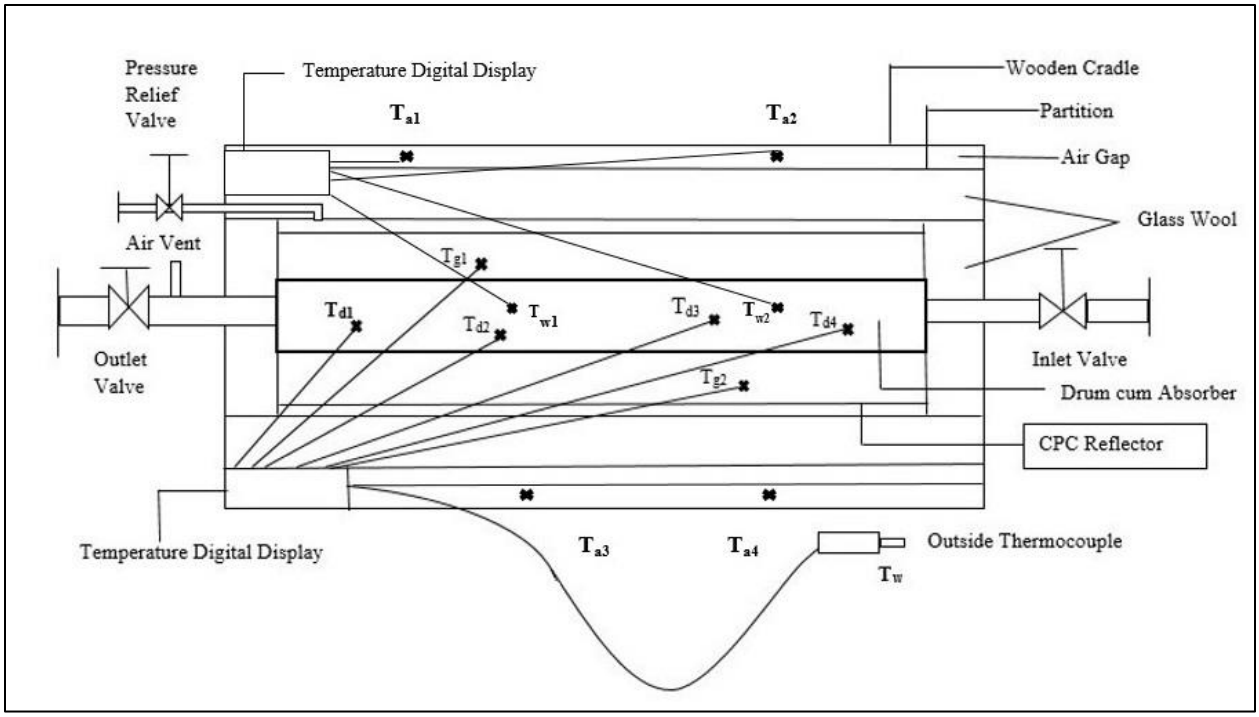

Fig 3.10 Experimental setup

3.2 Design of CPC profile

A two dimensional CPC is mounted with its length parallel to the horizontal east-west direction and aperture plane slopping towards the south. The tracking requirement and the frequency of adjustments required depend upon the concentration ratio. Since this collector is designed for households, one requires minimal or almost no tracking to facilitate minimum interference. Thus the CPC is designed for lower concentration ratio and wider acceptance angle. It is thus necessary to calculate the solar swing angle for the time period of the day for which collection is to be done. It may be noted that the solar swing angle is maximum on solstice days, i.e. June 21 and Dec 21. So, firstly the solar swing angle is calculated (Please refer Appendix. B), Page No. 159, and values worked out from 8:00 hrs. to 17:00 hrs. as shown in parametric Table 3.1.

Table 3.1 Time vs. Solar Swing Angle

Time hrs.	Solar swing α_v (degrees)
8:00	20.48◦
9:00	29.89◦
10:00	34.81◦
11:00	37.24◦
12:00	37.97◦
13:00	37.24◦
14:00	34.81◦
15:00	29.89◦
16:00	20.48◦

The minimum acceptance angle $2\theta_a$ required for the collector is equal to the solar swing angle α_v and the concentration ratio C.

$$C = \frac{1}{sin_{\theta a}} \quad (3.1)$$

where θ_a is the half acceptance angle. From results obtained shown in Table. 3.1, the concentration ratio may vary from 2 to 3. With known value of concentration ratio, other geometric parameters are obtained, for the geometry of CPC as shown in Fig.3.11, Page No. 43.

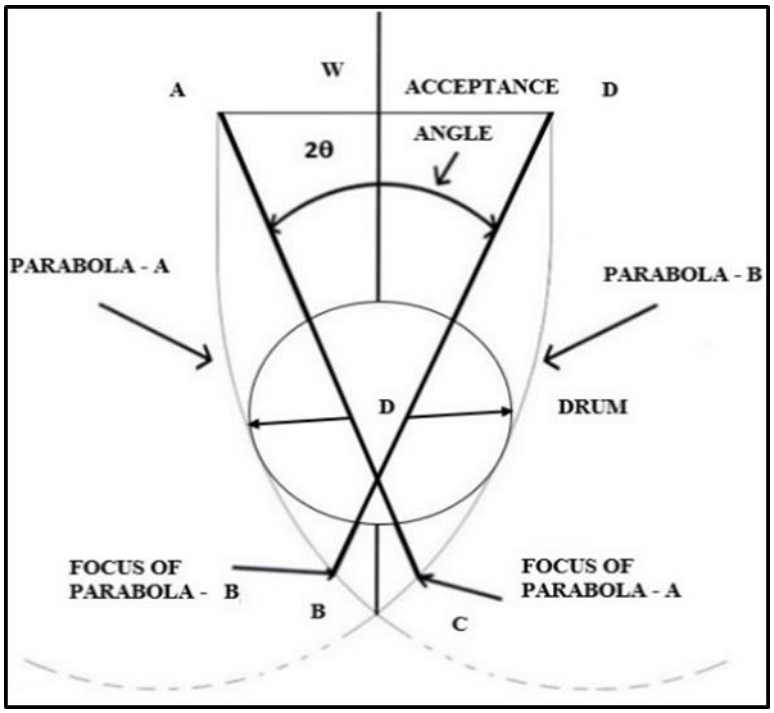

Fig 3.11 Geometry of CPC

Now from geometry of CPC, concentration ratio,

$$C = \frac{W}{b} \tag{3.2}$$

where W is the plane opening of the aperture and b is the width represented by BC.

In our case, it is the diameter of drum which is positioned at the focus. Since drum is for a capacity of 100 liters, suitable value for diameter which accounts to width 'b' is chosen and accordingly length of drum is obtained. Now with known value of 'b' from the relation of concentration ratio, W is obtained and the length of collector calculated for aperture area $1m^2$. The height to aperture ratio given by the expression , (Rabl [1976])

$$\frac{H}{W} = \frac{1}{2}\left(1 + \frac{1}{sin\theta_a}\right) cos\theta_a, \tag{3.3}$$

the height of the profile is obtained.

The system design parameters are shown in Table 3.2.

Table 3.2 System Design Parameters

S.no	Component	Material	Specification	Dimension
1	CPC Component			
	Wooden cradle	Ply wood Phenol bonded	l x b x h in m	1.4 x 0.72 x 0.91 m
	Reflector	Stainless steel (mirror finish)	Aperture area in m^2	1.008 m^2
2	Glass cover	Gauge 28	Concentration Ratio	2.06
		Clear Float glass	l x b in meters	1.4 x 0.72 m
			thickness in mm	4 mm
3	Storage component	MS 304 18 Gauge		
		Coating- Black paint nonselective	Capacity in litres	100 litres
4	Insulation	Glass wool	Front and rear face in m^2	1.14 m^2
			Side wall in m^2	2.66 m^2
			Bottom side	1.68 m^2
5	Air gap		in mm	80 mm

3.3 Calculation of insulation thickness

Theoretically the heat losses from the side and bottom should be minimum compared to the heat losses from the top. So the thickness of insulation has been theoretically determined to have minimum side heat loss coefficient and minimum bottom loss coefficient.

$$\text{i.e. } U_s + U_b < U_t \qquad (3.4)$$

Where U_s, U_b, and U_t represent the side, bottom and top heat transfer coefficients respectively in W/m^2-K.

Reconstructing the thermal network of the model, the heat flow from hot water in the drum to the environment is given by,

$$Q = Q_b + Q_s + Q_t \quad (3.5)$$

Where Q_b, Q_s, and Q_t are the heat loss from bottom, side and top of the collector.

For best performance of the heater,

$$Q_b + Q_s < Q_t \quad (3.6)$$

i.e. $K\left(\frac{A_s}{X_s}\right)\Delta T + K\left(\frac{A_b}{X_b}\right)\Delta T < U_t A_t \Delta T$ Or (3.7)

$$\left(\frac{A_s}{X_s}\right) + \left(\frac{A_b}{X_b}\right) < \frac{U_t}{K} A_t \quad (3.8)$$

K is the thermal conductivity of insulation in W/m^2-K, ΔT is the temperature difference of water in drum T_w in ◦ C and ambient temperature T_a in ◦C, A_s, A_b and A_t are the surface areas of side, bottom and aperture area respectively, X_s and X_b are the thickness of the back and side opaque insulation. Top loss coefficient is obtained using Klein's empirical equation for calculating top loss coefficient,

$$U_t = \left[\frac{M}{\left(\frac{C}{T_{pm}}\right)\left(\frac{Tpm-Ta}{M+f}\right)^{.33}} + \frac{1}{h_w}\right]^{-1} + \left[\frac{\sigma\left(T_{pm}{}^2+T_a{}^2\right)\left(T_{pm}+T_a\right)}{\frac{1}{\epsilon_{p+0.005M\left(1-\epsilon_p\right)}} + \frac{(2M+f-1)}{\epsilon_c}} - M\right] \quad (3.9)$$

Please refer Appendix B with notations having their usual meaning.

U_t = 3.04 W/m^2-K

A_s = 4.94 m^2 [inclusive of rear and front side]

A_b = 1.68 m^2

A_t = 1.008 m^2

K = 0.04 W/m^2-K [for glass wool insulation]

Substituting in equation (3.8)

$\left(\frac{4.94}{X_s}\right) + \left(\frac{1.68}{X_b}\right) < 76.6$ and (3.10)

$Q_b < Q_t$

$K\left(\frac{A_b}{X_b}\right) \Delta T < U_t A_t \Delta T$

$\left(\frac{A_b}{X_b}\right) < \frac{U_t}{K} A_t$

$\left(\frac{1.68}{X_b}\right) < 76.6$

$X_b > 0.0219$ m = 2.19 cm

Hence X_b is taken as 4 cm. Now substituting the value of X_b in equation (3.10)

$X_s > 0.142$ m = 14.2 cm.

So in the present design X_s is taken as 16 cm.

3.4 Instrumentation

The solar insolation falling on the aperture is measured with the help of solar power meter. For surface temperature measurement of the drum, glass cover and front, bottom and side panels of the collector J-Type thermocouples are used. These thermocouples are suitably mounted and fixed with the help of aluminium tape. The output was obtained on a digital display temperature indicator via a selector switch. The flow measurement was done by rotameter and inlet and outlet temperature of water measured by a scientific thermometer. The technical specifications of the instrumentation used are shown in Appendix D.

3.4.1 Fixing of thermocouple probes for surface temperature measurement

For surface temperature measurement of the drum and the top, side and bottom surfaces of the collector, thermocouples procured were reshaped by flattening the probe and properly fixed on the surface by aluminum tape at designated locations. The thermocouples were then connected to the digital display monitor. There are two monitors with six and eight selector switch respectively.

The proper numbering of thermocouples was done and accordingly connected to different points on selector switch as shown in Fig.3.12.

Fig. 3.12 Sequencing of Thermocouple

3.4.2 Calibration of Thermocouples

The thermocouples procured from the buyer were calibrated at their end. It was again calibrated at a reputed calibration centre in Delhi. The Thermocouple output in (mV) at an interval of 5^{o}C were obtained to a temperature of 300^{o}C. With this available output, the thermocouples were then checked with the help of multimeter, shown in Fig. 3.13, Page No. 48. To protect the electrical connections it was enclosed in a sheet metal box.

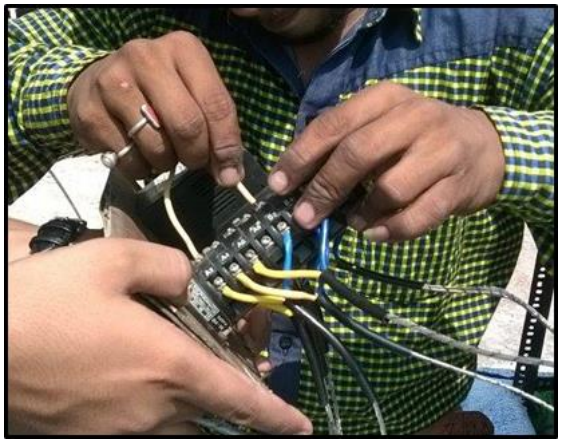

Fig. 3.13 Calibration check

3.5 Positioning of drum

The stainless steel reflector was wiped clean and which comprises the compound parabolic reflector. The drum is then positioned at the focus of the parabola. All plumber connections are restored. The top glass covers are then cautiously slid through the groove provided on the wooden cradle. To make it airtight, rubber seals were provided at the ends. The front panel which also functions as a door by the provision of hinges was locked. The airtight enclosure was now ready for thermal analysis.

3.6 Collector Installation

The prerequisite for any solar system installation is that the aperture is exposed to the most sunlight each day and throughout the year. Thus before installation of any solar equipment, the direction, solar geometry and location of the collector must be known. To ensure optimal heat output, the installation angle should be equal to or up to 15^{o} higher than the latitude of the location.

This solar water heater is installed on the rooftop at Aryabhata Institute of Technology, Delhi. The methodology adopted for rooftop installation was followed. Solar collectors need to face as close

as possible to the equator, which is the direction of the midday sun. Based on the requirement to face the equator, this means that in the northern hemisphere the collector should face south. To get precision in locating the direction due south, the surveyors (prismatic) compass was used. Since residential hot water demand is generally greater in the winter than in the summer, the collector ideally should be positioned to maximize wintertime energy collection, receiving sunshine during the middle six to eight daylight hours of each day. Care should be taken to avoid shading from other buildings, trees or adjacent boundary walls. The location therefore judiciously chosen was open terrace exposed to solar radiation throughout the day. The collector facing due south with the collector tilt equal to the latitude of the location which is 28^{o} for Delhi is obtained by mounting the collector at the prescribed angle on a structural C beam frame. The structural connection between the collector and frame and between the frame and building must be adequate to resist maximum potential wind loads. This was done by clamping the frame on a masonry foundation. The collector meeting the guidelines for roof top installation is shown in Fig. 3.14.

Fig. 3.14 Roof top installed collector

The rooftop installation of the system is completed as per the general recommendations by ASHRAE 93 – 97 for outdoor tests and the setup is ready for experimentation. The schematic layout of the experimental setup of BSWH is shown in Fig. 3.15.

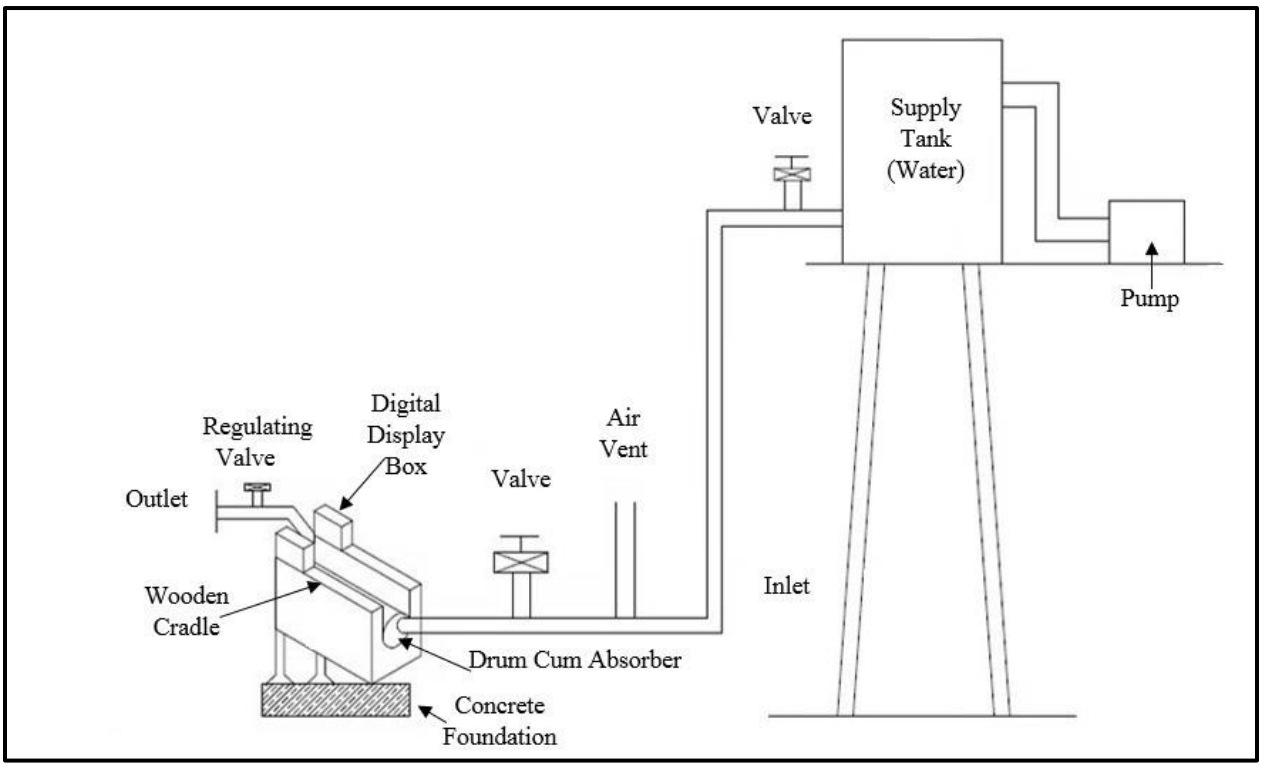

Fig. 3.15 Schematic Diagram of the experimental setup of BSWH

The complete making of the setup beginning from its infancy to the prototype is shown in Figs. 3.16 to 3.18, Page No. 51-54.

Fig. 3.16 Model of the prototype

Fig. 3.17 Template of CPC

Fig 3.18 Carpentry work (Wooden cradle)

Fig 3.19 Masonry work for roof top installation

Fig. 3.20 Instrumentation (a) Locating surface thermocouples on drum

(b) Output on digital display unit.

Fig 3.21 Plumbing Fittings

Fig 3.22 Setup ready for Installation

CHAPTER 4.0

EXPERIMENTAL PROCEDURE AND PERFORMANCE ANALYSIS

After achieving the experimental facility and installation of the setup, the next step is the testing of the collector. This chapter briefs about the testing procedure adopted and general guidelines to be met as per standards. It also includes the performance analysis and the methodology adopted to obtain collector performance parameters.

4.1 Testing procedure

Solar collector testing is undertaken with two types of approaches, the instantaneous approach and calorimetric approach. Fundamental characteristics of the collector can be established by these two approaches. However, the widely accepted is the instantaneous procedure. The input parameters for computation of system efficiency are $\dot{m}$ (rate of flow) of the working fluid, the temperature rise ($T_{fo} - T_{fi}$) between inlet and outlet, and the solar insolation on the plane of the collector. The solar collector system is equipped with necessary instrumentation for measurement of these parameters. The efficiency of the collector to convert solar radiation into thermal energy depends upon several meteorological and design parameters. The objectives of collector testing are:

(i) To predict collector performance in known meteorological conditions.

(ii) To permit evaluation of the performance of solar collectors for their commercial applications.

(iii) To establish performance standards.

During past several years, many standard collector test methods have been suggested based on whether it is undertaken indoor or as outdoor tests. Outdoor tests are hampered by meteorological conditions, are time-consuming and difficult to fix within exact boundaries. Indoor or laboratory

tests are performed in controllable environment and exclude meteorological variations and uncertainties. Suggested test methods are listed below:

(i) The test method suggested by the National Bureau of Standards (NBS) and modified by the 'American Society of Heating, Refrigeration and Air Conditioning Engineers'(ASHRAE).

(ii) The ISO (International standard of organisation), ISO 9806-1 prepared by the Technical committee Solar Energy, collectors and other components.

(iii) The test method suggested by the Bundesverband Solarenergie (BSE), Germany, a combined indoor-outdoor test method that does not respond very much to the meteorological conditions.

(iv) The test method proposed by Switzerland (EIR) that determines an "All day performance" of a collector on more or less statistical basis.

(v) (AFNOR) a test method proposed in France.

A well-laid procedure for testing and rating of solar collectors based on thermal performance was published by the National Bureau of Standards (NBS) in 1974. A modified version of the NBS procedure which was adopted in early 1977 as ASHRAE Standard 93 – 97 was developed by the 'American Society of Heating, Refrigeration and Air Conditioning Engineers'. (ASHRAE). The collector performance tests in the present model have been carried out by the ASHRAE Standard and ISO 9459-3:1993 for Solar heating – Domestic water heating systems for outdoor tests.

4.2 General recommendations adhered during installation for outdoor tests.

(i) The total aperture area of the collector should be atleast $1m^2$. In the model it is 1.008 m^2.

(ii) The collector must be installed in the open space in such a way that no shadows can obstruct during the test.

(iii) The collector should be located at a place where there will be no significant obstructions in the foreground of the collector subtending at an angle greater than 15^o to the horizontal. In the present case it is 28^o.

(iv) The collector testing carried on roof terrace should be located at least two meters away from the roof edge. Accordingly the collector is installed six meters away from roof edge.

(v) For open loop test a constant head device like a storage tank must ensure a constant mass flow rate. The requirement is met in the model by installing a storage tank at a height of 7.5 meters on a pavement and connected to the supply.

(vi) When the test loop is freshly charged with water, the system should be heated to its maximum operating temperature in order to expel the air dissolved in the water.

(vii) An air vent must be suitably placed in the system and outlet of collector.

(viii) The piping used in the test loop should be resistant to corrosion and suitable for operation at temperatures up to 95^oC.

(ix) The flow and temperature measuring devices should be installed with all due care, as greatest measuring errors are likely to occur in their measurement.

4.3 Instrumentation for collector testing

Instrumentation for measurement of the six primary experimental variables are ensured.

(i) Intensity of total solar radiation facilitated by a solar power meter.

(ii) The temperatures of water at inlet and outlet by scientific thermometer and surface temperatures to compute heat loss by J- Type surface thermocouple.

(iii) Ambient air temperature by thermometer.

(iv) Flow rate through the collector with the help of rotameter or any other measuring device.

(v) The surrounding wind speed by anemometer or other devices.

ASHRAE standard 93-77 for conduction of efficiency tests has laid down these standard testing requirements:

(i) The solar water heating device must be connected to an overhead tank to ensure constant flow rate.

(ii) For measurement of solar radiation a first class pyrometer need to be used.

(iii) Data need to be taken on good sunny days and mid-day hours and preferably when the solar incident angle is less than 30^{o}.

(iv) A series of tests need to be conducted, at interval of 15 minute or 30 minute period each of which determines the average efficiency. Tests were conducted half hourly and average of three days reading were taken.

(v) In computing efficiency, the gross frontal area of the collector need to be used.

(vi) The efficiency curve is drawn by plotting efficiency as a function of $\left(\frac{T_{fi}-T_a}{I_T}\right)$ where notations having their usual meaning.

(vii) After efficiency tests are completed, a series of tests is conducted to determine the collector's incident angle modifier. The collector's incident angle modifier test consists of a series of efficiency determination for a range of incident angles, with the inlet fluid temperature equal to the ambient temperature.

(viii) The time constant test is done to determine the transient thermal characteristics of the collector.

Thus, the collector performance tests are carried out in three steps. The first test is for calculation of instantaneous efficiency when the system is almost at steady state and the transient effects are almost negligible. So the test is undertaken few hours before solar noon, at solar noon and few hours after solar noon, when the incident beam is almost at right angles to the absorber surface. The second test is to obtain the incident angle modifier coefficient, and the third is to obtain collector time constant, indicative of thermal heat capacity. For measurement of the collector performance, the usual methodology adopted is keeping the collector from all shading and open to the sun and measure the gain in fluid temperature. The useful gain is then given by

$$q_u = \dot{m} c_{pw} \left(T_{fo} - T_{fi}\right) \tag{4.1}$$

Where $\dot{m}$ is the mass flow rate in Kg/sec, c_{pw} is the specific heat of water in kJ/Kg-K,

T_{fo} the outlet temperature of water and T_{fi} inlet water temperature of collector respectively in ◦C.

In addition, the incident energy, ambient condition, and wind velocity are also recorded. These data permit the characterization of a collector by parameters that indicates the systems capability to gain useful heat and how it losses heat to the surrounding. The thermal performance of a collector in terms of incident radiation can be described in the form:

$$q_u = A_c F_R \left[I_T (\tau\alpha)_{av} - U_l \left(T_{fi} - T_a\right)\right] \tag{4.2}$$

Here F_R is the heat removal factor and $(\tau\alpha)_{av}$ is the transmittance-absorptance product which is defined as the ratio of flux absorbed in the absorber plate to the flux incident on the cover system an appropriate subscript b or d being added to indicate the type of radiation, beam or diffused respectively. Out of the fraction τ which on transmission through the cover system, $\tau\alpha$ is absorbed and (1- α)τ is reflected back diffusely on to the cover system, so the fraction that comes back is diffused radiation and the fraction (1 - α) $\tau\rho_d$ is that which returns back from the glass covers. The process of absorption and reflection at the absorber surface goes on indefinitely, the quantities involved being successively smaller.

Thus the net fraction absorbed ($\tau\alpha$) = $\tau\alpha\left[1 + (1-\alpha)\rho_d + (1-\alpha)^2{\rho_d}^2 + \ldots\right]$ (4.3)

$$= \frac{\tau\alpha}{1-(1-\alpha)\rho_d} \quad (4.4)$$

The symbol ρ_d represents the diffuse reflectivity of the cover system. It is generally approximated to 0.15 for single cover system, 0.22 for two glass cover and 0.24 for three cover system, obtained for an incident angle of 60◦. During the course of collector testing, the standard testing recommendations suggest that beam radiation (I_b) should be high and diffused (I_d) portion be low. Thus one can replace the subscript for average (av) and consider $(\tau\alpha)$ as that which consists of only beam component. Thus instantaneous efficiency can be defined as:

$$\eta_i = \frac{q_u}{A_c I_T} = F_R(\tau\alpha) - \frac{F_R U_l (T_{fi} - T_a)}{I_T} \quad (4.5)$$

The quantity F_R is called the heat removal factor. The maximum heat gain and minimum heat losses occurs when entire collector surface is at inlet fluid temperature. Thus, the actual useful energy gain is equal to heat removal factor multiplied by the 'maximum possible useful energy gain', $(q_u)_{max}$ which occurs when plate temperature is equal to inlet temperature.

The experimental program is thus undertaken in two stages. The first outdoor tests as recommended by ISO 9458-2 and ASHRAE 93 – 77 conducted under clear sky day. In order to evaluate the daily energy gain in the system, the tank is charged at the start of the day and then left to operate during the day without any loads applied. At the end of the day, the useful accumulated energy and the temperature of the water in the tank measured. The second test is conducted as per the procedure of ISO 9459-3 and ASHRAE 93 - 77 to monitor the parameters namely daily thermal energy delivery (load), bulk mean delivery temperature, daily irradiation on the collector and ambient temperature. This test is carried out by varying the mass flow rate.

4.4 Test Period

The test conditions and permitted deviation of the measured parameters during the test for the steady-state and quasi-dynamic test are listed in Table 4.1. Basically, the demand for suitable test data is same for both types of approaches. The test data for quasi-steady state are collected during the whole day, from early in the morning to late in the afternoon. In contrast, for steady state, few instantaneous values during some hours around solar noon, each test day with clear sky and stable weather are collected, as shown in Fig. 4.1, Page No. 63. By measuring over the whole day, enough information about incidence angle modifier (IAM) – dependence is obtained. Also variable and partly cloudy conditions, Fig 4.2, Page No. 63 during the test period are prescribed, making it possible to identify the dependence of the diffuse part of irradiance as well as the thermal capacitance of the collector.

Table 4.1 (ASHRAE 93 – 97)
Test conditions and Permitted deviations

	Steady-state		**Quasi-dynamic**	
Parameter	**Value**	**Deviation from the mean**	**Value**	**Deviation from the mean**
Global solar irradiance G	> 700 W/m^2	± 50 W/m^2	300<G<1100 W/m^2	-
Incidence angle of the beam irradiance	< 20°	-	-	-
Diffuse fraction	< 30%	-	-	-
Surrounding air temperature	-	± 1 K	-	-
Surrounding air speed	3 m/s ± 1 m/s	-	-	-
Collector inlet temperature	-	±0,1 K	-	± 1 K

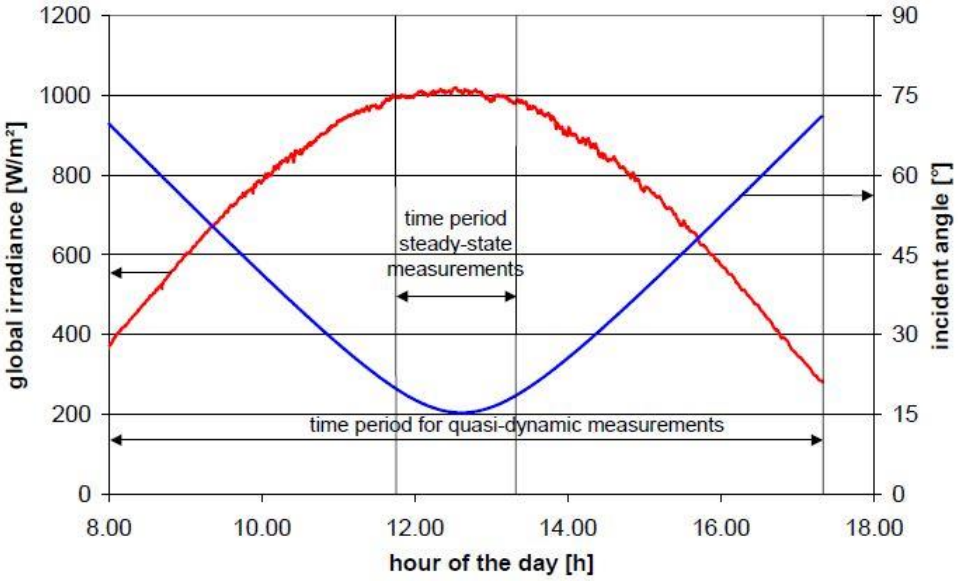

Fig 4.1 Acceptable time periods for steady-state and quasi dynamic measurements on a clear day as per ASHRAE 93 - 77

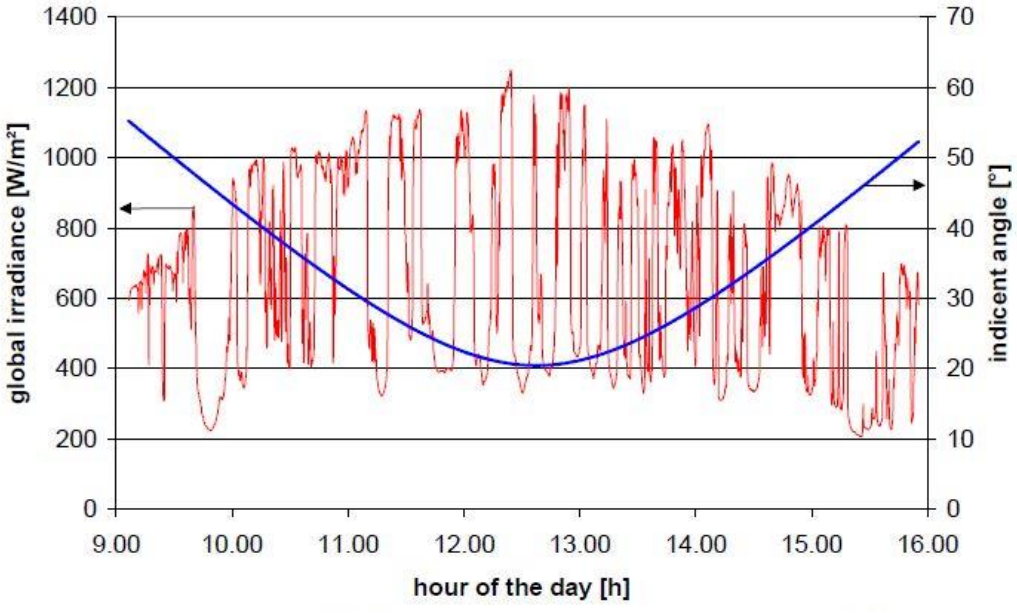

Fig 4.2 Time period only acceptable for quasi dynamic measurements on a day with variable irradiance as per ASHRAE 93 – 77

4.5 Parametric study

The parametric study of the model is undertaken using Engineering equation solver (EES), (Klein [2008]). The thermal performance of the collector is evaluated by computing the instantaneous efficiency of the collector by calculating the flux observed, heat loss and useful heat gain. It is convenient to express the heat lost from the collector in terms of overall heat transfer coefficient defined by the equation

$$q_l = U_l A_{ap} \left(T_{pm} - T_a\right) \tag{4.6}$$

where U_l is the overall heat transfer coefficient, A_{ap} effective area of absorber (drum) in m^2 and T_{pm}, T_a are mean plate (i.e. drum in this case) and ambient temperature respectively in ^{o}C. The heat lost from the collector is the summation of heat losses from the top, front, bottom and sides, and each expressed in terms of coefficients called top loss coefficient U_t, front loss coefficient U_f, bottom loss coefficient U_b and side loss coefficient U_s. Then overall heat transfer coefficient (please refer Appendix. C), Page No. 160, is given by:

$$U_l = U_t + U_f + U_r + U_s + U_b \tag{4.7}$$

The performance analysis proceeds in a similar manner to that of a cylindrical parabolic collector. However for a compound parabolic collector, because of its large acceptance angle, a CPC absorbs both the beam (I_b) and diffuse (I_d) component. The beam radiation falling on the aperture is $I_b R_b$ and diffuse radiation within the acceptance angle is $[I_b R_b + I_d/C]$,

and so the expression for flux absorbed is

$$S = \left(I_b R_b + \frac{I_d}{C}\right) \tau\, \alpha\, \rho_e \tag{4.8}$$

where notations having their usual meaning and C is the concentration ratio.

In order to obtain the useful heat gain, proceeding on similar lines to that adopted for cylindrical collector, q_u is obtained from the energy balance equation and given by:

$$q_u = \left[S - \frac{U_l}{C}\left(T_{pm} - T_a\right)\right](W - D_o)L \quad (4.9)$$

where W and L are width and length of aperture plane in m and D_o outside diameter of the drum. The instantaneous efficiency is then given by

$$\eta_{it} = \frac{q_u}{A_p I_T} \quad (4.10)$$

where A_p is the area of aperture in m^2.

4.6 Collector Characterization

Collector characterization parameters are obtained by performing thermal performance tests on the collector, under conditions meeting ASHRAE specifications for outdoor tests. To operate the system at nearly steady-state conditions, this means for outdoor tests, it becomes compulsive to carry the tests close to solar noon hours on clear days with beam radiation falling normal to the aperture plane. Thus, the transmittance – absorptance product ($\tau\alpha$) is approximately the normal incidence value$(\tau\alpha)_n$. To minimize the effects of scattering in data, the tests are made in identical pairs, one prior and other at the latter part of the solar noon, and the output obtained is then averaged. In addition, the general relevant conditions are also met during the experimentation. If the values of $F_R$and U_l does not vary greatly during operating range of collector, then long time performance estimates of the collector can be characterized by these two parameters $F_R(\tau\alpha)$ an indicator of "how energy is absorbed" and $F_R U_l$ indicator of "how energy is lost", which can be obtained from the plot of $\eta_i \; vs. \left(\frac{\bar{T}_f - T_a}{I_T}\right)$, where $F_R(\tau\alpha)$, is the intercept of the straight line and $F_R U_l$, the slope of the line. A collector constant that describes the effects of angle of

incidence is $K_{\tau\alpha}$ the incidence angle modifier represented by a single coefficient b_o. Souka and Safwat [1966], has suggested a general expression for angular dependence of $K_{\tau\alpha}$ for collectors

$$K_{\tau\alpha} = 1 - b_o\left(\frac{1}{cos\theta} - 1\right) \tag{4.11}$$

where b_o is a constant called the incidence angle modifier constant as shown in Fig. 4.3.

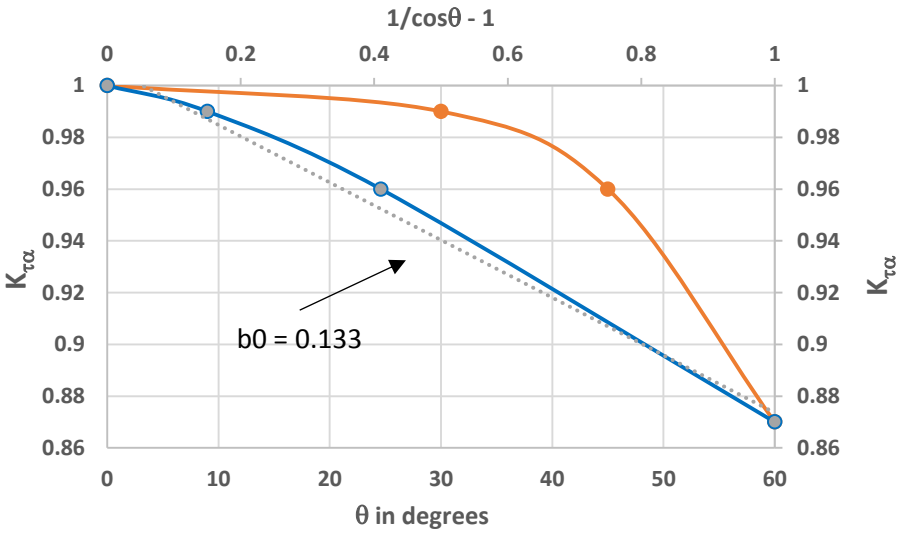

Fig.4.3 Incidence angle modifier $K_{\tau\alpha}$ as a function of θ and $\frac{1}{cos\theta - 1}$

The general guidelines as per standard testing methodology for outdoor tests, the tests should be conducted symmetrical about solar noon, i.e. few hours prior and after solar noon, when angles of the incident beam are approximately 30◦, 45◦ and 60◦ (Gillett and Moon [1985]). This approach is approximate to the test conditions, and the equation of flux absorbed is expresses as:

$$S = I_b R_b K_{\tau\alpha}(\tau\alpha) + I_d K_{\tau\alpha}(\tau\alpha)\left(\frac{1+cos\beta}{2}\right) + (I_b + I_d)K_{\tau\alpha}(\tau\alpha)\left(\frac{1-cos\beta}{2}\right) \tag{4.12}$$

Thus, the collector characterization is accounted by a three parameter model $[F_R(\tau\alpha), F_R U_l \; and \; b_o]$ in the present study.

4.7 Collector performance parameters

For any collector, it takes a few hours to reach its operating temperature from overnight conditions, after which it operates under quasi-steady conditions. The longtime performance estimates of the collector can be characterized by the optical efficiency factor$F_R(\tau\alpha)$ and heat loss factor $F_R U_l$ respectively. The parameters are obtained by plotting a graph of η vs. $\left[\frac{(\Delta T)_m}{I_T}\right]$, the slope of the line is $\frac{F_R U_l}{C}$ and the intercept is $F_R(\tau\alpha)$. The test was done in the month of April when the beam radiation is high and nearly normal to the aperture plane of the collector (readings were taken hourly from 11:00 hrs. to 15:00 hrs. Tabulated data is shown in Table 4.2 based on the average of three days readings on 21/04/2016, 22/04/2016 and 23/04/2016 respectively.

Table 4.2 Variation of parameters with time (April 2016 with clear sky)

I_T W/m^2	S W	q_u W	$\Delta T_m/I_T$ K-m^2/W	η_i %
827	550	275.4	0.0025	37.9
874	572	288.3	0.0035	37.7
788	624	310.8	0.0050	36.8
716	639	320	0.0080	35.8
630	654	324.9	0.0150	34.4

where $\Delta T_m = \overline{T}_f - T_a$

$$\overline{T}_f = \frac{T_{fi} + T_{fo}}{2}$$

In addition, the general relevant conditions are also met during the experimentation. Especially monitored are the operating parameters like mass flow rate kept at 450 ml/min - 1200 ml/min ± 10% per square meter of the collector aperture area and the total solar irradiance at the plane of the collector should be greater than 600W/m^2. The tank was charged at 11:00 hrs. and readings were taken at half hourly interval till 15: 00 hrs. The output of the thermocouples is obtained from

a digital display temperature indicator via a selector switch. The temperature of inlet and outlet water temperatures are measured by a scientific thermometer.

The definition of instantaneous efficiency, combined with the equation of useful heat gain, forms a basis for simulation models given by the equation:

$$\eta_i = \frac{q_u}{A_c I_T} = F_R(\tau\alpha)_{avg} - \frac{F_R\, U_l[(T_{fi} - T_a)]}{I_T} \qquad 4.13$$

Cooper and Dunkle [1981], showed that replacing fluid temperature with arithmetic mean of inlet and outlet temperature, i.e. $\overline{T}_f = \frac{T_{fi}+T_{fo}}{2}$ will result in very small errors for practical collector designs. The tank was charged at 11:00 hrs. and readings were taken at hourly interval till 15:00 hrs. Now from the plot of η_i vs. $\frac{\Delta T_m}{I_T}$, (Fig.4.4), where $\Delta T_m = \overline{T}_f - T_a$, the slope of the line is $F_R U_l$ and the intercept is $F_R(\tau\alpha)_{avg}$. Now for concentrating collectors, slope is $\frac{F_R U_l}{C} = -2.81$ i.e.,$F_R U_l = 5.7$ where C is the concentration ratio and intercept $F_R(\tau\alpha)_{avg} = 0.384$.

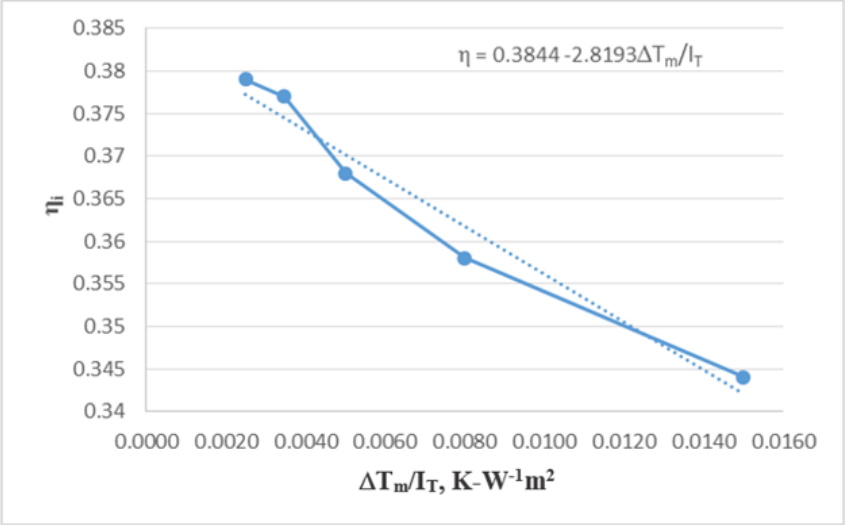

Fig 4.4 Performance curve to obtain optical loss and heat loss factor

To determine the time constant as a function of the thermal capacity of the collector is the third aspect of collector performance testing. The 'ASHRAE' standard test procedure recommends two methods for obtaining the same.

Firstly, the system is operated at almost steady state, with inlet temperature (T_{fi}) nearly equal to ambient temperature (T_a). After some useful heat gain, the collector is shielded by shading or moving the collector away from solar exposure and the fall in outlet temperature is noted a function of time. The second alternative method is obtaining the collector time constant with zero insolation testing i.e. at night, and record the fall in temperature till it reaches nearly the ambient temperature.

For integrated collector storage systems, describing the energy balance on tank, we get,

$$\frac{S - U_l(T_p - T_a)}{S - U_l(T_{pi} - T_a)} = \exp\left(\frac{A_c U_l}{(mC)_e}\right) t \qquad (4.13)$$

For concentrating collector, the time constant can be represented as a function of collector efficiency factor F',

where $F' = \frac{1}{U_l\left[\frac{1}{U_l} + \frac{1}{h_f}\right]}$ (as $D_o \cong D_i$) (4.14)

The characteristic dimension used for calculating Nu is D_i. Properties evaluated at the mean temperature $\frac{T_{fi} + T_{fo}}{2}$,

and $N_u = 3.66 = \frac{h_f D_i}{K}$ (4.15)

Analyzing over an infinitesimal time interval during sensible cooling of water,

the time taken dT, for a fall of dT_w in water temperature,

$$dT = -\frac{(MC)_w dT_w}{q_l} \qquad (4.16)$$

$$= -\frac{(MC)_w dT_w}{\pi D_o L F' U_l} \tag{4.17}$$

On integrating over time interval t during which the water temperature falls from T_{wo} to T_w,

$$t = -\frac{(MC)_w dT_w}{\pi D_o L F' U_l} \ln\left[\frac{(T_w - T_a)}{(T_{wo} - T_a)}\right] \tag{4.18}$$

Equation (4.13) can be rewritten as

$$\frac{T_w - T_a}{T_{wo} - T_a} = e^{-\left[\frac{\pi D_o L F' U_l}{(MC)_w}\right] t} \tag{4.19}$$

$$\text{At } t = \frac{(MC)_w}{\pi D_o L F' U_l} \tag{4.20}$$

$$\frac{T_w - T_a}{T_{wo} - T_a} = \frac{1}{e} \tag{4.21}$$

and t is called the time constant of the collector, generally given the notation as τ and $\frac{(MC)_w}{\pi D_o L F' U_l}$ is thermal capacitance of collector. In this case, compared to the heat capacity of water, the heat capacity of cover and other structures can be considered as negligible, the basic equation as a function of local fluid temperature can now be rearranged and written as

$$T_w^+ = T_a + \frac{S}{U_l} - \left[\frac{S}{U_l} - (T_w - T_a)\right] \exp\left[-\frac{F' \pi D_o L U_l}{\dot{m} C_{pw}}\right] t \tag{4.22}$$

Where T_w^+ the temperature of water after the end of each hour. Under zero insolation condition, T_w^+ can be reduced as a function of ambient temperature T_a. The output of 24-hr meteorological conducted in the month of October is shown in Table 4.3.

Table 4.3 Metrological Data (Outlet temperature with mass flow rate of 600 l/min)

Hour Ending	I_T W/m^2	T_a ◦C	T_w^+ ◦C	Hour Ending	I_T W/m^2	T_a ◦C	T_w^+ ◦C
17:50 on	14	32	42	5:00	0	-	-
19-10-16				6:00	-	-	-
18:00	0	31	41	7:00	-	-	-
19:00	0	29	41	8:00	-	-	-
20:00	0	29	40	9:00	744	28	33
21:00	0	28	40	10:00	868	31	33
22:00	0	-	-	11:00	891	33	35
23:00	0	-	-	12:00	924	33	37.5
0:00	0	-	-	13:00	888	33	38
20-10-16				14:00	790	35	41
1:00	0	-	-	15:00	640	36	44
2:00	0	-	-	16:00	610	35	46
3:00	0	-	-	17:00	301	35	44
4:00	0	-	-	17:50	-	-	-

With zero insolation and not much drastic changes in ambient temperature, the next steady state value obtained is 40◦C.

Theoretically, applying Newton's law of cooling,

$$T(t) = T_a + [T_{(0)} - T_{(a)}]e^{-kt} \quad (4.23)$$

where $T_{(0)}$ is the initial temperature at time t=0 in ^oC = 41^oC (at 18:00 hrs.)

T(t) is temperature of water after time interval t in ◦C = 40^oC (at 21:00 hrs.)

$T_{(a)}$ is the ambient temperature in ◦C = 28^oC.

Now using equation [4.23], value of k = - 0.027

general solution is $T(t) = 28 + 12\, e^{-0.027\, t}$ (4.24)

Assuming ambient temperature T(a) = 28°C constant, the next steady state value obtained is 33 °C. The time taken for the temperature of water to fall to 0.368*(41°C - 33 °C), the solution obtained from equation 4.24, the time constant τ = 2 hrs. 9 min.

Also from equation (4.20) and (4.22), $\tau = \frac{\dot{m}\, C_{pw}}{F'\, \pi\, D_o L U_l}$ [D_o = 0.38 m, L=1.34 m and $F'U_l = 3.58$]

Volume flow rate V=600 ml/min and ρ_w = 1000 Kg/m^3, Therefore $\dot{m} = \frac{600}{1000} * \frac{1}{60} * 1000 = 10\, \frac{kg}{s}$

Time constant τ = 2hr. 3 min. (4.25)

4.8 Uncertainty Analysis

No matter, regardless of the care that is taken, errors will occur in all experiments. The real errors are those that occur in experimental data that are always vague to some extent and carry some amount of uncertainty. The primary task is to determine just how uncertain a particular observation is and device a convenient way of specifying the uncertainty in analytical form. A reasonable definition of experimental uncertainty may be taken as the possible value the error may have. Depending upon the circumstances, this uncertainty may vary accordingly, and it is better to quantify it as experimental uncertainty rather than an experimental error, due to the uncertainty involved in the magnitude of the error.

To compute the uncertainty in the results from the estimates of uncertainty in the measurands, the result R is given as a function of the independent variables x_1, x_2, x_3,…, x_n. i.e. R = f(x_1, x_2, x_3,…, x_n). If the uncertainty in the independent variables are all given with same odds, then the uncertainty in the result having these odds is given by Kline [1953].

$$\omega_R = \left[\left(\frac{\delta R}{\delta x_1} w_1\right)^2 + \left(\frac{\delta R}{\delta x_2} w_2\right)^2 + \cdots \left(\frac{\delta R}{\delta x_n} w_n\right)^2\right]^{\frac{1}{2}} \tag{4.26}$$

where ω_R is the uncertainty in the result and, ω_1, ω_2, ω_3, … , ω_n, the uncertainty in independent variables. A precise method of estimating uncertainty in experimental results has been presented by Kline, [1953]. When the result function has a product form, uncertainty in product function can be expressed as R =$x_1^{a_1}$,$x_2^{a_2}$, $x_3^{a_3}$, ... $x_n^{a_n}$ and when partial differentiations are performed, we obtain,

$$\frac{\delta R}{\delta x_i} = x_1^{a_1}, x_2^{a_2}(a_i\, x_1^{a_{i-1}}), \ldots x_n^{a_n} \tag{4.27}$$

Dividing by R, we get, $\frac{1}{R}\frac{\delta R}{\delta x_i} = \frac{a_i}{x_i}$, substituting this equation in equation (4.26), gives

$$\frac{\omega_R}{R} = \left[\Sigma\left(\frac{a_i w_{x_i}}{x_i}\right)^2\right]^{\frac{1}{2}} \quad (4.28)$$

the fractional uncertainty in the result function in product form.

The measurands in the experiment are the solar insolation, the aperture area, and the temperature measurement by thermocouples.

The aperture area $A_p = L * W$ in m^2 (4.29)

L= 1.4m ± 0.001m (Least count)

W= 0.72 ± 0.001m (Least count)

The fractional uncertainty in area measurement $\frac{\omega_{Ap}}{A_p} = \sqrt{\left(\frac{\sigma L}{L}\right)^2 + \left(\frac{\sigma W}{W}\right)^2}$ = 1.56 x 10^{-3} (4.30)

Absolute uncertainty ω_{A_p} = 0.00157

A_p = 1.008 ± 0.00157 m^2 [Refer Appendix D]

At peak solar insolation

Incident radiation I_T = 842 ± 5.7 W/m^2 [Refer Appendix D], Page No.163.

Temperature measurement $(T_{pm} - T_a)$ = 15 ± 0.1°C

Combined uncertainty ω_c = 0.00962

At maximum outlet water temperature

Incident radiation I_T = 485± 2.66 W/m^2

Temperature measurement $(T_{pm} - T_a)$ = 10 ± 0.1°C

Combined uncertainty ω_c = 0.0115

The combined uncertainty and its influence on efficiency is shown in Table 4.4 and Table 4.5.

Table 4.4 Uncertainty Analysis

Time hrs.	A_p m^2	ω_{Ap}	$(T_{pm} - T_a)$ ^oC	$\omega_{\delta T}$	I_T W/m^2	ω_{IT}	Combined uncertainty ω_c
13:30 **(At Peak Solar)**	1.008	± 0.001	15	± 0.1	842	± 5.7	0.00962
15:00 **(Max. Outlet) Temp.**	1.008	± 0.001	10	± 0.1	495	± 2.66	0.0115

Table 4.5 Influence on efficiency

Condition at	Error in %	Nominal value of η_c %	$\omega_c \eta_c$
Peak Solar	2.50	37.60	± 0.36
Max outlet Temp	3.25	35.33	± 0.41

4.9 Model analysis by multiple linear regression (MLR) in SPSS

Statistical package for social sciences (SPSS) is a window based program that can be used for data analysis and to create tables and graphs. During model development, variables are divided into two groups, the influencing parameters as the predictor (input) and response (target or output) variables. To obtain the linearity between study variable and explanatory variables, the scatter plot matrix of the data can be used, which also checks-in on the assumption of linearity. A scatterplot matrix is a two-dimensional array of two dimension plots where each form contains a scatter diagram except for the diagonal. It gives information in the light of the relationship between a pair of variables rather than just the correlation coefficient between each pair of variables and thus it gives a sense of linearity or nonlinearity of the relationship. In the present analysis, the data-

driven method for energy use evaluation is the empirical approach. In the empirical approach, the most accepted technique is the linear or multivariate regression model (MLR) operated between measured energy use parameter as output (dependent) variable and the various influential parameters such as climatic factors, collector design parameters etc. as independent variables. This approach can be used for any time scale (hourly, sub-hourly, daily or monthly). Least-squares regression is the most common regression techniques to determine the coefficient of the model. Secondly, it also checks for multivariate normality. The MLR model summary and overall fit statics are depicted in tables. The statistics menu allows to include additional statistics to access the validity of the linear regression analysis.

The first table in the results output tells about the variables in the analysis. The second table shows the multiple linear regression model summary, the R^2 and adjusted R^2 value. R^2 and adjusted R^2 have distinct inferences, with the former which gives the percentage of explained variation as if all independent variables in the model affect the dependent variable whereas the latter gives the percentage of variation explained by only those independent variables that really affects the dependent variable.

The third output table is the F-Test. When $R^2 = 0$, the linear regression's F-test has a null hypothesis, that the model explains zero variance in the dependent variable. In case we assume that the model explains a significant amount of variance in the dependent variables, it means the F-test is highly significant. Regression coefficients represent the mean change in the response variable for one unit of change in the predictor variable while holding other input variables as constant. The multiple linear regression estimates are shown in the next table which includes the intercepts and significance levels. Lastly one can check for normality of residuals with a normal P – P plot.

A low p-value (< 0.05) indicates that one can reject the null hypothesis. In other words, a predictor that has a low p-value is likely to be a useful addition to the model because any changes in the predictor's value bring about necessary changes in the response variable. The residual is defined as the difference between the observed and fitted value of study variable. Residual is a measure of the variability in the response variable that is not explained by the regression model, which can be viewed as the deviation between the data and the fit. In case the residues are normally distributed, the plot shows that the points that generally follow the normal (diagonal) line with no strong deviations. By obtaining these scatter plots one can indicate whether there exits a good or weak linear relationship between these independent and dependent variables.

The MLR model analysis is based on following hypotheses:

Hypotheses 1

- In order to extrapolate the experimental results, the temperature difference at different points on the collector can be predicted by multiple linear regression with a dependent variable which can be outlet temperature of water or collection efficiency and four independent variables solar radiation intensity, incident angle, average drum surface temperature and ambient temperature at fairly constant inlet temperature.

Hypotheses 2

- As an estimator for heat collection efficiency η_c as the dependent variable, the system can be modeled as a function of following independent variables solar incident radiation on the titled plane $I_{T,}$ heat loss factor $F_R(U_l)$ and optical loss factor $F_R(\tau\alpha)$.

Going by these set of assumptions, the standardized residuals ought to resemble a sample from a standard normal distribution. A comparison of these residuals with a standard normal distribution

allows an assessment of the distributional assumption. A plot of the residuals against fitted values allows an assessment of the variance structure. The model fitting is done by considering the normal P-P plot and the Q-Q plot.

This chapter thus summarises the general recommendations of conducting tests as per test standards, and inferences derived from the analysis are explained in the next chapter.

CHAPTER 5

RESULTS AND DISCUSSIONS

5.1 Brief Review

In order to be practical, direct water heater solar devices must contain sufficient volume of stored water and achieve significant water temperature rise during the day and satisfactory temperature preservation during the night. These aspects have been taken into consideration in the design and construction of this system. The drum (absorber cum storage tank) is sized 100 liters to cater the needs of a family of four based on the normal consumption pattern. BSWH units are thicker units compared to FPC due to storage tank mounted on system trough. To increase the solar fraction a reflector of the type compound parabolic is incorporated in the design, supported on a wooden cradle. The wooden cradle which not only supports the reflectors but is also an important entity to concentrate the insolation onto the receiver drum. The reflector is made of stainless steel of 18 gauge. The advantage of the compound parabolic is that it can increase the collection efficiency due to increase in the concentration ratio and with the minimum of tracking required due to increased acceptance angle is best suited for the domestic purpose. The optical principle of a reflecting parabola is that all rays of light parallel to its axis are reflected a point. A parabolic trough, on the other hand, is line-focus concentrators, where as a result of the linear translation, the focal point becomes a line. The drum painted black is so positioned on the wooden cradle so as that its periphery lies on the focus of the parabolic reflector, so as to intercept maximum reflected rays which fall on the focal axis. For maintaining good thermal storage which is a major cause of concern in the case of integrated SWH systems, glass wool insulation is provided on the front, bottom and side panels of the SWH. To provide higher delivery temperatures throughout the day an additional thermal resistance is added by introducing an air gap at the arms of CPC.

The parameters investigated in this study are:

i) Performance prediction and validation with experimental data

ii) Effect of air gap on collector performance parameters

iii) Effect of mass flow rate on system performance

iv) Collector characterization parameters

v) Heat preservation capability as a function of Time constant

vi) Comparative model studies

5.2 Regression analysis

The efficiency of a solar collector depends on many factors such as collector temperature, ambient temperature, insolation and mass flow rate of the fluid. It is, therefore, important to specify the conditions in which the efficiency has been measured and calculated. Using the energy balance equation to obtain thermal efficiency and the plots obtained satisfying the equation in the form

$$\eta_{it.}A_p = \frac{S}{I_T} - \frac{U_l}{C}\frac{(T_{pm} - T_a)}{I_T} \quad (5.1)$$

where A_p is aperture area in m^2, I_T is incident solar radiation in W/m^2, U_l is overall heat transfer coeffient in W/m^2-K, C is the concentration ratio and T_{pm} mean plate (absorber drum) temperature in ◦C and T_a is ambient temperature in ◦C.

The fact that U_l is not always a constant but depends on the collector operating temperature and ambient conditions. As the heat loss coefficient varies non-linearly with the rise in collector temperature, the graph of efficiency vs $(T_{pm} - T_a)/ I_T$ represented as Collector performance parameter CP (in ◦C- m^2/W) should bend slightly downwards as the ratio increases. The magnitude of this effect may be quite small making straight line representation adequate. Thus the y-axis intercept would be flux absorbed and $\frac{U_l}{C}$ would be the slope of the line. To obtain the dependence

of thermal efficiency on the ratio of temperature difference between collector mean temperature and ambient i.e. ($T_{pm} – T_{a)}$ relative to global solar radiation I_T, regression analysis was carried out on obtained data. The trend line is indicative of the fact that, as CP increases, efficiency decreases as shown in Fig. 5.1. Theoretical values of efficiency are higher for CP between 0.015 - 0.016 compared to experimental values. Also reflected in Fig. 5.2, Page No. 83. For CP between 0.016 – 0.0175 the experimental values of efficiency cluster around almost 37 % – 37.5 % without much drop in efficiency. This is because of the presence of air gap. The air in the gap is heated up as the day progresses and reduces the effective temperature difference between system and surrounding. So although I_T decreases after solar noon the efficiency values remain almost same. For theoretical analysis, the introduction of the air gap is done as an added thermal resistance in the heat transfer circuit but experimental values reflect that the temperature of air has also an important bearing in suppressing the heat loss. Thus the results show that there is a slight increase in efficiency for CP between 0.019 – 0.02 in comparison to theoretical values.

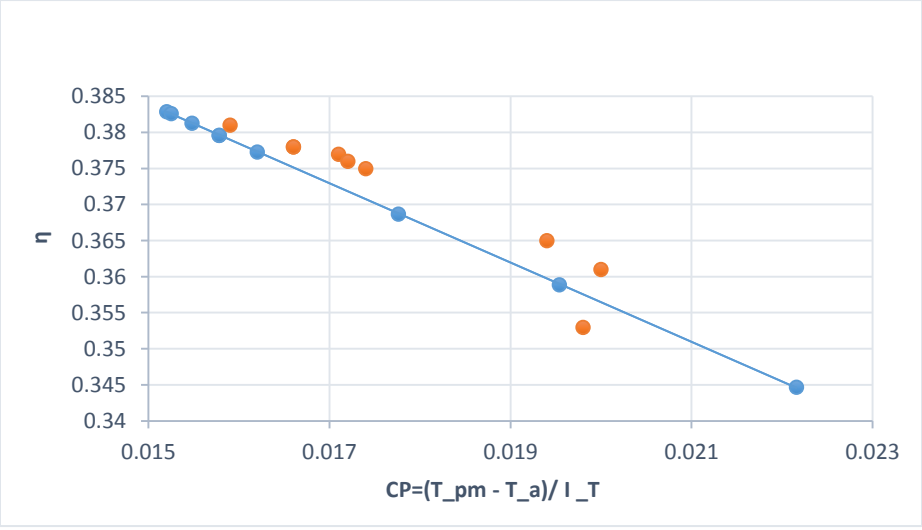

Fig 5.1 CP vs η

5.3 Parametric study of the model

The variation of the solar intensity, useful heat gain, collector efficiency with time is shown in Fig.5.2 and Fig.5.3, Page No. 83-84, both experimental and theoretical with a maximum outlet temperature of 53^{o}C attained at 15:00 hrs. as shown in Fig. 5.4, Page No. 84. It is also seen that the theoretical and experimental values of various performance parameters complement each other, (Table. 5.1 and Table.5.2). The solar intensity increases from 11:00 hours to 13:30 hours, reaching a maximum value of 842 W/m^2 at 13:30 hours. It has been observed that with air gap introduced at the arms of the CPC, even with the fall of solar insolation, there is a rise in temperature of outlet water, Fig. 5.4, Page No. 84 wherein the trend of increase in outlet temperature continues even after the drop in efficiency after solar noon, Fig.5.5, Page No. 85. It is also depicted in the diurnal curve, Fig.5.6, Page No. 85. This is because the air gap acts as a thermal barrier between absorber cum drum and outside ambient air.

Table.5.1 Parametric Table (Theoretical)

Time hrs.	I_T W/m^2	q_u W	S W	CP	η_c %
11:00	887	339.5	678.9	0.0157	37.9
11:30	904	347.6	692.8	0.0154	38.2
12:00	921	355.4	706.3	0.0152	38.2
12:30	918	354	703.9	0.0152	38.2
13:00	887	339.5	678.9	0.0157	37.9
13:30	864	328.6	660.1	0.0162	37.7
14:00	788	292.9	598.6	0.0177	36.8
14:30	716	259.2	540.5	0.0195	35.8
15:00	631	219.5	472.0	0.0221	34.4

Table.5.2 Parametric Table (Experimental)

Time hrs.	I_T W/m^2	CP	ΔT ◦C	T_{wo} ◦C	S W	q_u W	η_c %
11:00	697	0.0166	12	24	550.3	275.4	37.8
11:30	725	0.0159	12	26	572.5	288.3	38.1
12:00	790	0.0171	14	32	624.0	310.8	37.7
12:30	810	0.0166	14	38	639.7	320.0	37.8
13:00	829	0.0174	15	40	654.5	324.9	37.5
13:30	842	0.0172	15	44	664.2	330.6	37.6
14:00	694	0.0194	14	47	544.7	264.9	36.5
14:30	529	0.0200	11	50	413.3	199.6	36.1
15:00	485	0.0198	10	53	372.0	179.3	35.3

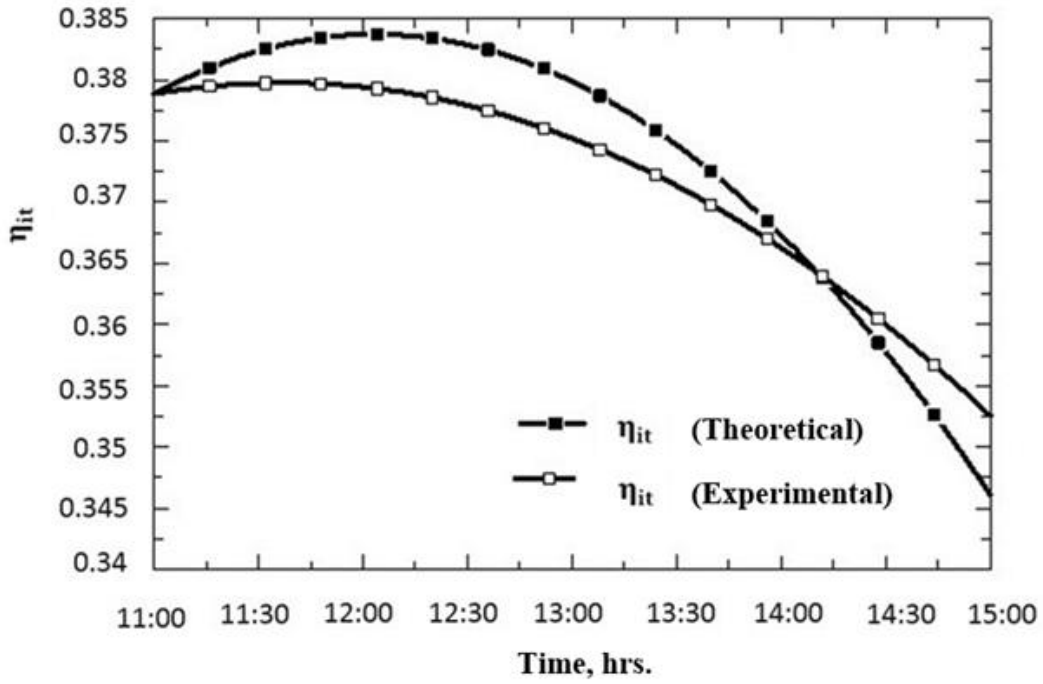

Fig. 5.2 Efficiency vs. Time (Theoretical and Experimental)

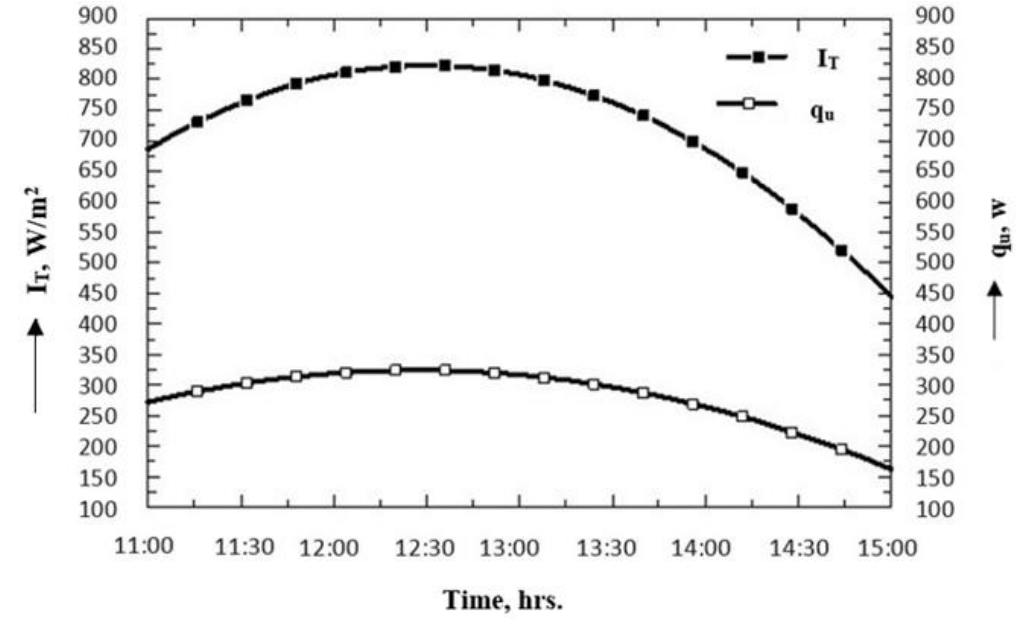

Fig. 5.3 Variation of I_T and q_u vs Time (Experimental)

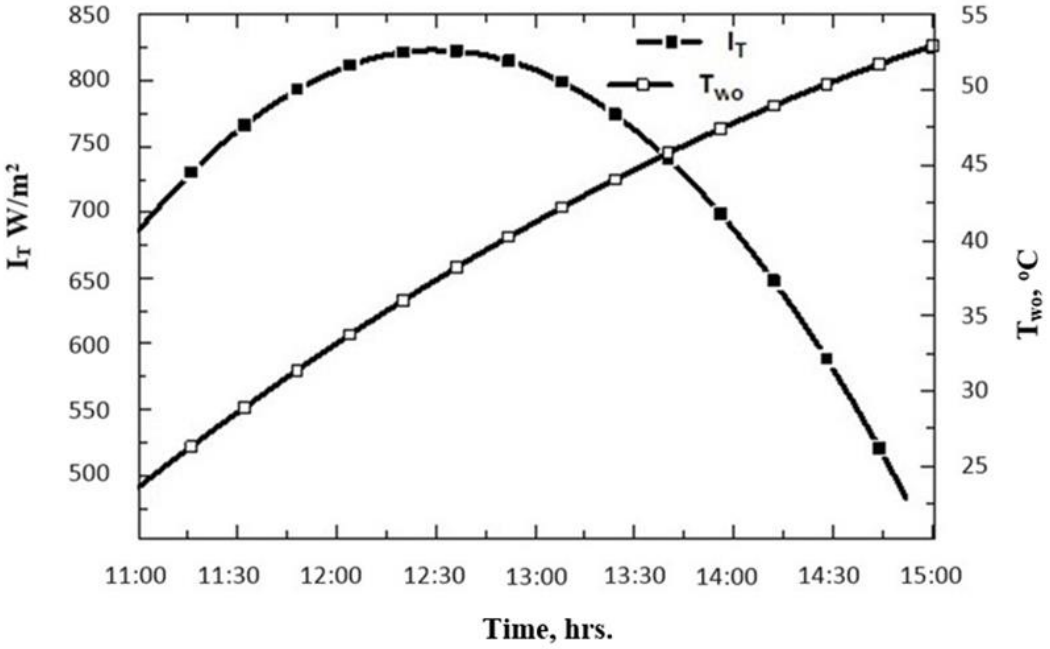

Fig 5.4 Variation of incident solar insolation and outlet temperature with Time (Experimental)

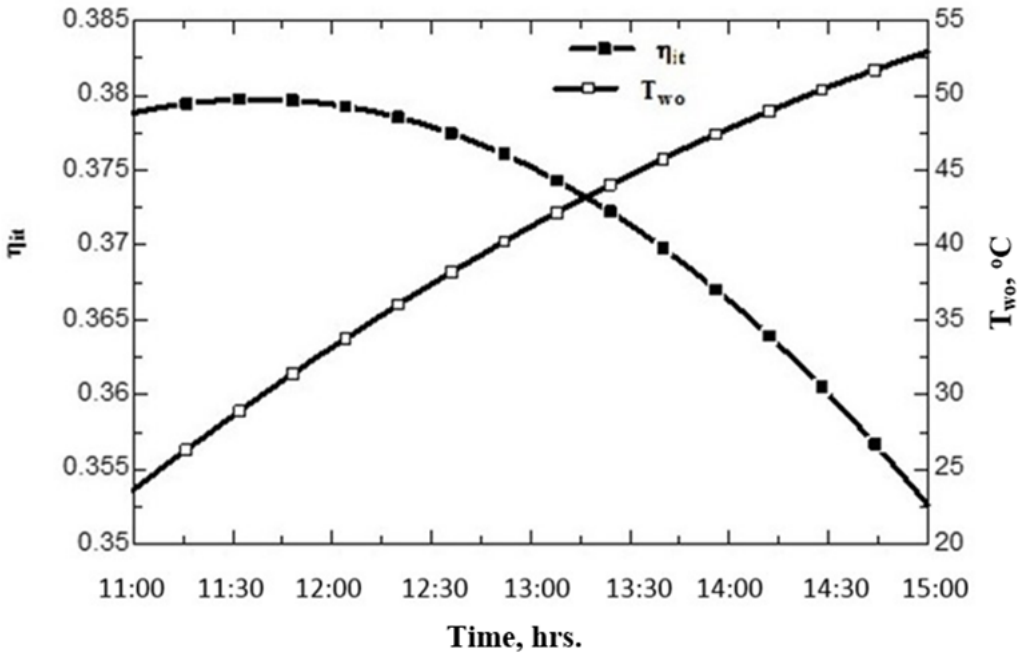

Fig. 5.5 Variation of efficiency and outlet temperature with Time (Experimental)

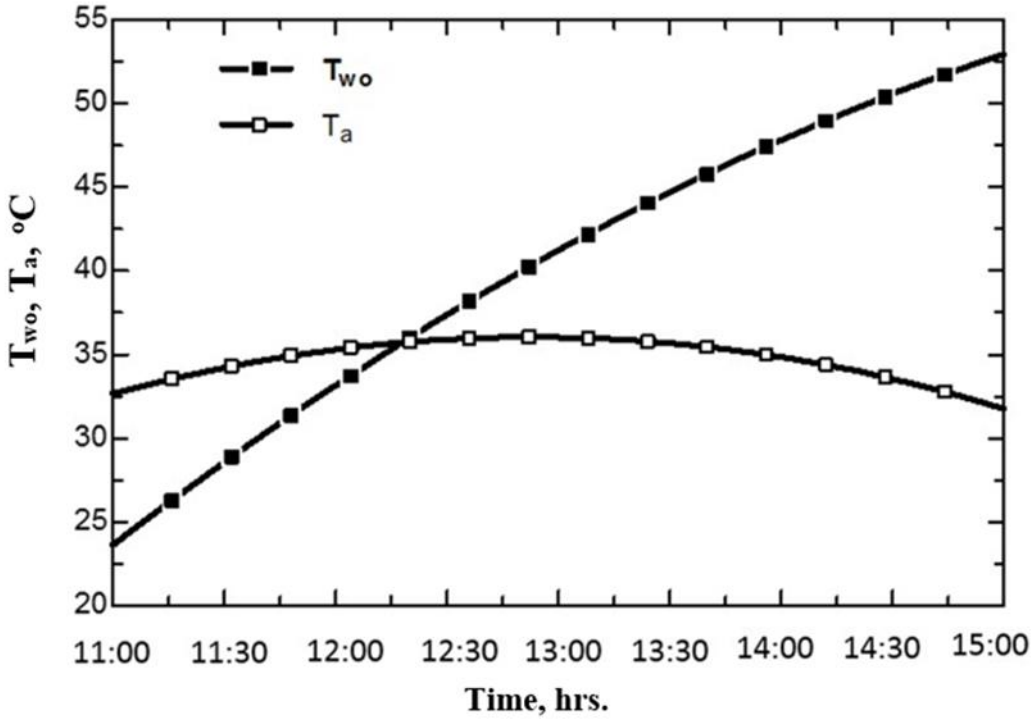

Fig. 5.6 Diurnal variation

5.4 Comparative study with a model without an air gap

A comparison with a similar model developed by Varghese et al. [2007] but without an air gap, it is observed that in contrast to the model with an air gap, the outlet temperature reduces with the decrease in solar insolation.

A few assumptions are done for comparison in the analysis:

(i) Since the objective of the study is the comparison between the two models, the heat stored within the walls of the drum is not considered and also being the two collectors designed for the same capacity. Only the quantity of heat stored by water is used in the computation of mean collector efficiency.

(ii) The models have been tested at different locations and on different days, but for the comparative study, the readings when the mean solar radiation incident on the aperture plane on the two models is in close proximity has only been taken into consideration.

(iii) As both the models have low concentration ratio, optical losses have not been worked out for the analysis.

For calculation of the mean collector efficiency for the test duration computation is done using the formula

$$\eta_c = \frac{Q_{wd}}{Q_a} \tag{5.2}$$

Where Q_{wd} in joules is the amount of heat quantity of stored water in the drum and Q_a is the 'solar insolation' impinging on the aperture plane during four hour duration of experimentation. If T_i is initial temperature of water at the time of charging at 11:00 am and T_f is the temperature of water at 3:00 pm, then:

$$Q_{wd} = m_w c_{pw}(T_i - T_f) \tag{5.3}$$

where m_w is the mass of water in storage cum absorber drum in Kg

The solar energy Q_a in joules intercepted by the aperture surface A_a is determined by the integration of the solar radiation intensity (global) G(t) measured on the aperture plane;

$$Q_a = A_a \int_{t_i}^{t_f} G(t)dt \quad (5.4)$$

Now $\int_{t_i}^{t_f} G(t)dt = G_m\ the$ mean solar radiation for the time period from t_i (11:00am) to t_f (3: 00 pm.)

Thus the mean collection efficiency $\eta_c = \frac{m_w c_{pw}(T_i - T_f)}{A_a * G_m * \Delta t}$ (5.5)

The results of the study has been depicted in Table 5.3

Table 5.3 Comparative Table

Inlet Temp. of water	**Without air gap Varghese et al.[2007]** 30 ^oC		**With air gap (Proposed model)** 24 ^oC	
Time	Temp. of outlet water $T_{wo,}$ ^0C	Collection efficiency η %	Temp. of outlet water $T_{wo,}$ ^0C	Collection efficiency η %
1 hr. prior to solar noon	43	24.67	38	38.10
At solar noon	44	29.70	47	37.54
At 3 pm	41	28.56	53	35.33

It is observed that maximum temperature difference of water obtained with air gap is 29^{o}C and that obtained without air gap is 14^{o}C and the average percentage increase in collector efficiency is 24.6 % (on condition of no withdrawal) with an air gap introduced on the side arms of the CPC.

5.4.1 Thermal loss coefficient vs mean temperature difference ΔT i.e. ($T_{pm} - T_a$)

For these type of systems, the thermal losses are significant as no thermal insulation can be provided on the drum which is also the absorber. To overcome this problem the system has to be thermally insulated from outside. Both the models are well insulated by glass wool insulation on the bottom and side and backed by plywood. In addition in the discussed model an air gap has been introduced at the arms of the CPC which not only adds to the thermal resistance, but also the air gets heated up which reduces the temperature difference between the drum and surrounding. From the values of regression coefficients obtained, it is seen that the average values of overall loss coefficient vary from 9-10 W/m^2-K as also obtained from heat loss calculations. The thermal loss coefficient per unit absorber area with and without air gap is shown in Fig 5.7.

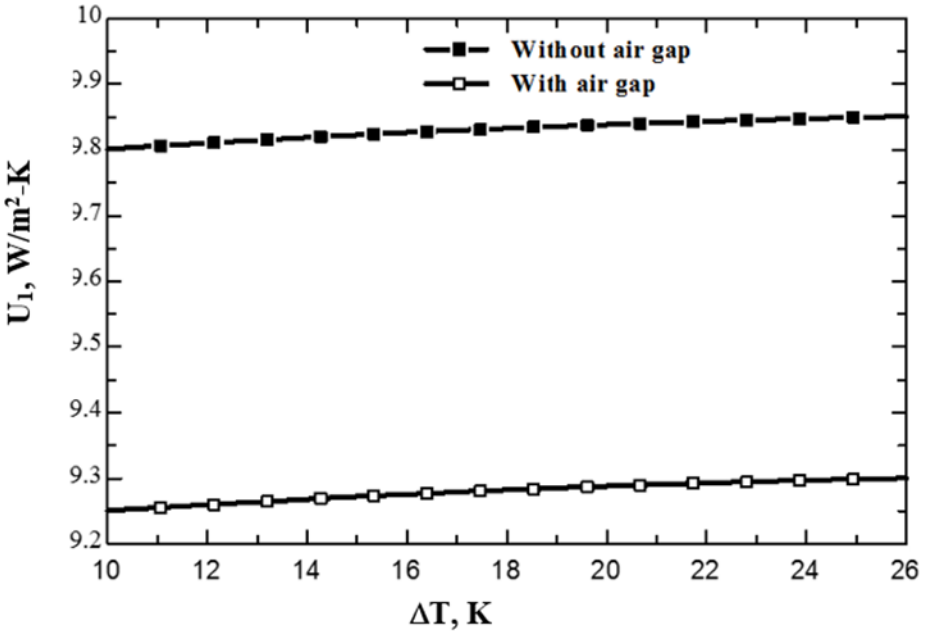

Fig 5.7 Thermal loss coefficient with and without air gap

5.4.2 Side loss coefficient with and without an air gap

The parametric study made on the model with and without an air gap has shown that there is a percentage reduction of heat loss from the side walls from 13.4 % to 52.5 % as ΔT increases from 14°C to 26°C. Initially, when the temperature difference is lower and air in the gap is not heated up, heat losses are higher but as the day progresses and temperature in air gap increases, it acts as a thermal barrier between the drum and ambient air. Later the heat loss remains fairly constant. The side loss coefficient with air gap, averages about 1.41 W/m^2-K and without an air gap was 2.81 W/m^2-K. Variation of the heat lost from the side walls in both cases is shown in Fig.5.8.

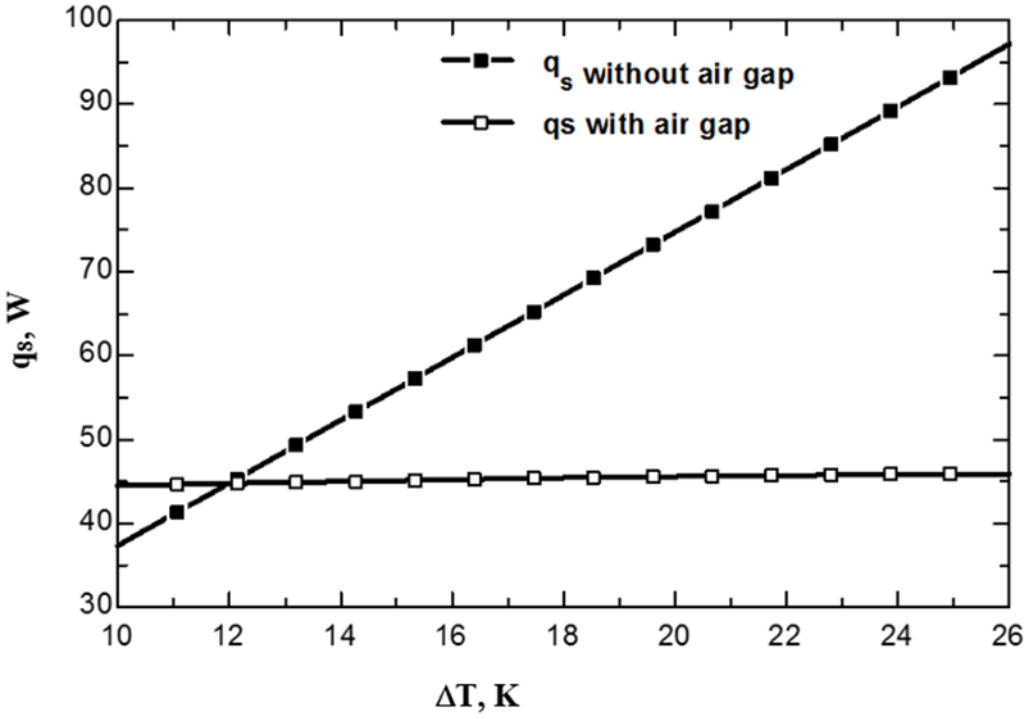

Fig.5.8 Heat loss from side walls of the CPC panel with and without air gap

5.5 Effect of mass flow rate on outlet temperature (average readings taken for time duration 12:30 hrs. to 16:30 hrs.) for 7 days

The effect of mass flow rate on outlet temperature on different days with solar insolation is shown in Fig.5.9, (Page No. 91).

5.5.1 Case 1 and case 6 (No- flow condition)

Higher the solar insolation, higher is the useful heat gain and higher the temperature of outlet water.

5.5.2 Case 3 and case 5 (Almost same outlet temperature in both cases)

In normal cases as flow rate increases, the maximum water temperature decreases although the system efficiency increases due to lower heat losses caused by lower operating temperature. But with this collector, it is seen that the variation in the outlet temperature of water is minimal, except for drastic variations in flow rate

5.5.3 Case 2 and case 5 (Almost same average solar insolation)

Here the marginal higher temperature of outlet water in case 2 is due to marginally higher system efficiency due to higher mass flow rate (from 16 kg/hr. to 18 kg/hr.), although the difference in temperature is not much significant.

5.5.4 Case 2 and case 7 (At very high mass flow rate)

Almost same average solar insolation but very high mass flow rate, there is significant drop in outlet temperature from 49.5^{o}C to 41.5^{o}C.

Thus, it can be concluded that the effect of mass flow rate is not much profound and for households, with normal consumption pattern, this system is capable of providing hot water with average temperatures ranging from 45°C to 55°C throughout the day, even late evenings.

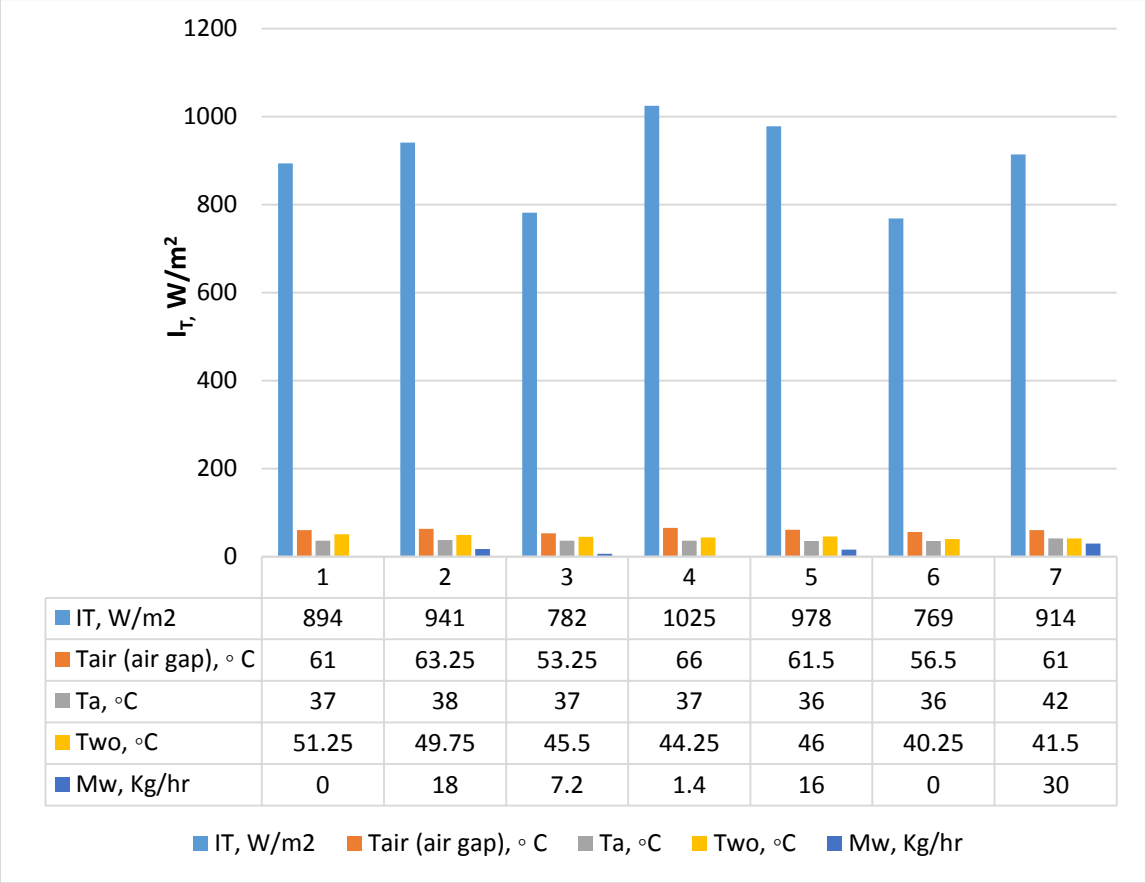

	1	2	3	4	5	6	7
IT, W/m2	894	941	782	1025	978	769	914
Tair (air gap), ◦ C	61	63.25	53.25	66	61.5	56.5	61
Ta, ◦C	37	38	37	37	36	36	42
Two, ◦C	51.25	49.75	45.5	44.25	46	40.25	41.5
Mw, Kg/hr	0	18	7.2	1.4	16	0	30

Fig. 5.9 Effect of mass flow rate on outlet temperature

1. 30/3/2016 (normal sunshine hrs.) Avg. wind speed 4.4 kmph
2. 31/3/2016 (normal sunshine hrs.) Avg. wind speed 3.2 kmph
3. 6/4/2016 (partial cloud) windy day, wind speed 7.5 kmph
4. 7/4/2016 (normal sunshine hrs.) Avg. wind speed 4.3 kmph
5. 8/4/2016 (normal sunshine hrs.) Avg. wind speed 3 kmph
6. 9/4/2016 (partial cloud) Avg. wind speed 6.7 kmph
7. 19/5/2016 (dust haze) Avg. wind speed 6.4 kmph

5.6 Effect of mass flow rate on system efficiency

By measuring the mass flow rate $\dot{m}$ and the temperature drop ($(T_{fi} - T_{fo})$ across the collector, the heat loss factor $F_R U_l$, can also be obtained as $F_R U_l = \frac{\dot{m} C_p (T_{fi} - T_{fo})}{\bar{T}_{f-} T_a}$ (5.6)

The variation of heat loss factor $F_R U_l$ with mean temperature of fluid $\overline{T}_f = \frac{T_{fi}+T_{fo}}{2}$ is shown in Fig.5.10 for varying mass flow rates. Using least square fit of data obtained, heat loss factor can be represented as a function of surrounding air temperature in the form

$$F_R U_l = a_0 + a_1 \left[\frac{T_{fi}+T_{fo}}{2} - T_a\right] \quad (5.7)$$

Using the non-linear model fitting function in excel, the value of $a_0 = 4.18$ and a_1= 0.11, and the equation is rewritten as $F_R U_l = 4.18 + 0.11 \left[\frac{T_{fi}+T_{fo}}{2} - T_a\right]$ (5.8)

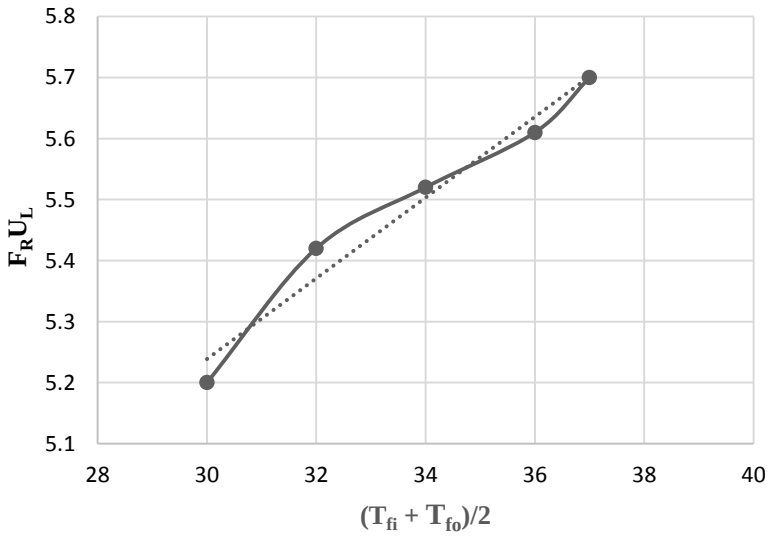

Fig. 5.10 Heat loss factor vs. mean fluid Temperature

Rewriting equation 4.13,

$$\eta_i = \frac{q_u}{A_c I_T} = F_R(\tau\alpha) - \frac{F_R\, U_l[(\bar{T}_f - T_a)]}{I_T}$$

From the sample of data taken for different values of solar insolation, both for summer and winter seasons and using equation (4.13) and equation (5.8), the test curves are plotted as shown in Figs. 5.11 to 5.15, (Page No. 94 – 96) with suffix 'S' for summer and 'W' for winter respectively. For summer, the tests were performed in the months of March, April, and May and for winter the months chosen were October, November, and December for Delhi. It has been observed that for this model, the efficiencies obtained with lower values of solar insolation i.e. 200 W/m^2, 400W/m^2, and 600 W/m^2 are higher in summer than in winter. However, for solar insolation of 800W/m^2 and 1000W/m^2, the values are marginally higher in winter than in summer. This is because the average wind speed in Delhi in summer is 3.6 m/s and in winter is 2.1 m/s respectively, which is comparatively lower. The overall heat coefficient U_l and F_R are function of temperature and wind speed, although F_R is weak function of temperature. Thus scatter in data is expected, because of variation in wind speeds, the angle of incidence and temperature dependence. Added to that some variations also occur due to the relative quantum of the beam (I_b), diffuse (I_d) and ground-reflected radiations. Except for few days at the far end of December and early January due to fog, the solar insolation obtained in Delhi is reasonably good. Now with air gap introduced on the side walls, the efficiency of the collector is in close range throughout the year. For all year round performance of the collector, the average value of collector efficiency hovers between 38% - 40%, and with water delivery temperature of 40^{o}C to 50^{o}C obtained throughout the year, which is reasonably good for a domestic solar water heater with no separate thermally insulated storage tank.

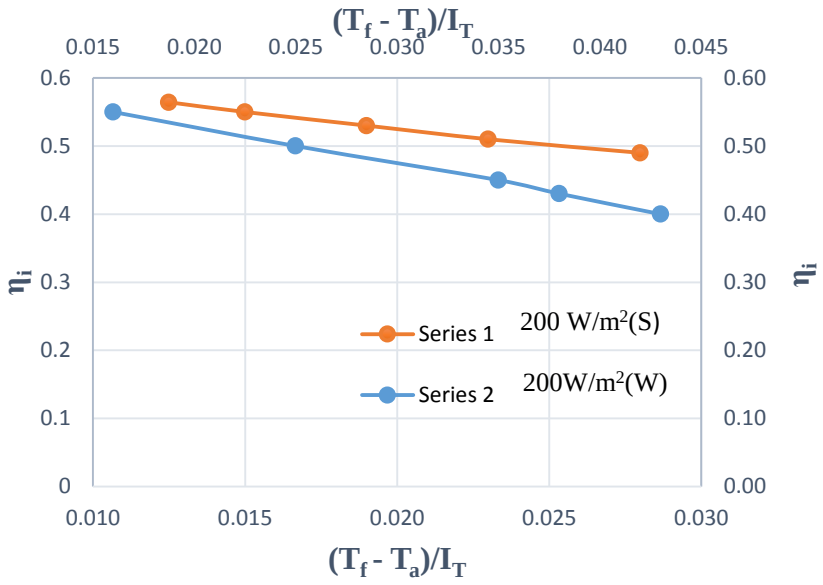

Fig. 5.11 $\eta_i \; vs. \left(\frac{\overline{T}_f - T_a}{I_T}\right)$

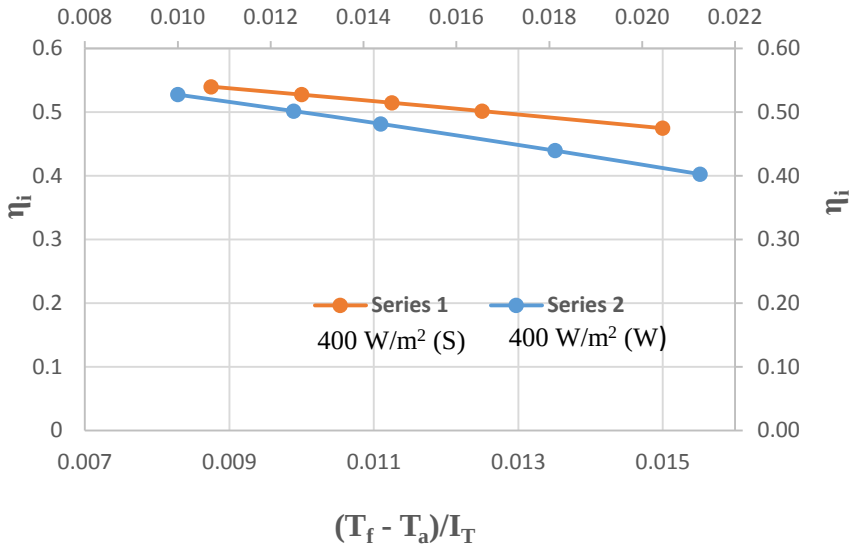

Fig. 5.12 $\eta_i \; vs. \left(\frac{\overline{T}_f - T_a}{I_T}\right)$

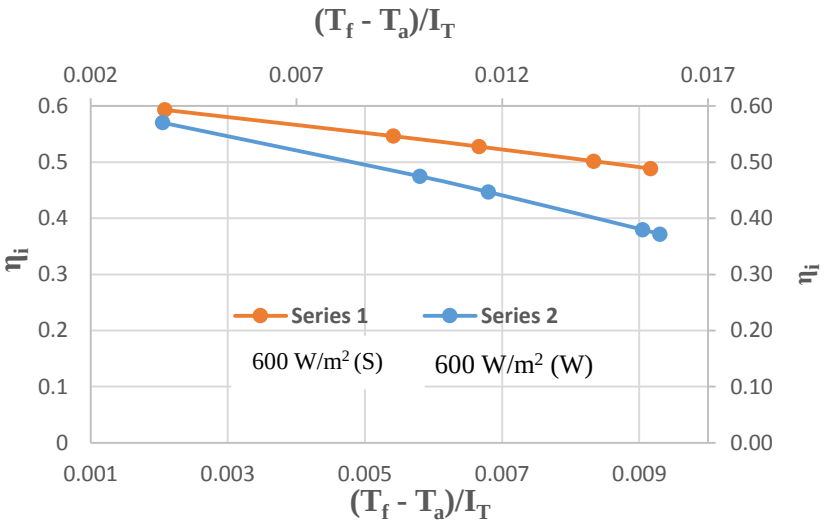

Fig. 5.13 $\eta_i \; vs. \left(\frac{\overline{T}_f - T_a}{I_T}\right)$

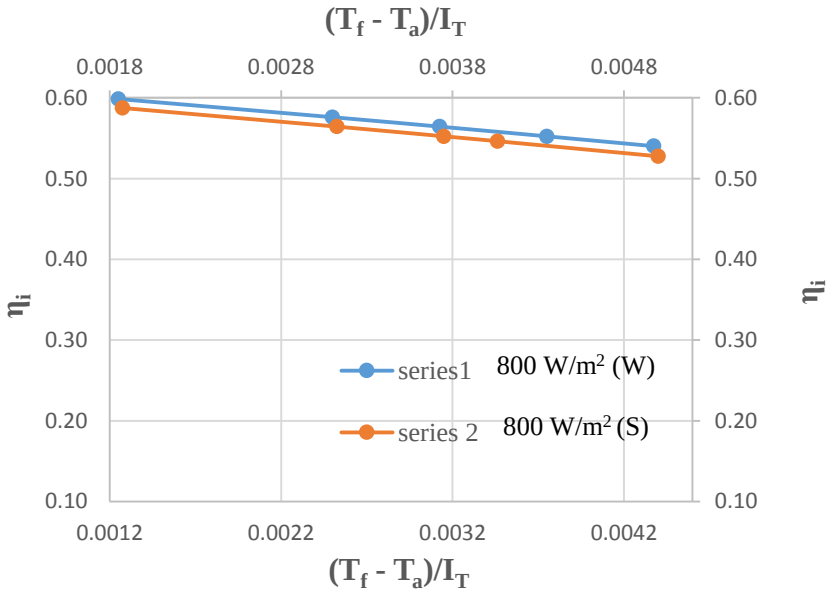

Fig. 5.14 $\eta_i \; vs. \left(\frac{\overline{T}_f - T_a}{I_T}\right)$

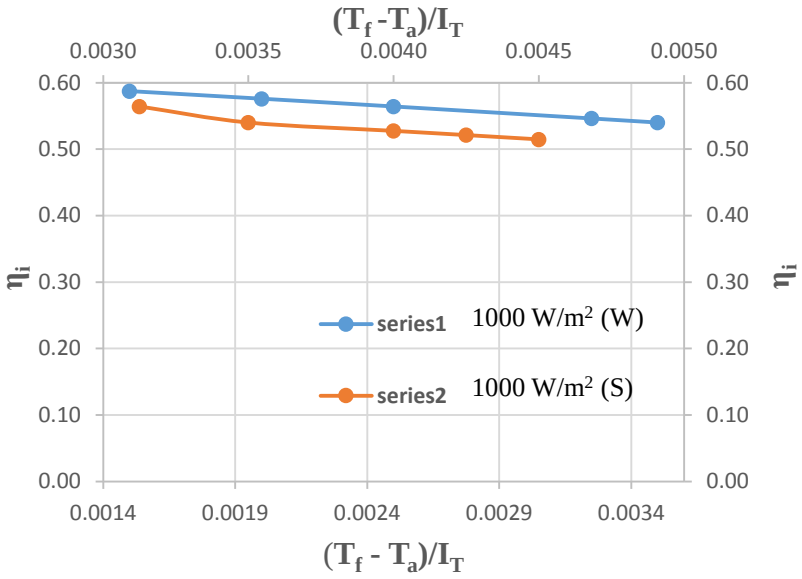

Fig. 5.15 $\eta_i \; vs. \left(\frac{\bar{T}_f - T_a}{I_T}\right)$

5.7 Time constant by zero (no insolation) Testing

Experimentally to obtain the time constant τ, the temperatures measured after dusk is taken into consideration and as already outlined with inlet temperature of fluid almost equal to ambient temperature, i.e. ($T_{fi} \cong T_a$). With this in view, experimental data, obtained for the month of November has been taken into consideration. The 24-hr meteorological data is shown in Table 5.4, Page No. 97.

Table 5.4 Time Constant (from 24-hr Metrological data) 4th Nov 2016, Delhi

Hour Ending	I_T W/m^2	T_a in ◦C	T_w^+ in ◦C	Hour Ending	I_T W/m^2	T_a in ◦C	T_w^+ in ◦C
17:50(sunset)				5:00	0	14	22
on 17-11-16	0	24	41	6:00	88	15	23
18:00	0	24	40	7:00	110	17	25
19:00	0	23	37	8:00	403	19.5	26.5
20:00	0	22	35.5	9:00	650	22.5	27.5
21:00	0	22	35	10:00	861	24	31
22:00	0	18	31	11:00	969	25	35
23:00	0	18	30	12:00	1065	27	40
0:00	0	17	28	13:00	1061	27	42
on 18-11-16				14:00	942	29.5	45
1:00	0	16	27	15:00	760	29	45
2:00	0	15	24	16:00	456	27	44
3:00	0	14	23	17:00	119	25	41
4:00	0	14	22	17:50	-	24	39

Now with zero insolation and no water withdrawal from the tank, the cooling curve as shown in Fig.5.16 (Page No. 98) is plotted on a semi-logarithmic scale of ln ($T_w - T_a$) with time. Time (0) hrs. is at 17:50 Hrs. IST (sunset), and the beginning of experiment at zero insolation at time t = 0. The slope of this line is equal to ($-1/\tau$) = 0.0639, i.e. k = 0.0639 and the time elapsed for the temperature to drop by 0.368*[(35ºC – 22ºC)], is 1hr. 36 min. This also validates to that obtained theoretically, although there is a slight difference of 33 minutes. This is because the positioning of the outlet valve is slightly below the top circumference of the drum. Also to avoid any leakage through holes drilled for inserting thermocouple knobs in the drum, the drum is not filled to its full

capacity of 100 liters. The result obtained is thus indicative that, the system heat retention capability is reasonably good and is capable to deliver warm water with temperatures of even more than 25^{o}C early morning, even in winter seasons, when the ambient temperature is less than 20^{o}C.

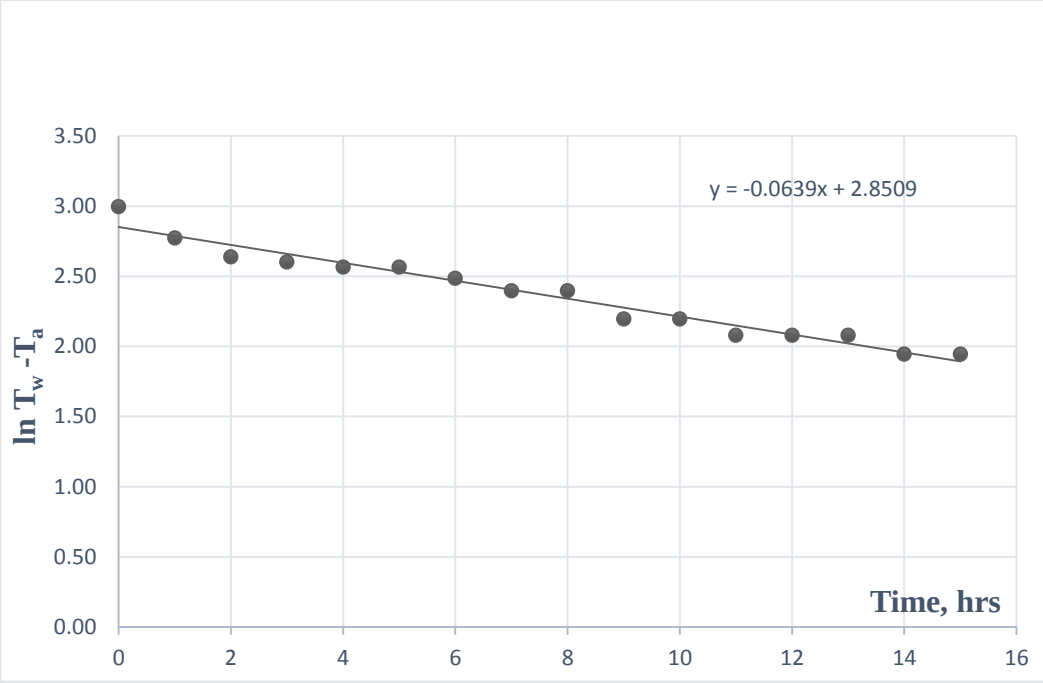

Fig. 5.16 Cooling Curve

5.8 Performance characteristic curve of collector

On similar lines to that of the performance of a paraboloid solar concentrator solar cooker, knowing time constant, heat loss factor ($F'U_l$) and optical efficiency factor ($F' \eta_o$), it is possible to approximately predict, the sensible heating period of the collector under any given climatic conditions, with available data of solar insolation and ambient temperature.

The maximum average temperature attained by the collector is 53°C, the time of sensible heating from ambient temperature to 53°C, can be obtained from equation 5.9.

$$\tau_{heating} = \tau \ln \left[\frac{1}{1 - \frac{F' U_l}{F' \eta_o} \left(\frac{53 - T_a}{I_b} \right)} \right] \quad (5.9)$$

A plot of $\tau_{heating}$ versus the climatic parameter $\left(\frac{53 - T_a}{I_b} \right)$ can be referred as the characteristic curve of the solar water heater as shown in Fig. 5.17.

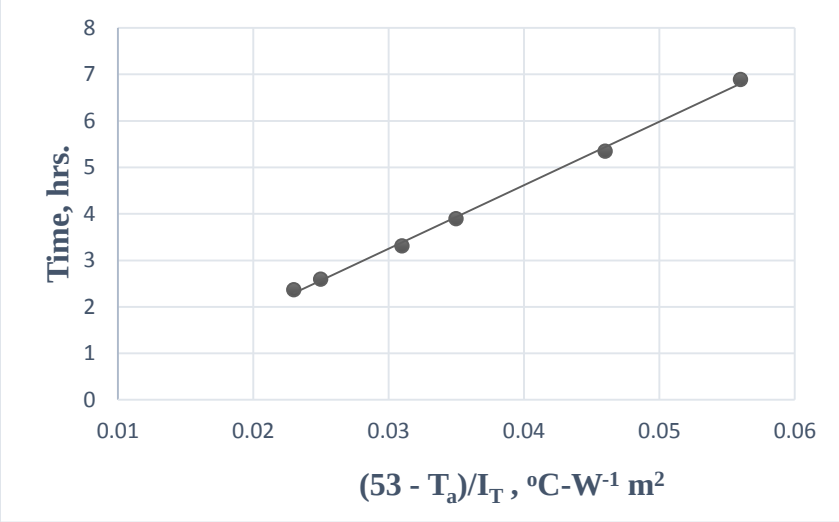

Fig. 5.17 Characteristic curve $\left(\textbf{Time vs.} \frac{53 - T_a}{I_T} \right) \left(\frac{°C}{W/m^2} \right)$

On any sunny day with average solar insolation of 600 W/m^2 – 800 W/m^2, it takes only 3-4 hrs. and even less for the system to attain its maximum temperature. The temperature then remains fairly constant. The unique feature of this design is its capability to prolong this temperature for longer hours even after dusk with zero insolation.

5.9 Water temperature preservation

To obtain its wider acceptability in the domestic sector, the need is to improve the water temperature rise during the daily operation and water temperature preservation during the night. With the introduction of an air gap, the system is capable of delivering hot water at an average temperature of 45^{o}C - 55^{o}C throughout the day. To obtain the heat storage capacity of the system, the temperature of outlet water just before dusk was recorded and the system was left alone under no drain off condition and with no shield or top cover. The next day, the temperature of water at 6:00 am was recorded. The same methodology was adopted in both cases i.e. with an air gap and without an air gap. It was found that in both the cases the average temperature difference between the inlet and outlet water temperature was between 10^{o}C - 12^{o}C. This is indicative of the fact that few hours after the dusk, the heat lost from the side walls increases as the temperature in the air gap starts decreasing, the mean temperature difference between the system and ambient increases and the air in the gap does not make any meaningful contribution to suppress heat loss. The system behaves more like that without an air gap. The heat preservation obtained was due to glass wool insulation provided at the sides and bottom of the collector. However, in northern India, the temperature drop of air during the night is relatively less and the system is capable of delivering reasonable hot water in the range of 28^{o}C - 30^{o}C early next morning.

The system efficiency is comparable to other systems despite the fact that nothing additional is provided to enhance the system performance like TIM, PCM etc. so as not to incur the high cost. On comparison with an ICS system with and without TIM (Chaurasia et al. [2001]), the system efficiency without TIM is 11.1 % and that with TIM 38.1 %. The system efficiency of this design also averages close to 38 %. Also, the maximum temperatures obtained are comparable to other systems in the range of 50^{o}C to 60^{o}C, but with this design, the temperatures attained are

prolonged for longer periods even with drop in solar insolation. The air in the gap attained a maximum temperature of 66^{o}C (averaging above 60^{o}C), whereas the ambient temperature hovered between 36^{o}C – 38^{o}C. Thus the air in the gap at the arms of CPC acts as a thermal barrier between the system and ambient which improves heat retention and suppresses heat loss.

5.10 Influence of mass flow rate on design parameters

As the mass flow rate increases, the heat losses to the surrounding decreases, which is reflected by an increase in the value of F_R. The maximum possible value of useful heat gain, $(q_u)_{max}$ occurs when the entire collector surface is at inlet fluid temperature, T_{fi} and in such a case the q_l heat losses to the surrounding are minimum. Then F_R can be expressed as

$$F_R = \frac{\dot{m}C_{pw}}{\pi D_o L U_l}\left[1 - \exp\left(-\frac{\pi D_o L U_l F'}{\dot{m}C_{pw}}\right)\right] \quad (5.10)$$

The values of F_R and flow factor F'' obtained for varying flow rates is shown in Table 5.5.

In this system the effect of reduced F_R is offset by the reduced mean fluid temperature due to the larger diameter of the drum. The collector flow factor $F'' = \frac{F_R}{F'}$ where F' is essentially a constant for a collector referred to as the collector efficiency factor. A plot of collector flow factor and $\frac{\dot{m}C_{pw}}{\pi D_o L U_l}$ is indicative of the collector capacitance rate and is a dimensionless collector parameter. High flow rates will make for a thermally efficient collector but may require a pump and larger diameter pipes. Flow rates at the low end may be attainable with a smaller pump and lower diameter pipe but will be less thermally efficient. This is very much true for active systems. However, since this collector operates on thermosyphon principle and with a larger diameter drum, pressures losses are less significant. The effect of mass flow rates is, therefore, less profound on

its performance as shown in Fig. 5.18, Page No. 103. For a mass flow rate of 600 l/min – 1000 l/min, the values of flow factor approaches close to unity.

Table. 5.5 Values of F_R and F'' for varying flow rates

Mass flow rate ml/min $\dot{m}$	Dimensionless collector capacitance $\frac{\dot{m}\, C_p}{A_c U_l F'}$	Heat Removal factor F_R	Flow factor F''
450	3.46	0.54	0.86
650	5.00	0.59	0.94
850	6.54	0.60	0.96
1050	8.07	0.61	0.97
1200	9.22	0.63	1

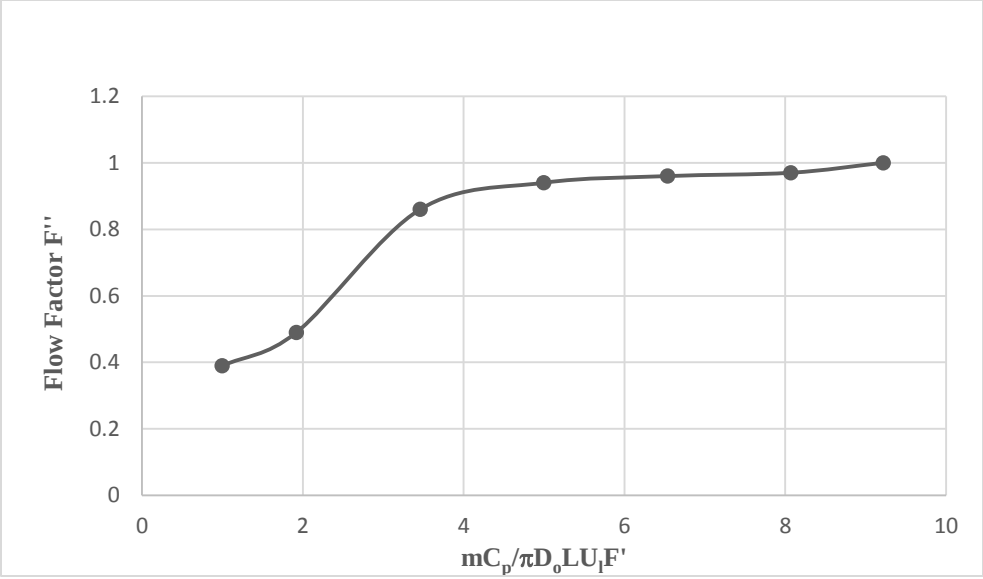

Fig. 5.18 Collector flow factorF''as a function of $\frac{\dot{m}C_p}{\pi D_o L U_i F'}$

A comparison with similar studies made on models, based on their collector efficiency is shown in Table 5.6. It is observed that the system efficiency of (SYS-4), the proposed model is comparable to that obtained with SYS-1 and SYS-2 (Souliotis et al. [2011]; higher than that obtained with SYS-3, Varghese et al. [2007]). The ICS vessel design of SYS 1 consists of two concentric stainless steel cylinders one within the other, the created annulus evacuated and partly filled with water. During daytime operation, the water evaporates and act as a thermal bridge during nighttime operation. In comparison, this modified design makes use of air as a thermal barrier. Initially, when the air in the gap is not heated up, heat losses are higher but as the day progresses and temperature in air gap increases and it acts as a thermal barrier between the drum and ambient air. The parametric study made on the model with and without air gap has shown that there is percentage reduction of heat loss from the side walls from 13.4% to 52.5 % as ΔT increases from 14^{o}C to 26^{o}C. Later the heat loss remains fairly constant. The side loss coefficient with air

gap averages about 1.41 W/m^2-K. The slight increase in efficiency seen in SYS-1 and SYS-2 is due to difference in the ratio of stored water volume to aperture area V_T/A_a. The V_T/A_a ratio of SYS-1 is 54.36 l/m^2 and that of SYS-4 is 99 l/m^2.

Table. 5.6 Comparison with similar model studies

System Nomenclature	System	Reference	Collector efficiency η_c
SYS 1	ICS with partial vacuum	Souliotis[2011]	0.394 - 1.814 ($\Delta T_m / I_T$)
SYS 2	ICS without partial vacuum	Souliotis[2011]	0.420 - 2.152 ($\Delta T_m / I_T$)
SYS 3	ICS without air gap	Varghese[2007]	0.28 - 1.59 ($\Delta T_m / I_T$)
SYS 4	ICS with air gap at arms of CPC	Present model	0.384 - 2.819($\Delta T_m / I_T$)

5.11 Influence of air gap on heat losses and outlet temperature using MLR statistical tool

The performance of the model is predicted for both summer and winter conditions. The tabulated readings for the month of April 2016 based on the average of three days readings and a total of 16 observations made in the month of March and April are shown in Tables 5.7, 5.8 (Table showing significant variables for MLR analysis) and 5.9 respectively (Page No. 106-107). From the summary output of the regression analysis, the R^2 value is 0.874 and adjusted R^2 is 0.811, which is indicative of a good fitness fit for the model. To postulate the performance in summer days, the summary output of 16 days observations inclusive of both months, March (beginning of the advent of summer in Delhi) and April is analyzed. Based on the F-significance level which has a value of 0.0041 in April and 0.0038 for the entire period, means at 95% confidence level, the model is statistically significant. Now from ANOVA table, (Page No. 110) if we look at the actual variables and their p-values (p-value < 0.05), it is seen that the variables effecting the output are, the temperature of air in the air gap and heat losses (although not much predominant). In other words, the model is able to predict outlet/delivery temperature as a function of the temperature of air in

the gap and heat losses. In summer, the solar insolation I_T becomes less significant once the system attains the steady state. The temperature rise of air in the gap serves as a thermal barrier between the system and surrounding, such that the reduced solar insolation after solar noon and even till late evening does not adversely affect the outlet temperature of water. It is also reflected by the low value of the coefficient for heat losses $U_l (T_d - T_a)$ in the ANOVA Table. The normal probability plot is linear (Fig. 5.19, 5.24), (Page No. 108, 111) and the residual plots (Fig. 5.21, 5.22, 5.26 & 5.27), (Page No. 109-112) for the temperature of the air gap and heat losses are scattered uniformly which means that relationship exists between the predictor and response variable.

However in winter, in the month of December, (Table 5.10, 5.11), Page No. 113 and from the output of ANOVA table it is seen that the significant variables are solar insolation and heat losses. It is indicative that in severe winter the air gap does not serve the purpose it is intended, necessitating the use of an auxiliary heater. But on combining with good sunny days of December and the month of October (Table 5.12), Page No.116, 16 observation results are tabulated and summary of the output obtained by MLR analysis. It is seen from ANOVA table, Page No. 117, the significant variables (p-value < 0.05%), are I_T and temperature of the air gap and as also seen in the normal probability plots and residual plots, shown in Fig's 5.28 to 5.34, Page No. 118, 119. It can thus be summed up that except for few days in the month of December and January in Delhi, this collector has good heat preservation capability. In winter, however, the influence of I_T becomes more significant in comparison to summer months.

Table 5.7 Tabulated Readings in the month of April 2016 with T_{fi} = 34◦C (based on average of three days readings.)

Time hrs.	T_{wo} ◦C	T_a ◦C	$(T_d)_{avg}$ ◦C	I_T W/m²	$U_l(T_d - T_a)$ W/m²	$(T_{air})_{gap}$ ◦C
9:00	40	33	41.5	825	76.5	44.75
10:00	44	36	47.5	1000	103.5	56.5
11:00	46	37	47.25	1114	92.25	58
12:00	48	37	50.25	1065	119.25	59
13:00	49	40.5	50.75	1050	92.25	60.25
14:00	47.5	39	48.5	895	85.5	56.25
15:00	50	41.5	45.75	870	38.25	55.75
16:00	50	41	46.25	765	47.25	54.75
17:00	48	39	44.25	288	47.25	51.25
17:30	46.5	39	44	280	45	51

Table 5.8 Output and Input variables for MLR analysis (Summer)

Time hrs.	T_{wo} ◦C	I_T W/m²	$U_l(T_d - T_a)$ W/m²	$(T_{air})_{gap}$ ◦C
9:00	40	825	76.5	44.75
10:00	44	1000	103.5	56.5
11:00	46	1114	92.25	58
12:00	48	1065	119.25	59
13:00	49	1050	92.25	60.25
14:00	47.5	895	85.5	56.25
15:00	50	870	38.25	55.75
16:00	50	765	47.25	54.75
17:00	48	288	47.25	51.25
17:30	46.5	280	45	51

Table 5.9 Tabulated Readings in the month of March 2016 with T_{fi}= 34◦C

Time hrs.	T_{wo} ◦C	T_a ◦C	$(T_d)_{avg}$ ◦C	I_T W/m²	$U_l(T_d - T_a)$ W/m²	$(T_{air})_{gap}$ ◦C
9:00	39	33	42	837	81	42.5
10:00	40.5	34	44.5	935	94.5	54.5
11:00	42.6	38	46.5	975	76.5	60.25
12:00	44	39	46.75	1040	69.75	62.5
13:00	44.6	40	47.75	990	69.75	64.5
14:00	45	38	46.75	850	78.75	62
15:00	45	36	47.25	630	101.25	61.75
16:00	44.3	32	45.25	318	119.25	55.5
17:00	44.3	31	44.5	218	121.5	52.75
17:15	44	31	43.5	125	112.5	47.25

SUMMARY OUTPUT of April 2016

Regression Statistics	
Multiple R	0.93
R Square	0.87
Adjusted R Square	0.81
Standard Error	1.32
Observations	10

ANOVA

	df	SS	MS	F	Significance F
Regression	3	72.91	24.30	13.90	0.0041
Residual	6	10.48	1.74		
Total	9	83.40			

	Coefficients	Standard error	t Stat	P-value
Intercept	15.35	5.80	2.64	0.038
X Variable 1 I_T W/m²	0.0022	0.0023	-0.92	0.389
X Variable 2 $U_l(T_d - T_a)$ W/m2	0.069	0.0228	-3.05	0.022
X Variable 3 $(T_{air})_{gap}$ ◦C	0.70	0.12	5.85	0.0010

RESIDUAL OUTPUT				PROBABILITY OUTPUT	
Observation	Predicted T_{wo}	Residuals	Standard Residuals	Percentile	T_{wo}
1	39.71	0.28	0.268	5	40
2	45.71	1.71	-1.58	15	44
3	47.30	1.30	-1.20	25	46
4	46.23	1.76	1.63	35	46.5
5	49.03	0.030	-0.027	45	47.5
6	47.02	0.47	0.43	55	48
7	50.02	-0.028	-0.026	65	48
8	48.92	1.07	0.99	75	49
9	47.51	0.48	0.44	85	50
10	47.51	1.01	-0.938	95	50

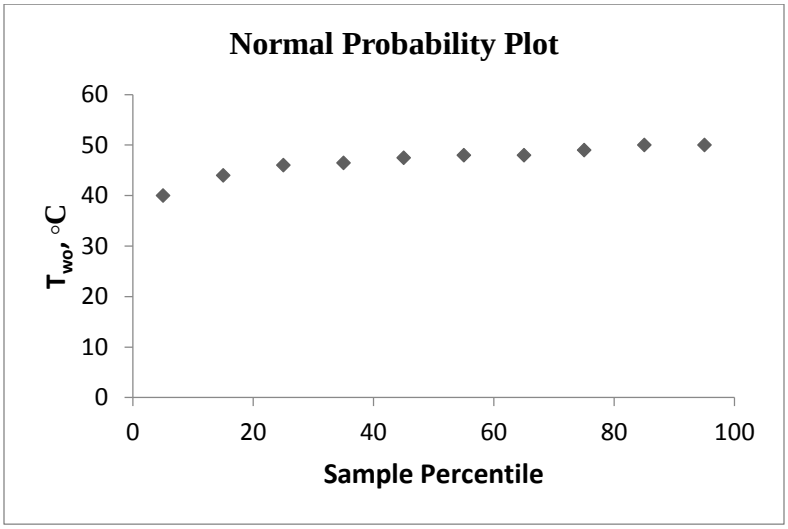

Fig. 5.19 Normal probability plot (April 2016)

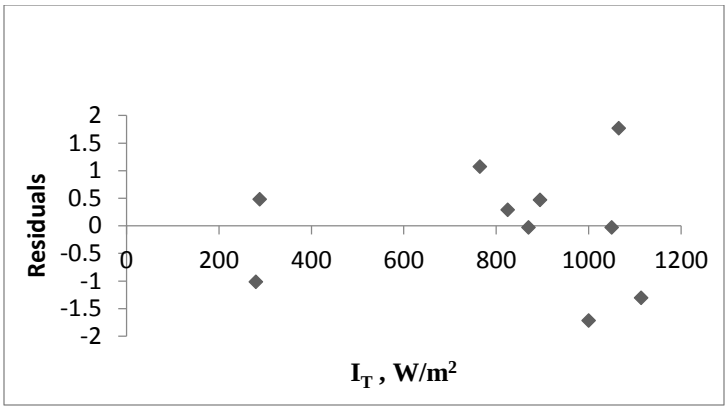

Fig 5.20 I_T Residual output (April 2016)

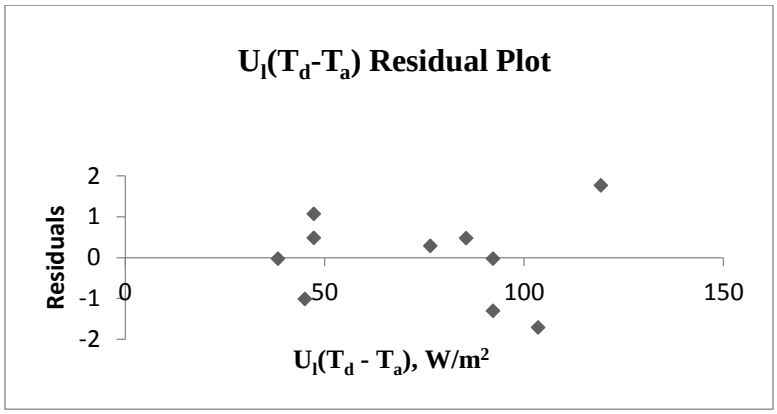

Fig 5.21 Heat loss Residual output (April 2016)

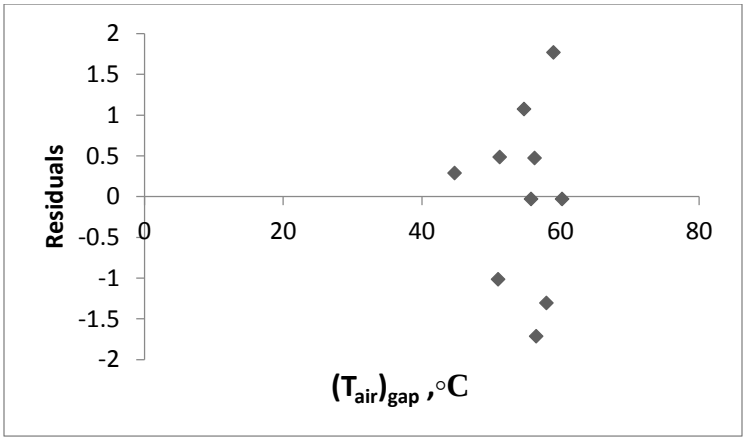

Fig 5.22 $(T_{air})_{gap}$ Residual output (April 2016)

Summary Output of 16 observations made in the months of March and April 2016

Regression Statistics	
Multiple R	0.81
R Square	0.65
Adjusted R Square	0.57
Standard Error	1.64
Observations	16

ANOVA

	df	*SS*	*MS*	*F*	*Significance F*
Regression	3	62.64	20.88	7.75	0.0038
Residual	12	32.29	2.69		
Total	15	94.93			

	Coefficients	*Standard Error*	*t Stat*	*P-value*
Intercept	22.62	5.751	3.93	0.0019
X Variable 1 $\mathbf{I_T}$ **in W/m²**	0.318	0.163	1.94	0.0751
X Variable 2 $\mathbf{U_l(T_d - T_a)}$ **in W**	-0.0035	0.0016	-2.16	0.0514
X Variable 3 $\mathbf{(T_{air})_{gap\ in}}$ **°C**	0.219	0.097	2.25	0.043

RESIDUAL OUTPUT				PROBABILITY OUTPUT	
Observation	Predicted T_{wo}	Residuals	Standard Residuals	Percentile	T_{wo}
1	42.75	-0.754	-0.51	3.125	42
2	46.62	-2.62	-1.79	9.375	42.5
3	46.47	-0.47	-0.32	15.625	43.5
4	47.82	0.17	0.12	21.875	44
5	48.30	0.69	0.47	28.125	46
6	47.26	0.23	0.16	34.375	46.5
7	48.83	-1.33	-0.90	40.625	46.5
8	48.08	-1.08	-0.74	46.875	47
9	41.45	1.04	0.70	53.125	47.5
10	44.86	-1.36	-0.93	59.375	47.5
11	47.64	-1.14	-0.78	65.625	48
12	48.43	0.56	0.38	71.875	48
13	47.95	2.04	1.39	78.125	49
14	46.67	3.32	2.26	84.375	49
15	46.94	1.05	0.71	90.625	50
16	46.84	-0.34	-0.23	96.875	50

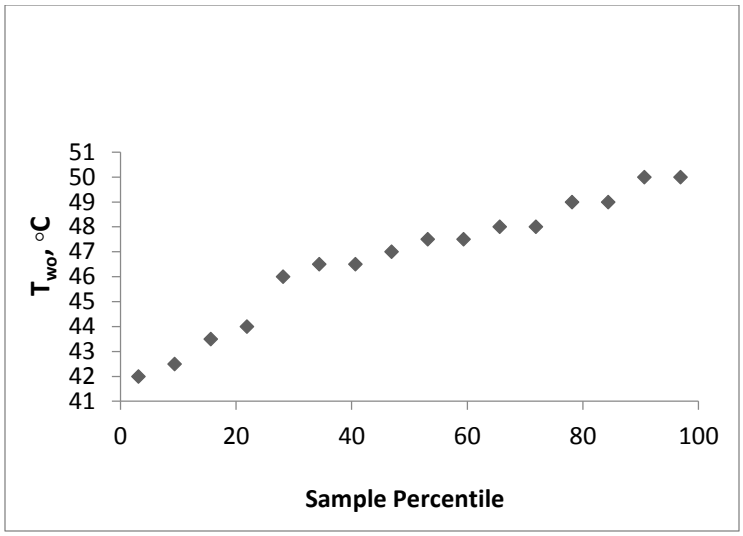

Fig 5.23 Normal probability plot

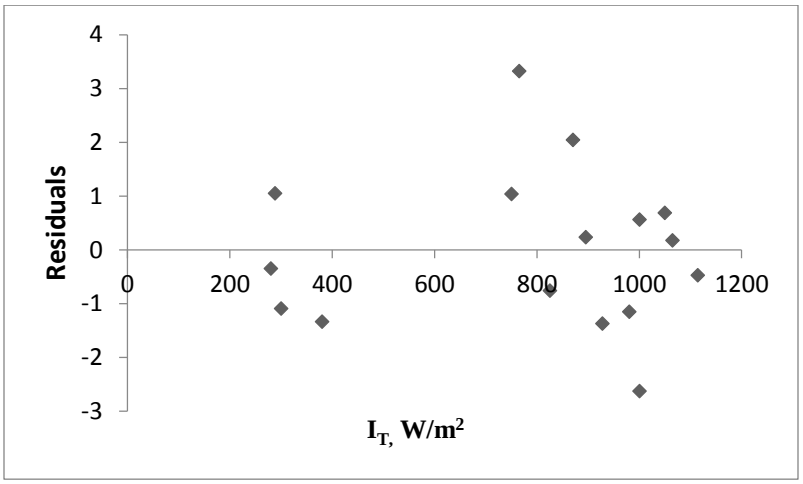

Fig 5.24 I_T Residual output

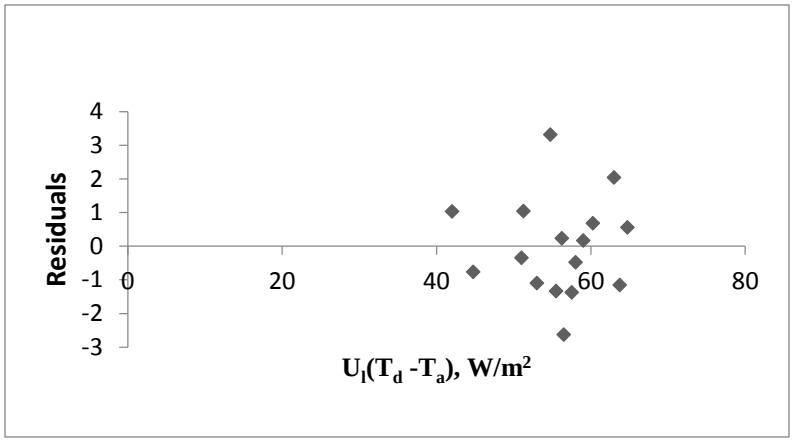

Fig 5.25 Heat loss Residual output

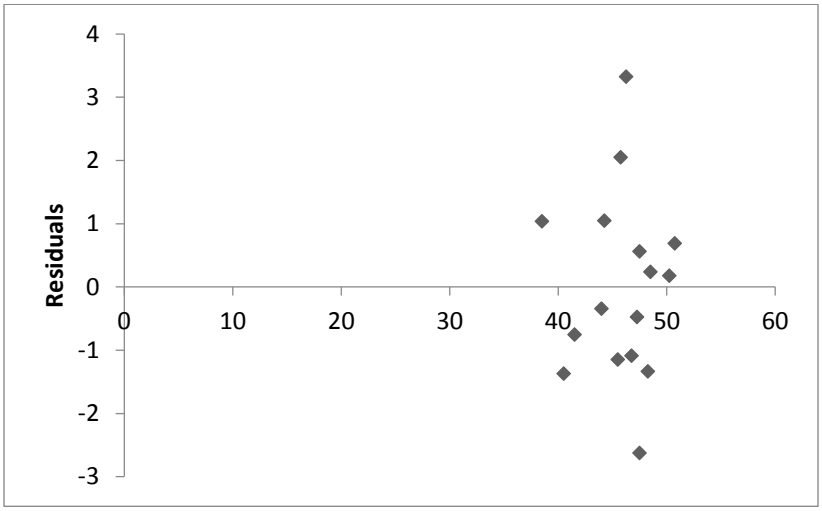

Fig 5.26 (T_{air}) $_{gap}$ Residual output, ◦C

Table 5.10 Tabulated readings during the month of December 2016 with $(T_{fi})_{avg} = 22^{\circ}C$ based on average three days readings

Time	T_{wo} ◦C	T_a ◦C	$(T_d)_{avg}$ ◦C	I_T W/m²	$U_l(T_d - T_a)$ W/m²	$(T_{air})_{gap}$ ◦C
10:00	24	18	33	552	180	39.5
11:00	29	20	34	824	168	44.5
12:00	33	21.5	34.75	864	159	46
13:00	37	23	35.75	891	153	46.5
14:00	37.5	24	41	882	204	50.5
15:00	40	24	43.25	688	231	49
16:00	41	23.5	43	314	234	44.5
17:00	39	21	42.5	108	258	40.5

Table 5.11 Output and Input variables for MLR analysis (Winter)

Time	T_{wo} ◦C	I_T W/m²	$U_l(T_d - T_a)$ W/m²	$(T_{air})_{gap}$ ◦C
10:00	24	552	283	39.5
11:00	29	824	342.5	44.5
12:00	33	864	390	46
13:00	37	891	437.5	46.5
14:00	37.5	882	443	50.5
15:00	40	688	472.5	49
16:00	41	314	484	44.5
17:00	39	108	459.5	40.5

SUMMARY OUTPUT during the month of December 2016

Regression Statistics	
Multiple R	0.999997
R Square	0.999994
Adjusted R Square	0.999990
Standard Error	0.018001
Observations	8

ANOVA

	df	*SS*	*MS*	*F*	*Significance F*
Regression	3	248.21	82.739	255321.44	5.11327E-11
Residual	4	0.00129	0.00032		
Total	7	248.21			

	Coefficients	*Standard Error*	*t Stat*	*P-value*
Intercept	0.058	0.135	0.429	0.68
I_T in W/m^2	-0.00019	6.63E-05	-2.912	0.043
Ul(T_d - T_a) in w	0.0843	0.00024	348.13	4.08E-10
(T_{air}) gap in ◦C	0.0049	0.0057	0.869	0.43

RESIDUAL OUTPUT

Observation	Predicted T_{wo}	Residuals	Standard Residuals
1	24.00	-0.0072	-0.531
2	28.99	0.0041	0.304
3	33.00	-0.00022	-0.0168
4	37.00	-0.0021	-0.157
5	37.48	0.0125	0.922
6	40.00	-0.00458	-0.336
7	41.02	-0.02405	-1.767
8	38.97	0.0215	1.584

PROBABILITY OUTPUT

Percentile	T_{wo}
6.25	24
18.75	29
31.25	33
43.75	37
56.25	37.5
68.75	39
81.25	40
93.75	41

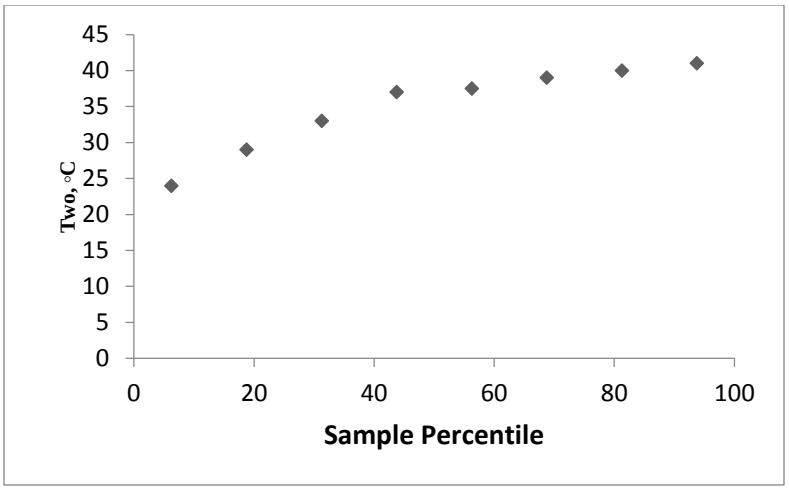

Fig 5.27 Normal probability plot (December 2016)

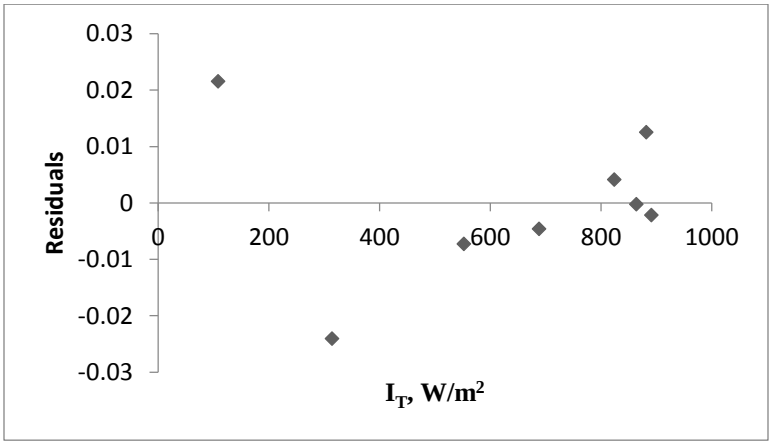

Fig 5.28 I_T Residual output (December 2016)

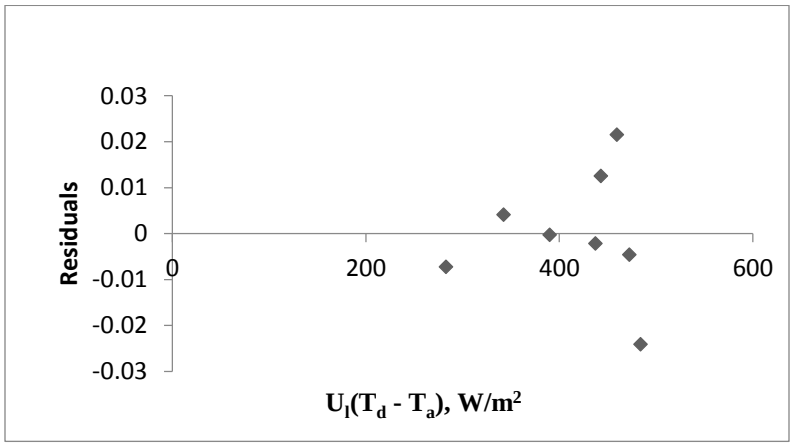

Fig 5.29 Heat loss Residual output (December 2016)

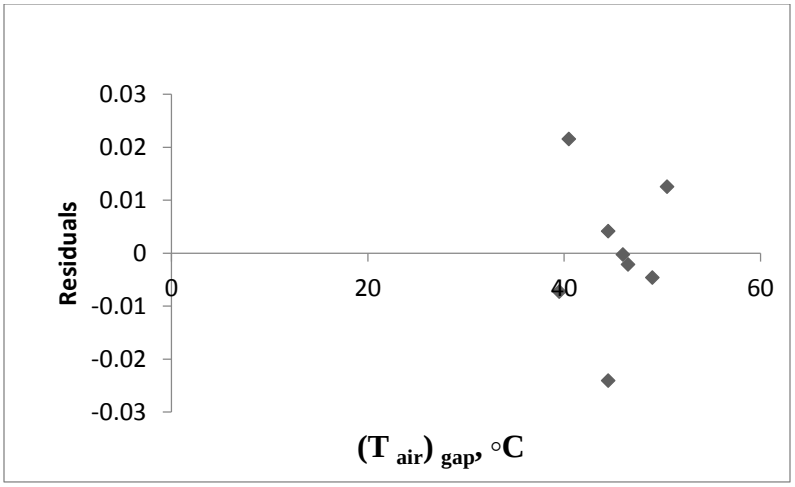

Fig 5.30 $(T_{air})_{gap}$ Residual output, ◦C

Table 5.12 Tabulated readings for the month of October 2106 with $(T_{fi})_{avg} = 32$◦C

Time hrs.	T_{wo} ◦C	T_a ◦C	(T_d)avg ◦C	I_T W/m²	$U_l(T_d - T_a)$ W	$(T_{air})_{gap}$ ◦C
10:00	33.25	32.5	36	861	31.5	41.75
11:00	34	32	40	969	72	46
12:00	34.5	33	41	1065	72	47.75
13:00	39.5	34	49	1061	135	47.75
14:00	42	36	53	942	153	51.5
15:00	42	35	51	760	144	50.75
16:00	41	34	50.5	456	148.5	45.25
17:00	38	34	47.5	119	121.5	42.75

SUMMARY OUTPUT of 16 observations in the months of October and December 2016

Regression Statistics	
Multiple R	0.841
R Square	0.707
Adjusted R Square	0.6346
Standard Error	3.0323
Observations	16

ANOVA

	df	*SS*	*MS*	*F*	*Significance F*
Regression	3	267.18	89.06	9.685	0.001582
Residual	12	110.34	9.195		
Total	15	377.52			

	Coefficients	*Standard Error*	*t Stat*	*P-value*
Intercept	-15.66	10.47	-1.495	0.160
I_T in W	-0.014	0.0038	-3.650	0.0033
$U_l(T_d - T_a)$ in ◦C	-0.0156	0.0160	-0.976	0.348
(T air) gap in ◦C	1.402	0.2711	5.17	0.00023

RESIDUAL OUTPUT				PROBABILITY OUTPUT	
Observation	Predicted T_{wo}	Residuals	Standard Residuals	Percentile	T_{wo}
1	30.23	3.01	1.11	3.12	24
2	34.03	-0.038	-0.014	9.37	29
3	35.137	-0.63	-0.23	15.62	33
4	35.96	3.53	1.30	21.87	33.25
5	40.86	1.13	0.41	28.12	34
6	44.97	-2.97	-1.09	34.37	34.5
	39.03	1.96	0.72	40.62	37
8	40.70	-2.70	-0.99	46.87	37.5
9	29.12	-5.12	-1.88	53.12	38
10	32.48	-3.48	-1.28	59.37	39
11	34.16	-1.16	-0.42	65.62	39.5
12	34.57	2.42	0.89	71.87	40
13	39.51	-2.01	-0.74	78.12	41
14	39.72	0.27	0.10	84.37	41
15	38.64	2.35	0.86	90.62	42
16	35.57	3.42	1.26	96.87	42

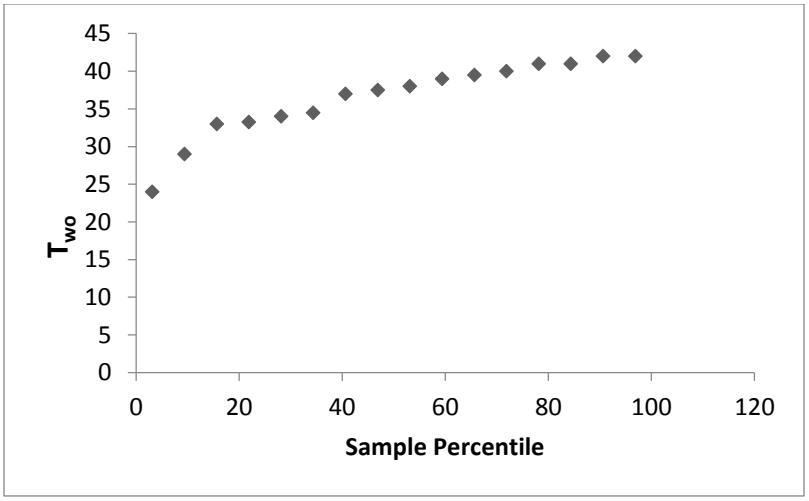

Fig 5.31 Normal probability plot (October and December 2016)

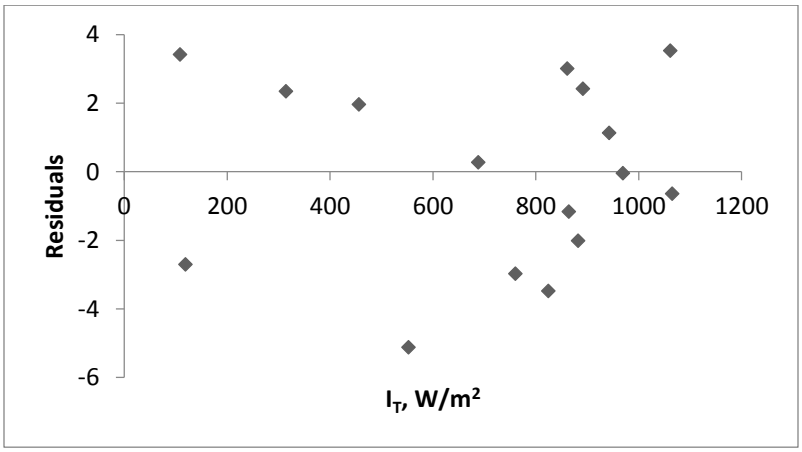

Fig 5.32 I_T Residual output

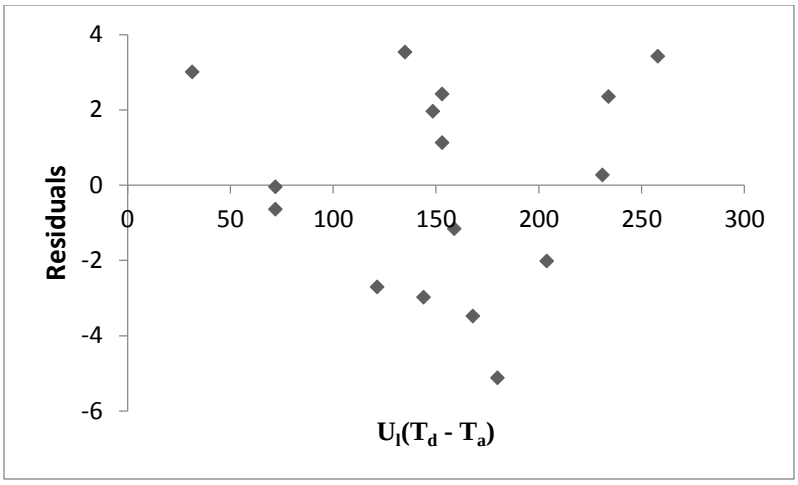

Fig 5.33 Heat loss Residual output

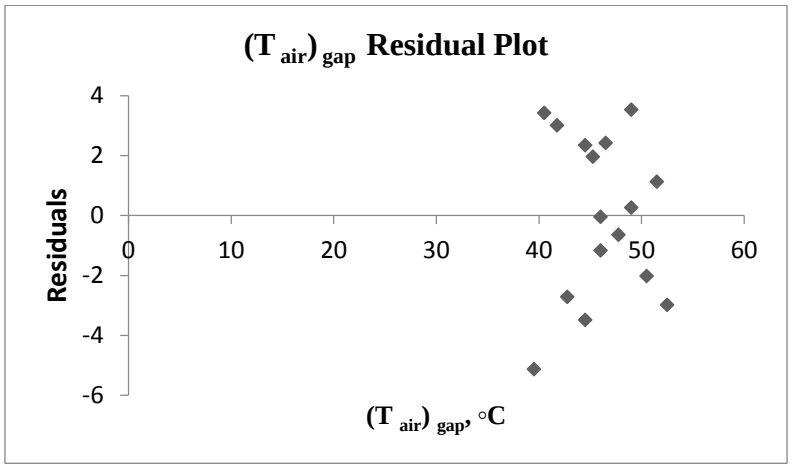

Fig 5.34 $(T_{air})_{gap}$ Residual output

5.12 Techno- economic analysis of the collector

Few countries bank on solar water heating systems (SWHS) to meet their domestic hot water needs, instead prefer to use fuel or electric/gas geysers. The reason being the former having relatively high initial investment and performance marred by poor maintenance and the latter having low initial cost. In this light, we need to compare the economic feasibility of a SWH system with the other alternatives. In almost all solar energy systems, the annual heat loads are met by combing solar and non-solar alternatives i.e. auxiliary or conventional energy source. The primary objective of the economic analysis is to determine the cost method which is optimal.

5.12.1 Economic criteria for analysis

Solar economics on this model has been computed by EES using the f-chart method which showed that the 55% of the annual thermal load can be obtained by solar in a household of a family of four with a normal consumption of 100 LPD. The f-chart method is a design method by Klien et al. [1976] with correlations in terms of dimensionless variables, which are the results of many numerical experiments and simulations which form a basis for further correlations. The collector is designed to meet the heating load of households of a family of four based on the normal consumption pattern shown in Table 5.13, Page No.121. The parametric study (Varghese et al.[2017]) done on the model by EES to compute the system design parameters like heat removal factor, flow factor, and collector capacitance rate is shown in Table 5.14, Page No. 121. These parameters obtained from collector test results, form the basis to develop the correlations between dimensionless variables (defined later) and f. (i.e. the fraction of the monthly loads supplemented by solar).

Table 5.13 Consumption Pattern(Delivery Temperature 40°C- 60 °C)

Details	100 LPD	200 LPD	300 LPD	500 LPD
No of persons	4–6	8–10	12–14	20–25
No of bathroom	2	3	4	7
No of panels	1	2	3	4
Electricity saved/month	120 units	240 units	360 units	600 units

Source: JNNSM (wwww.seci.co.in)

Table 5.14 Values of F_R and F'' for varying flow rates

Mass flow rate in ml/min $\dot{m}$	Dimensionless collector capacitance $\frac{\dot{m}\,C_p}{A_c U_l F'}$	Heat Removal Factor F'_R	Flow factor F''
450	3.46	0.54	0.86
650	5.00	0.59	0.94
850	6.54	0.60	0.96
1050	8.07	0.61	0.97
1200	9.22	0.63	1

5.12.2 Solar Economics

For obtaining the economics of solar gain, (Beckman et al. [1977]), gave the concept of solar savings, in terms of difference in the costs of energies (conventional and solar). It can be simply stated in equation form as:

Solar savings = costs of conventional energy – costs of solar energy

The cost of solar energy includes cost of installation of solar equipment and operating cost. Installation cost is the sum of two entities, one proportional to aperture or collector area and the other independent of area:

$$C_s = C_A A_c + C_E \qquad (5.11)$$

Where C_s = total cost of installed solar energy equipment

C_A = total area dependent cost in rupees

A_c = collector area in m^2

C_E = total cost of equipment which is independent of collector area in rupees

C_A includes all system components such as purchase and installation.

C_E includes costs independent of area such as transportation, construction and erection.

System running costs are which includes cost of auxiliary energy, (like auxiliary heater), operating pump and other axillaries if any.

The breakup cost of the model is shown in Table 5.15, Page No. 123.

Table 5.15 Costing of ICS solar water heater

Costing Breakdown	Component	Description	Total cost in Rupees
Material Cost	Wooden Cradle	2 full size (4'x 2')	4690/-
		Phenol bond Plywood	
	Reflector	Stainless steel(18 gauge)	6050/-
		mirror finish (1.4m x 1m)	
	Absorber cum storage	MS 304	4920/-
	Tank	(18 gauge)	
	Coating	Black Paint	600/-
		(Non-selective)	
	Insulation	Glass wool	860/-
		(25 Kg.)	
	Top cover	Glass	1120/-
		1.4 m x 0.72 m (2 No's)	
	Gaskets	Rubber	100/-
	Piping and Plumbing	PVC pipes, Inlet & outlet valve, Pr.	652/-
		gauge and relief valve	
	Support structure	C-beam channel structure steel	850/-
Assembly Cost	Wooden cradle	Carpentry work	1200/-
	Plumbing connections	Plumber work	800/-
	Platform and support for C - beam channel	Masonry work	800/-
Instrumentation	Thermocouples	J- Type (13 No's)	5785/-
	Selector switch with	L&T make	1600/-
	Digital display Rotameter	(2 No's) Borosilicate Glass body Range(0.5 - 1500 LPH)	850/-
	Aluminum Tape	1 Roll	225/-
Miscellaneous		Fevicol, nails, gloves,	150/-
		Transportation cost	900/-
		Total Cost	**32150/- ($ 535)#**

 # 1$ = Rs. 64 in the month of July'2017

In practice, the economic problem pertains to system size for a known load, with other parameters fixed with respect to the gross area of collector. Thus, given a system configuration and given load which is function of time throughout a year, the primary design variable is the collector area. The economic figures of merit for the model is postulated by the f-chart method. This method is based on the outcome of numerous thermal simulations to evolve the factor f as a function of two dimensionless variables. The two dimensionless groups are

$$X = \frac{A_c F_R' U_l (T_{ref} - \overline{T}_a)\Delta t}{L} \quad \text{i.e. ratio} \quad \left(\frac{\text{Collector losses}}{\text{Heating Loads}}\right) \tag{5.12}$$

$$Y = \frac{A_c F_R' (\overline{\tau\alpha}) \overline{H}_T N}{L} \quad \text{i.e. ratio} \quad \left(\frac{\text{Absorbed solar radiation}}{\text{Heating Loads}}\right) \tag{5.13}$$

where $A_c -$ Collector area in m^2

$F_R' -$ Heat removal factor

$U_l -$ Collector overall loss coeffient in W/m^2 = 9.2 W/m^2-k, Varghese [2017]

$T_{ref} -$ Reference temperature (60^oC in our case)

$\overline{T}_a -$ Monthly average ambient temperature

$\Delta t -$ Total number of seconds per month

$\overline{\tau\alpha} -$ Monthly average transmittance – absorptance product

$\overline{H}_T -$ Monthly average daily radiation incident on collector surface per unit area in J/m^2

$N -$ Days in month

L– Monthly heating load in GJ

$F'_R U_l$ and $F'_R(\overline{\tau\alpha})$ as obtained from collector test results.

The annual fraction SF= $\frac{\sum f_i L_i}{\sum L_i}$ (5.14)

is obtained by repetition of X, Y and f calculation for each month and then getting the summation for the year.

The annual solar fraction as computed by EES (Klein [2008]) is shown in Table 5.16, Page No. 126. The heating load may vary marginally during peak summer and winter, but assumed constant throughout the year. Monthly variance may lead to higher solar fraction than computed.

Table 5.16 Annual performance of the ICS system at Delhi

Month	$\overline{H}_T$ MJ/m^2	$\overline{T}_a$ ^{o}C	L GJ	X	Y	f	fL GJ
January	14.30	14.3	0.38	1.418	0.5188	0.3796	0.14
February	18.00	16.8	0.38	1.319	0.6522	0.4849	0.18
March	21.96	29.2	0.38	0.8264	0.7956	0.6122	0.23
April	24.96	36	0.38	0.5563	0.9043	0.6962	0.26
May	26.32	39.8	0.38	0.4053	0.9503	0.7324	0.28
June	23.55	38.2	0.38	0.4688	0.8532	0.6709	0.25
July	19.20	34.7	0.38	0.6079	0.6956	0.5591	0.21
August	18.20	33.6	0.38	0.6516	0.659	0.5308	0.20
September	20.16	34.2	0.38	0.6278	0.7304	0.5816	0.22
October	19.20	33	0.38	0.6755	0.6956	0.5549	0.21
November	16.20	28.3	0.38	0.8622	0.5869	0.4653	0.18
December	13.80	22.9	0.38	1.077	0.5	0.3856	0.15
			4.56				**2.53**

Annual solar fraction SF= $\frac{fL}{L} = 0.55$

For computation of solar savings calculation, the total installation cost is exclusive of the instrumentation cost, as it is restricted to experimental test rig only. The total cost of installation rounded off to Rs.23700/- ($ 395) which includes material cost, assembly cost and transportation, as that obtained from equation (5.11), the collector area being 1.008 m^2. To obtain the economic collector size and the annual load fraction corresponding to different storage capacities, X calculated for a capacity of 100 litres must employ the storage size correction factor $\frac{X_c}{X} = \left(\frac{\text{actual stoarge capacity}}{\text{standard storage capacity}}\right)^{0.25}$ and accordingly the value of $\frac{X_c}{X}$ varies as 2, 3, 4, and 5 respectively. The annual load fraction vs collector area computed by EES is shown in Fig. 5.35.

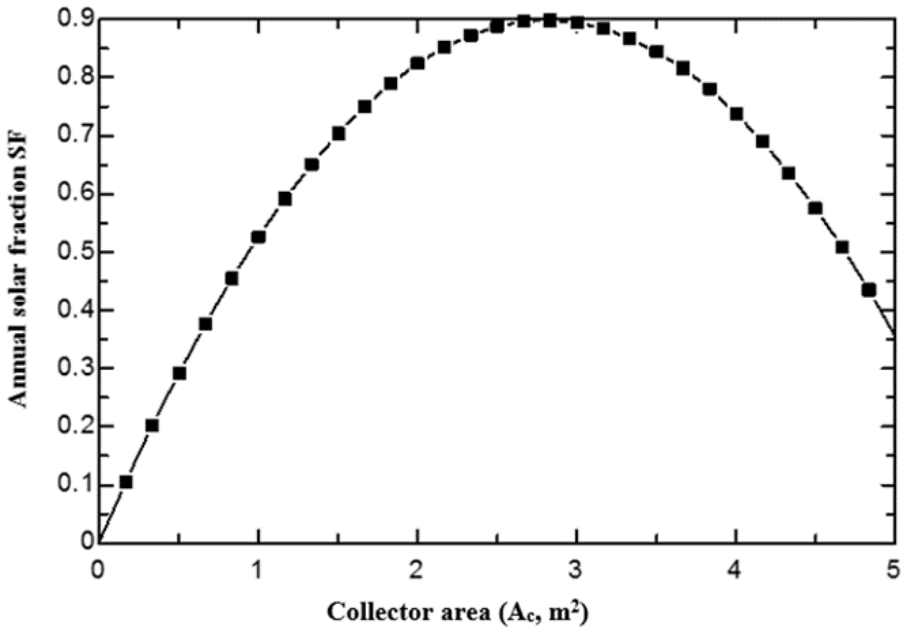

Fig. 5.35 Annual solar fraction vs. collector area

The annual solar savings calculated in terms of energy units is shown in Table.5.17 and the payback period is 2 years and 7 months for the collector. The (Heat load) $_{non\text{-}solar}$ calculation is based on the energy consumption of the commonly used heating appliance in households, an electric geyser. 100 litres water for a temperature rise of 30^{o}C requires 12.6 MJ of heat equivalent to 3.5 KWh. A 1000W geyser would thus consume 4 units of energy per day assuming conversion efficiency of heater as 90% and for a BEE star rating geyser with PUF insulation, the average standing losses is 0.2 - 0.3 kWh per day and operate 3.5 hrs. per day to attain 12.6 MJ of heat. To compute solar savings in Rupees, the unit charge is Rs.4/kWh, as per billing charges for (0 – 200 units) per month.

$$(\text{Heat Load})_{non\text{-}solar} = [(\text{Energy consumption} * \text{hrs. of operation per day})] * 365 \text{ days} \quad (5.15)$$

$$(\text{Heat Load})_{solar} = SF*[\text{Annual heating load in KWh}] \quad (5.16)$$

Table 5.17 Payback period calculations

Collector Area m^2	*SF*	Installation cost in Rs.	(Heat Load)$_{non\text{-}solar}$ kWh	(Heat Load)$_{solar}$ kWh	Solar Savings		Payback Period in Years
					kWh	Rs.	
1	0.55	23700	5110	2810	2300	9200	2 yrs. 7 month
2	0.82	47400	10200	8364	1836	7344	6 yrs. 01 month
3	0.89	71100	15300	13617	1683	6732	10 yrs. 02 months

It is observed that, (from Fig.5.35), although the maximum value of solar fraction is for 3m^2 collector area, but the payback period is 10 years. Taking this factor into account, with this type

of design, the optimum collector size suits is $1m^2$ to $2m^2$, which also matches with the consumption pattern of a medium sized household.

5.12.3 Life cycle cost (net present worth) LCC

Life cycle cost computation has been done using Excel NPV function and represented on excel spreadsheet as shown in Table 5.18, Page No. 131. The cost incurred has been categorized under two heads, the acquisition cost, and operational cost. The acquisition cost includes cost of installation and operational cost which includes the cost of auxiliary energy and cost incurred for good up keeping. The other negative cash flows like incremental costs on interest on payment, insurance, property tax, mortgage payment etc. are not within the scope of this analysis. The positive cash flows are the energy savings by solar over the life cycle period of 15 years. An (LCC) analysis includes inflation when estimating future expenses and that expected future costs are brought back to the present worth (cost) discounted by calculating postulated investments at a market discount rate so as to have funds available when needed.

It can be better understood as the difference between the LCC of a $(\text{Fuel system})_{\text{conventional}} - (\text{solar system})_{\text{solar+auxillary system}}$

Estimated annual cost of auxiliary heater = (365*3.5 kWh/day) / (SEF * Unit cost of electricity)

For this collector unit, solar energy factor (SEF) is 1.22. The ICS SWH, do not need significant maintenance requirements. Occasional leakages in the plumbing could be easily repaired by common plumbers. In case quality of water is hard, scale deposition in the collector may result over the years. This may require de-scaling with acids. But in this design, because of the larger diameter of the drum, compared to small size tubes in conventional SWH's, quality of water and scaling is not an issue of major concern. This is a major added advantage of the model. The

drum/storage tank is housed in the wooden cradle, there is no need to paint the outside exposed surface. The drum which serves the dual role of storage and absorber, the painting may have to be redone every 2-3 years. For computation of the total present worth of solar savings, it is postulated that (based on previous data), that the electricity cost may inflate by 6% in five years, 8% in next five years and 10% the remaining next five years and market discount rate at 8%.

At the Nth period, the cost is P $(1+i)^{N-1}$ and the present worth of the N^{th} cost is

$$PW_N = \frac{P(1+i)^{N-1}}{(1+d)^N} \tag{5.17}$$

Where P is the payments made at the end of each period, i the inflation rate and d is the market discount rate.

Sample Calculation (From excel spread sheet)

		KWH			
$(\text{Heat load})_{\text{non-solar}}$		5110			
(Heat load)solar		2810	SF*(Annual heating load)=0.55(5110)		
Energy savings		2300	x Rs.4/-	unit charge upto 200 units	
			9200/-	which will vary as per	
Cost of auxillary	Rupees	-230	**8970/-**	inflation rate.	

Table 5.18 Net present worth calculations

Year	Negative cash flows	Amount	Positive cash flows	Amount	Net present worth
		in Rupees		in Rupees	of solar savings in Rs.
0	Installation	-23700.00	Energy savings	-23700.00	-23700
1	Added cost of auxiliary Energy	-230.00		8970.00	8306
2		-230.00		8740.00	7943
3		-230.00		8510.00	7590
4		-230.00		8280.00	7249
5	Added cost of maintenance	-1830.00		6450.00	5542
6		-244.00		6206.00	5746
7		-244.00		5962.00	5520
8		-244.00		5718.00	5294
9		-244.00		5474.00	5069
10	Added cost of maintenance	-2644.00		2830.00	2620
11		-264.00		2566.00	2854
12		-264.00		2302.00	2608
13		-264.00		2038.00	2352
14		-264.00		1774.00	2085
15	Added cost of maintenance	-3264.00		-1490.00	-1784
16		**Total present worth of solar savings**			**45295**

The annual solar fraction for the model is 0.55 and the payback period is two years. It may be noted that the PW('Present Worth') decrease when i < d and increase when i > d. NPV is positive till 14 years and the negative value from the 15^{th} year is indicative that system has to be replaced after 14 years as the returns will not be worth the investment. The total NPV value of Rs.45295/- promises good return, which means it is more lucrative to install this collector unit for households.

CHAPTER 6.0

CONCLUSIONS AND SCOPE FOR FUTURE WORK

6.1 Conclusions

The solar heating system of this type defers to active flat plate collector (FPC) systems which are commonly employed for domestic applications both in design and operation. The FPC's are normally fixed in position and do not track the sun. To obtain maximum incidence of the solar radiation it has a larger surface area but with the large surface area, about 30% - 50 % heat losses also occur and mainly the convective and radiative losses from the front face of the collector. To obtain higher collection efficiency one can opt for concentrating collectors as it increases the solar intensity by concentrating the energy available over a large surface onto a smaller surface (absorber) in this case.

The present design is a batch solar water heater in principle but incorporated with a CPC reflector and with an air gap introduced at the arms of the CPC so as to suppress the heat loss from the side walls of the solar water heater. Due to the concentration on a smaller area, the heat loss area is reduced. Further, the thermal mass is much smaller than that of an FPC and hence transient effects are small. The solar water heater is a simple passive system with a single storage cum absorber unit housed in a thermally insulated wooden cradle with CPC reflector. It is, therefore, less expensive and also has less installation and maintenance cost.

Because of the use of a single larger diameter drum unlike a number of small tubes in conventional solar heating systems, this system as a whole operates at a lower temperature which reduces the overall convective and radiative losses and results in an increase in useful heat gain. The additional problems of freezing and scaling in tubes are eliminated in the present design. This system does not require tracking owing to its large acceptance angle which makes it a hassle-free operating system. The annual solar fraction for the model is 0.55 and the payback period is two years.

The parametric study conducted on the model and comparative study with a similar model but without air gap has revealed that there is an improvement in the collection efficiency. The maximum temperature difference of water obtained with an air gap is 29^{o} C and that obtained without air gap is 14^{o} C and average percentage increase in collector efficiency is 24.6% (on condition of no withdrawal) with an air gap introduced on the side walls of the CPC. The effect of mass flow rate on outlet temperature is less profound when compared to ICS's with plane surfaces and even with extended storage units. Thus this model is an amicable alternative to conventional flat plate/ evacuated collectors as it cuts down the cost of a separate storage tank and working on thermos-syphon principle also eliminates the cost of other auxiliaries. As the delivery temperatures being high, a thermodynamic match between temperature level and the task occurs. The side loss coefficient with air gap averages the value about 1.41 W/m^2-K. Also, the effect of mass flow rate is less profound and for households, with normal consumption pattern, this system is capable of providing hot water with average temperatures ranging from 45^{o}C to 55^{o}C after solar noon on good sunny days and even late evenings. The heat preservation of the system is significant with 8^{o}C to 10^{o}C temperature difference of water with ambient obtained early morning, even in the winter season on any day with good sunshine hours.

On the life cycle environmental impacts of the two types of solar thermal systems used for domestic water heating, the flat plate and evacuated tube collectors, suggests higher environmental impacts due to the greater energy consumption for the production of these systems. Manufacturing is the main contributor which accounts for (60%) to the environmental impacts.
In comparison, this low cost integral solar water heater is simple in design and can be built with a minimum of carpentry and plumbing work. The total NPV value of Rs.44701/- promises good return, which means it is more lucrative to install this collector unit for households.

6.2 Major outcome of the work

The novelty in the design is the use of concentrator for the domestic solar water heater. A compound parabolic concentrator (CPC) is used in this setup to improve the optical efficiency. Another key feature of this system is that, the longer periods of heat retention is achieved by incorporating an air gap at the arms of the CPC, unlike most commonly used methods of using TIM and PCM, which also increases the cost. The detailed studies have established that the air in the gap acts not as a thermal barrier alone, but the temperature of air increases as the day progresses. This reduces the temperature gradient between system and surrounding, and the system is capable of delivering hot water even after dusk with reasonable hot water available the next morning also. In other words, the air in the gap also serves as a thermal storage. It is observed that there is significant improvement in system parameters compared to conventional FPC system employed for households. A comparison of the collector parameters of the present model is made with the conventionally used flat plate collectors for households as shown in Table 6.1. The key system parameters compared to FPC are indicative of the improved performance of the system.

Table 6.1 Comparison of present model with FPC - SWH

Collector Parameters	ICS-SWH Present model	FPC - SWH Singh.R[2016]
Temperature difference across the collector surface in ^oC	8 - 15	2 - 10
Instantaneous efficiency η_{is} in %	0.34 - 0.40	0.21 - 0.35
Heat Removal Factor F_R	0.59 - 0.63	0.52 - 0.58
Collector Efficiency Factor F'	0.62	0.66
Overall heat loss coefficient W/m^2-^oC	9.20 - 9.80	6.90 - 7.50

The cost of FPC system as offered by National Bank for Agriculture and Rural Development (NABARD) for 100 LPD capacity is Rs.22000/- and for a 200 LPD capacity is Rs.42000/- (Source: www.solarwaterheater.gov.in.). A majority of the households owning SWH fall under the rich and striver categories as per affluence layers distribution based on household income (Veeraboina and Ratnam [2012]; Chandrashekar and Kandpal [2004]). The target population should be the middle class which still strive on the use of electric geysers, the most common water-heating device in the households. An estimated cost for this model could be much lower than Rs. 20000/- if manufactured in bulk.

For a 100 litres capacity tank the FPC requires $2m^2$ collector area, whereas for this collector with the same capacity the aperture area is $1m^2$ only. The active FPC system also requires pump and other auxiliaries, in addition to a separate well-insulated storage tank, unlike this ICS system. The present system, thus, occupies less space and being a passive system is environment-friendly. The added advantage of using CPC reflector is that it is capable of capturing diffuse radiation. 25% – 30% of the total radiation is diffused component and this collector is capable to trap even diffused component of radiation. This means that even in cloudy weather the system is capable to deliver hot water. With wider acceptance angle and with a reasonably good concentration ratio between 2 to 3, system efficiency close to 40% which is sufficient to meet the requirement of hot water for household purposes. In short, the present system is compact, cost-effective, aesthetically attractive, can be easily integrated with building design and environment-friendly.

6.3 Scope for future work

- Good thermal heat retention, to suppress nocturnal heat loss are an increasingly important entity in BSWH systems. To suppress the nocturnal heat loss conventional techniques can be used but the results can be more encouraging if, in addition to these conventional

techniques, the thermal inertia of the collector can be increased. The application of the concept of thermal mass in the design is thus proposed. Thermal mass is a concept used in building design that provides inertia against temperature fluctuations. This concept can be introduced in such heaters by the use of Insulated Concrete Form (ICF) that can be placed as extended surfaces on the exterior of the drum, thereby increasing the thermal capacity.

- To make the system more compact, the CPC can be truncated, reducing its height (h) which also results in saving in reflector area. However, truncation does change the 'height-to-aperture' $\left(\frac{h}{A_a}\right)$ ratio, the 'concentration ratio', C and the average number of reflections reaching the absorber surface, although within limits truncation does not affect the acceptance angle. Thus studies need to be carried out to analyse the effects of truncation of CPC as a function of concentration ratio C and half acceptance angle θ_c, by obtaining plots of height-aperture ratio vs concentration ratio, reflector area-aperture area ratio vs concentration ratio and the average number of reflections to concentration ratio.
- System may be made in a more packaged form for better commercial acceptance and adaptability by the end users.

REFERENCES

1. Abdul Jabbar Khalifa, N., Kadhim Suffe, H., Mahmoud Sh. Mahmoud, 2013. A Storage domestic solar hot water system with a back layer of phase change material. Experimental Thermal and Fluid Science, 44, 174-81.

2. Allen, S. R., Hammond, G. P., Harajli, H. A., McManus, M. C., Winnett, A. B., 2010. Integrated appraisal of a solar hot water system. Energy, 35, 1351-1362.

3. Asif, M., Muneer, T., 2006. Life cycle assessment of built-in-storage solar water heaters in Pakistan. Building Service Engineering Research and Technology, 27, 63-69.

4. Abedin A. H., Marc Rosen, A., 2011. A Critical Review of Thermochemical Energy Storage Systems. The Open Renewable Energy Journal, 4, 42-46.

5. Abunabbi, J. R., Loveday, D. L., 2002. TRNSY model of a thermosyphon solar domestic water heater with a horizontal store and mantle heat exchanger. Solar Energy, 72, 89-98.

6. Akuffo, F. Jackson, E., 1988. Simulation studies on a compact solar water heater in the tropics. Solar & Wind Technology, 5, 229-237.

7. Alvarez, A., Tarrio-Saavedra, J., Zaragoza, S., Lopez-Beceiro, J., Artiaga, R., Naya, S., Alvarez, B., 2016. Numerical and experimental study of a corrugated thermal collector. Case Stud. Therm. Eng., 8, 41-50.

8. Ardente, F., Beccali, G., Cellura, M., Lo Brano, V., 2005. Life cycle assessment of a solar thermal collector. Renewable Energy, 30, 1031-1054.

9. Atul Jadhav, S., Ajit Kumar Gundekar, P., Ramchandra, Jyeshraj Joshi, 2013. Performance analysis of a novel cost effective CPC system. Energy Conversion and Management, 66, 56-65.

10. Barley, C. D., Winn, C. B., 1978. Optimal sizing of solar collectors by the method of relative areas. Solar Energy, 21, 279-283.

11. Beckman, W. A., Klein, S. A., Duffie, J. A., 1977. Solar heating design by f-chart method. Wiley-Interscience, New York.

12. Bliss, R. W., 1959. The derivations of several "Plate-efficiency factors" useful in the design of flat-plate solar heat collectors. Solar Energy, 3, 55-64.

13. Boy, E., Boss, R., Lutz, M., 1987. A collector storage module withy integrated phase change material. In: Proceeding ISES.

14. Braun, J. E., Klein, S. A., Pearson, K. A., 1983. An improved design method for solar water heating systems. Solar Energy, 31, 597-604.

15. Braun, M. R., Altan, H., Beck, S. B. M., 2014. Using regression analysis to predict the future energy consumption of a supermarket in the UK. Applied Energy, 130, 305-313.

16. Buckles, W. E., Klein, S. A., 1980. Analysis of solar domestic hot water heaters. Solar Energy, 25, 417-424.

17. Buker, M. R. S., 2015. Building integrated solar thermal collectors-A review. Renewable and Sustainable Energy Reviews, 51, 327–346.

18. Cabeza, L., Castell, A., Barreneche, C., De Gracia, A. F. A., 2011. Materials used as PCM in thermal energy storage in buildings: A review. Renewable and Sustainable Energy Reviews, 15, 1675-1695.

19. Carrillo Andres, A., Cejudo Lopez, J. M., 2002. TRNSYS model of a thermosiphon solar domestic water heater with a horizontal store and mantle heat exchanger. Solar Energy, 72, 89–98.

20. Castro, C. D., Mediavilla, M., Miguel, L. J., Frechoso, F., 2013. Global solar electric potential: a review of their technical and sustainable limits. Renewable and Sustainable Energy Reviews, 28, 824-835 `

21. Chaabane, M., Mhiri, Bournot, P., 2014. Thermal performance of an integrated collector storage solar water heater (ICSSWH) with phase change materials (PCM). Energy Conversion and Management, 78, 897-903.

22. Chandrasekar, B., Kandpal. T., 2004. Techno-economic evaluation of domestic solar water heating systems in India. Renewable Energy, 29, 319-332.

23. Chauhan, R., Kadambi, V., 1976. Performance of a collector-cum-storage type of solar water heater. Solar Energy, 18, 327-335.

24. Chaurasia, P. B. L., Twidell, J., 2001. Collector cum storage solar water heaters with and without transparent insulation material. Solar Energy, 70, 403-416.

25. Chinnappa, J., Gnanalingam, K., 1973. Performance at Colombo, Ceylon, of a pressurised solar water heater of the combined collector and storage type. Solar Energy, 15, 195-204.

26. Chen, Z., Gu, M., Peng, D., 2010. Heat transfer performance analysis of a solar flat-plate collector with an integrated metal foam porous structure filled with paraffin. Applied Thermal Engineering, 30, 1967-1973.

27. Cobble, M. H., 1964. Irradiation into transparent solids and the thermal trap effect. Journal of Franklin Institute, 278, 383-394.

28. Cobble, M. H., Fang, P.C., Lumsadine, E., 1966.Verification of the theory of the thermal trap. Journal of Franklin Institute, 282, 102-107.

29. Colangelo, G., Favale, E., Miglietta, P., De Risi, A., 2016. Innovation in flat solar thermal collectors: A review of the last ten years experimental results. Renewable and Sustainable Energy Reviews, 57, 1141-1159.

30. Cooper, P. I., Duckle, R.V., 1981. A non-linear flat plate collector model. Solar Energy, 20, 133-140.

31. Cruz, J. M. S., Hammond, G. P., Reis, A. J. P. S., 2002. Thermal performance of a trapezoidal-shaped solar collector/energy store. Applied Energy, 73, 195-212.

32. Devanarayanan, K., Kalidasa Murugavel, K., 2014. Integrated collector storage solar water heater with compound parabolic concentrator - Development and progress. Renewable and Sustainable Energy Reviews, 39, 51-64.

33. De Beijer, H. A., 1998. Product development in solar water heating. In: 5th World Renewable Energy Congress, Florence.

34. Diakoulaki, D., Zervos, A., Sarafidis, J. M. S., 2001. Cost benefit analysis for solar water heating systems. Energy Conversion and Management, 42, 1727-1739.

35. Dincer, I., Rosen, M., 2011. Thermal energy storage. Systems and applications. Ed. Wiley, Second Eddution, New York.

36. Duffie, J., Beckman, W., 2006. Solar Engineering of Thermal Processes, John Wiley & Sons, 3rd edition, New York.

37. Ecevit, A., Al-Shaiah, A. M., Apodin, E. D., 1989. Triangular built-in-storage solar water heater. Solar Energy, 42, 253-265.

38. Eisenmann, W., Vajen, K., Ackermann, H., 2004. On the correlations between collector efficiency factor and material content of parallel flow flat-plate solar collectors. Solar Energy, 76, 381-387.

39. Evarts, J. C., Swan, L. G., 2013. Domestic hot water consumption estimates for solar thermal system sizing. Energy and Buildings, 58, 58-65.

40. Faiman, D., Hazan, H., Laufer, I., 2001. Reducing the heat loss at night from solar water heaters of the integrated collector-storage variety. Solar Energy, 71, 87-93.

41. Fanney, A. H., Klein, S.A., 1983. Performance of solar domestic hot water systems at the National Bureau of Standards – measurements and predictions. ASME Solar Energy Engineering 105, 311-321.

42. Farghally, H. M., Ahmed, N. M., 2014. Design and sensitivity analysis of photovoltaic/thermal solar collector. World academy of Science, Engineering and Technology, 18, 730-737.

43. Furundzic, A. K., Kosoric, V., Golic, K., 2012. Potential for reduction of CO2 emissions by integration of solar water heating systems on student dormitories through building refurbishment. Sustain. Cities Soc., 2, 50-62.

44. Garg, H. P., 1975. Year round performance studies on a built-in storage type solar water heater at Jodhpur, India. Solar Energy, 17, 167-172.

45. Garg H, Rani, U., 1982. Theoretical and experimental studies on collector/storage type solar water heater. Solar Energy, 29, 467-478.

46. Garnier, C., Currie, J., Muneer, T., 2009. Integrated collector storage water heater: Temperature stratification. Applied Energy, 86, 1465-1469.

47. Gautam, A., Chamoli, S., Kumar, A., Singh, S., 2017. A review on technical improvements, economic feasibility and world scenario of solar water heating system. Renewable and Sustainable Energy Reviews, 68, 541-562.

48. Ghoneim, A. A., 2005. Performance optimisation of solar collector equipped with different arrangement of square-celled honeycomb. International Journal of Thermal Sciences, 44, 95-105.

49. Giglio, T., Lamberts, R., Barbosa, M., Urbano, M., 2014. A procedure for analysing energy savings in multiple small solar water heaters installed in low-income housing in Brazil. Energy Policy, 72, 43-55.

50. Gianluca Seralea, Enrico Fabriziob, Marco Perinoa, 2015. Design of a low-temperature solar heating system based on a slurry Phase Change Material (PCS). Energy and Buildings, 106, 44-58.

51. Gillet, W. B., Moon, J. E., 1985. Solar Collectors, Test methods and design guidelines. Reidel, (for the commission of European communities) Dordrecht.

52. Greening, B., Azapagic, A., 2014. Domestic solar thermal water heating: A sustainable option for the UK. Renewable Energy, 63, 23-36.

53. Grimmer, D. P., 1979. A comparison of compound parabolic and simple parabolic concentrating solar collectors. Solar Energy, 22, 21-25.

54. Halliot, D., Goetz, V., Py, X., Benabdelkarim, M., 2011. High performance storage composite for the enhancement of solar domestic hot water systems: Part 1: Storage material investigation. Solar Energy, 85, 1021-1027.

55. Helal, O., Chaouachi, B., Gabsi, S., 2011. Design and thermal performance of an ICS solar water heater based on three parabolic sections. Solar Energy, 85, 2421-2432.

56. Hollands, K. G. T., 1965. Honeycomb devices in flat plate solar collectors. Solar Energy, 9, 159-164.

57. Hollands, K. G. T., Iynkaran, K., 1985. Proposal for a compound honeycomb collector. Solar Energy, 34, 309-316.

58. Holeman, J. P., 2008. Heat Transfer, Tata Mcgrow - Hill Publication, 9th edition, New York.

59. Hou, H. J., Wang, Z. F., Wang, R. Z., Wang, P. M., 2005. A new method for the measurement of solar collector time constant. Renewable Energy, 30, 855-865.

60. Hottel, H. C., Woertz, B. B., 1942. The performance of flat-plate solar heat collectors. Trans. ASME, 64, 64-91.

61. Jordan, U., Furbo, S., 2005. Thermal stratification in small solar domestic storage tanks caused by draw-offs. Solar Energy, 78, 291-300.

62. Kablan, M. M., 2004. Techno-economic analysis of the Jordanian solar water heating system. Energy, 29, 1069-1079.

63. Kalogirou, S. A., Papamarcou, C., 2000. Modelling of thermosphon solar water heating system and simple model validation. Renewable Energy, 21, 471-493.

64. Kalogirou, S. A., 2009. Thermal performance, economic and environmental life cycle analysis of thermosiphon solar water heaters. Solar Energy, 83, 39-48.

65. Kalogirou, S. A., 2004. Solar thermal collectors and applications. Progress in energy and combustion science, 30, 231-295.

66. Kalogirou, S. A., Tripanagnostopoulos, Y., Souliotis, M., 2005. Performance of solar systems employing collectors with colored absorber. Energy and Buildings, 37, 824-835.

67. Kaptan, I. N., Kilic, A., 1996. A theoretical and experimental investigation of a novel built in storage solar water heater. Solar Energy, 57, 393-400.

68. Kaushik, S. C., Ranjan, K. R., 2016. Energetic and Exergetic Performance Evaluation of Natural Circulation Solar Water Heating System. Applied Solar Energy, 52, 16-26.

69. Kaushik, S. C., Rakesh Kumar, Garg, H. P., Prakash, J., 1994. Transient analysis of a triangular built-in-storage solar water heater under winter conditions. Heat Recovery Systems and CHP, 14, 337-341.

70. Kaushik, S. C., Kumar, R., Garg, H. P., 1995. Effect of baffle plate on the performance of a triangular built in storage solar water heater. Energy Conversion & Management, 36, 337-342.

71. Kaushika, N. D., Sumathy, K., 2003. Solar transparent insulation materials: A review. Renewable and Sustainable Energy Reviews, 7, 317-351.

72. Klein, S. A., Beckman, W. A., Duffie, J. A., 1976. A design procedure for solar heating systems. Solar Energy, 18, 113-127.

73. Klein, S. A., Engineering equation solver, version 8.158. F Chart Software; 2008.

74. Kline, S. J., Mc Clintock, F. A., 1953. Describing Uncertainties in single sample experiments. Mechanical Engineering, 75, 3-8.

75. Koroneos, C. J., Nanaki, E. A., 2012. Life cycle environmental impact assessment of a solar water heater. J. Clean. Prod., 37, 154-161.

76. Kumar, R., Rosen, M. A., 2010. Thermal performance of integrated collector storage solar water heater with corrugated absorber surface. Applied Thermal Engineering, 30, 1764–1768.

77. Kumar, R., Rosen, M. A., 2011. Integrated collector-storage solar water heater with extended storage unit. Applied Thermal Engineering, 31, 348-354.

78. Lamnatou, C., Notton, G., Chemisana, D., Cristofari, C., 2014. Life cycle analysis of a building-integrated solar thermal collector, based on embodied energy and embodied carbon methodologies. Energy Building, 84, 378-387.

79. Lamnatou, C., Mondol, J. D., Chemisana, D., Maurer, C., 2015. Modelling and simulation of Building-Integrated solar thermal systems: Behaviour of the coupled building/system configuration. International Journal of Ambient Energy, 48, 178-191.

80. Lien, A. G., Hestnes, A. G., Aschehoug, O., 1997. The use of transparent insulation in low energy dwellings in cold climates. Solar Energy, 59, 27-35.

81. Lin, W. M., Chang, K. C., Chung, K. M., 2015. Payback period of residential solar water heaters in Taiwan. Renewable and Sustainable Energy Reviews, 41, 901-906.

82. Madhlopa, A., Mgawi, R., Taulo, J., 2006. Experimental study of temperature stratification in an integrated collector–storage solar water heater with two horizontal tanks. Solar Energy, 80, 989-1002.

83. Mahmut Sami, B., Saffa, B. R., 2015. Building integrated solar thermal collectors-A review. Renewable and Sustainable Energy Reviews, 51, 327-346.

84. Mazman, M., Cabeza, L. F., Mehling, H., Nogues, M., Evliya, H., Paksoy, H. O., 2009. Utilization of phase change materials in solar domestic hot water systems. Renewable Energy, 34, 1639-1643.

85. Misra, R. S., 1993. Evaluation of thermal stratification in thermosyphonic solar water heating systems. Energy Conversion and Management, 34, 347-361.

86. Misra, R. S., 1994. Thermal stratification with thermosyphon effects in solar water heating systems. Energy Conversion and Management, 35, 193-203.

87. Mohamad, A., 2013. A Storage domestic solar hot water system with a back layer of phase change material. Experimental Thermal and Fluid Science, 44, 174-181.

88. Mohsen, M. S., Akash, B. A., 2002. On integrated solar water heating system. Int. Commun. Heat Mass Transfer, 29, 135-140.

89. Mohsen, M. S., Al-Ghandoor, A., Al-Hinti, I., 2009. Thermal analysis of compact solar water heater under local climatic conditions. Int. Commun. Heat Mass Transfer, 36, 962-968.

90. Morse, R. N., 1961. Water heating by solar energy. UN Conf. New Sources of Energy, Rome, 38, 62-73.

91. Munroe, M. M., 1981. A method of determining the time constant of the flat-plate solar collector. Energy Conversion and Management, 21, 185-189.

92. Nahar, N., 2003. Year round performance and potential of a natural circulation type of solar water heater in India. Energy and Buildings, 35, 239-247.

93. Nayak, J. K., Dhiman, N. K., Tiwari, G. N.; 1982. Thermal optimisation of a built-in storage solar water heater. Applied Energy, 10, 169-176.

94. Nordgaard, A., Beckman, W. A., 1992. Modelling of flat plate collectors based on monolithic silica aerogel. Solar Energy, 49, 387-402.

95. Notton, G., Motte, F., Cristofari, C., Canaletti, J. L., 2014. Performances and numerical optimization of a novel thermal solar collector for residential building. Renewable and Sustainable Energy Reviews, 33, 60-73.

96. Ortabasi, U., Dyksterhuis, F. H., Kaushika, N. D., 1983. Honeycomb stabilized salt less solar pond. Solar Energy, 31, 229-236.

97. Pierson, P., Padet, J., 1990. Time constant of solar collectors. Solar Energy, 44, 109–114.

98. Pinel, P., Cruickshank, C. A., Beausoleil-MorrisonI, Wills, A., 2011. A review of available methods for seasonal storage of solar thermal energy in residential applications. Renewable and Sustainable Energy Reviews, 15, 3341-359.

99. Parkash, J., Garg, H. P., Datta, G., 1985. Performance prediction for a built-in, storage-type solar water heater. Energy, 10, 1209-1213.

100. Purohit, P., Michaelowa, A., 2010. CDM potential of solar water heating systems in India. Solar Energy, 82, 799-811.

101. Rabl, A., 1976. Optical and thermal properties of compound parabolic concentrators. Solar Energy, 18, 497-511.

101. Rabin, Y., Korin, E., Mikic, B., 1995. Integrated solar collector storage system based on a salt hydrate phase change material. Solar Energy, 60, 119-126.

102. Reddy, B. S., 1995. Electrical vs solar water heater: a case study. Energy Conversion & Management, 36, 1097-1106.

103. Reddy, K. S., Kaushika, N. D., 1999. Comparative study of transparent insulation materials cover systems for integrated-collector-storage solar water heaters. Solar Energy Materials and Solar Cells, 58, 431-446.

104. Richards, S. J., Chinnery, D. N. W., 1967. A solar water heater for low cost housing NBRI Bull, 41, CSIR Research Report 237, South Africa.

105. Sadhishkumar, S., Balusamy, T., 2014. Performance improvement in solar water heating systems - A review. Renewable and Sustainable Energy Reviews, 37, 191-198.

106. Samuel, T. D. M. A., Wijeysundera, N. E., 1981. Optimal performance of thermal trap collectors. Solar Energy, 26, 65-76.

107. Saif-Ul-Rehman, M., 1967. Prospects and limitations of solar energy utilization in developing countries. Solar Energy, 11, 98-108.

108. Schmidt, C. A., Goetzberger, A., 1990. Single-tube integrated collector storage systems with transparent insulation and involute reflector. Solar Energy, 45, 93-100.

109. Senthilkumar, S., Yasodha, N., 2012. Design and Development of a Three Dimensional Compound Parabolic Concentrator and Study of Optical and Thermal performance. International Journal of Energy Science, 2, 64-68.

110. Shariah, M., Lof, G., 1996. The optimisation of the tank volume-to-collector area ratio for a thermosyphon solar water heater. Renewable Energy, 7, 289-300.

111. Shariah, M., Lof, G., 1997. Effects of Auxillary Heater on annual performance of thermosyphon SWH simulated under variable operating conditions. Solar Energy, 60, 19-126.

112. Shi, J., Su, W., Zhu, M., Chen, H., Pan, Y., Wan, S., Wang, Y., 2013. Solar water heating system integrated design in high-rise apartment in China. Energy Building, 58, 19-26.

113. Shimoda, Y., Okamura, T., Yamaguchi, Y., Yamaguchi, Y., Taniguchi, A., Morikawa, T., 2010. City-level energy and CO2 reduction effect by introducing new residential water heaters. Energy, 35, 4880-489.

114. Sharma, A., Tyagi, V.V., Chen, C. R., Buddhi, D., 2009. Review on thermal energy storage with phase change materials and applications. Renewable and Sustainable Energy Reviews, 13, 318-345.

115. Shukla, S. K., Ajeet Kumar, 2008. Analytical thermal modelling of double slope solar still by using inner glasss cover temperature. Thermal Science, 12, 139-152.

116. Shukla, A., Buddhi, D., Sawhney, R. L., 2009. Solar water heaters with phase change material thermal energy storage medium: A review. Renewable and Sustainable Energy Reviews, 13, 2119-2125.

117. Shi, L., Chew, M. Y. L., 2012. A review on sustainable design of renewable energy systems. Renewable and Sustainable Energy Reviews, 16, 192-207.

118. Singh, R., Lazarus, I. J., Souliotis, M., 2016. Recent developments in integrated collector storage (ICS) solar water heaters: A review. Renewable and Sustainable Energy Reviews, 54, 270-298.

119. Smyth, M., Eames, P.C., Norton, B., 2001. Annual performance of heat retaining integrated collector/storage solar water heaters in a northern maritime climate. Solar Energy, 70, 391-401.

120. Smyth, M., Zacharopoulos, Eames, P. C., Norton, B., 1999. An experimental procedure to determine solar energy flux distributions on the absorber of line-axis compound parabolic concentrators. Renewable Energy, 16, 761-764.

121. Smyth, M., Eames, P.C., Norton, B., 2003. Heat retaining integrated collector/storage solar water heaters. Solar Energy, 75, 27-34.

122. Smyth, M., Eames, P. C., Norton, B., 2004.Techno-economic appraisal of an integrated collector/storage solar water heater. Renewable Energy, 29, 1503-1514.

123. Smyth, M., Eames, P. C., Norton, B., 2006. Integrated collector storage solar water heaters. Renewable and Sustainable Energy Reviews, 10, 503-538.

124. Sodha, M. S., Nayak, J. K., Kaushik, S. C., Sabberwal, S. P., Malik, M. A. S., 1979. Performance of a collector/storage solar water heater. Energy Conversion, 19, 41-47.

125. Sodha, M. S., Tiwari, G. N., Shukla, S. N., 1983. Transient analysis of a natural circulation solar water heater with a heat exchanger. Journal of Energy, 7, 107-111.

126. Sokolov, M. V., Vaxman, M., 1983. Analysis of an integral compact solar water heater. Solar Energy, 30, 237-246.

127. Souka, A. F., Safwat, H. H., 1966. Optimum orientations for the double exposure flat plate collector and its reflectors, Solar Energy, 10, 170-174.

128. Soteris Kalogiroua, A., Christos Papamarcou, 2000. Modelling of a thermosyphon system and simple model validation. Renewable Energy, 21, 471-493.

129. Soteris Kalogirou, 2009. Thermal performance, economic and environmental life cycle analysis of thermosiphon solar water heaters, Solar Energy, 83, 39-48.

130. Souliotis, M., Quinlan, P., Smyth, M., Tripanagnostopoulos, Y., Zacharopoulos, A., Ramirez, M., Yianoulis, P., 2011. Heat retaining integrated collector storage solar water heater with asymmetric CPC reflector. Solar Energy, 85, 2474–2487.

131. Souliotis Chemisana, D., Caouris, Y. G., Tripanagnostopoulos, Y., 2013. Experimental study of integrated collector storage solar water heaters. Renewable Energy, 50, 1083-1094.

132. Souliotis, M., Kalogirou, S., Tripanagnostopoulos, Y., 2009. Modelling of an ICS solar water heater using artificial neural networks and TRNSYS. Renewable Energy, 34, 1333–1339.

133. Souliotis, M., Singh, R., Papaefthimiou, S., Lazarus, I. J., Andriosopoulos, K., 2016. Integrated collector storage solar water heaters: survey and recent developments. Energy Systems, 7, 49-72.

134. Souza, J. V. D., Fraisse, G., Pailha, M., Xin, S., 2014. Experimental study of a partially heated cavity of an integrated collector storage solar water heater (ICSSWH). Solar Energy, 101, 53-62.

135. Sridhar, A., Reddy, K. S., 2007. Transient analysis of modified cuboid solar integrated-collector-storage system. Applied Thermal Engineering, 27, 330-346.

136. Suman, S., Khan, M. K., Pathak, M., 2015. Performance enhancement of solar collectors-A review. Renewable and Sustainable Energy Reviews, 49, 192-210.

137. Suri, R. K., Al-Marafie, A. M. R., Al-Homoud, A. A. A., Maheshwari, G. P., 1998. Cost-effectiveness of solar thermal and electrical energy production. International Journal of Ambient Energy, 9, 177-184.

138. Symons, J. G., 1984. Calculation of the transmittance-absorptance product for flat-plate collectors with convection suppression devices. Solar Energy, 33, 637-644.

139. Tabor, H., 1969. Honeycomb (cellular) insulation. Solar Energy, 25, 269-274.

140. Tanishita, I., 1970. Present situation of commercial solar water heaters in Japan. International Solar Energy Society Conference, Melbourne, Australia.

141. Tayeb, A. M., 1993. A simulation model for a phase change energy storage system: experimental and verification. Energy Conversion Management, 34, 243-250.

142. Tian, Y., Zhao, C.Y., 2013. A review of solar collectors and thermal energy storage in solar thermal applications. Applied Energy, 104, 538-553.

143. Tiwari, G. N., Shukla, S. K., Singh, I. P., 2002. Computer modelling of Passive/Active solar stills using inner glass temperature. Desalination, 154, 171-185.

144. Thirugnanasambandam, M., Iniyan, S., Goic, R., 2010. A review of solar thermal technologies. Renewable and Sustainable Energy Reviews, 14, 312-322.

145. Tripanagnostopouios, Y., Yianoulis, P., 1992. Integrated collector storage systems with suppressed thermal losses. Solar Energy, 48, 31-43.

146. Tripanagnostopoulos, Y., Yianoulis, P., Papaefthimiou, S., Zaferatos, S., 2000. CPC solar collectors with bifacial absorbers. Solar Energy, 69, 191-203.

147. Tripanagnostopoulos, Y., Souliotis, M., Nousia, T. H, 2002. CPC type integrated collector storage systems. Solar Energy, 22, 327-350.

148. Tripanagnostopoulos, Souliotis, M., 2006. ICS Solar systems with two water tanks. Renewable Energy, 31, 1698-1717.

149. Tripanagnostopoulos, Y., 2014. New designs of building integrated solar energy systems. Energy Procedia, 57, 2186-2194.

150. Tzivanidis, C., Bellos, E., 2016. The use of parabolic trough collectors for solar cooling – A case study for Athens climate. Case Stud. Thermal Energy, 8, 403-413.

151. Ulrike, Furbo, Simon, 2005. Thermal stratification in small solar domestic storage tanks caused by draw-offs. Solar Energy, 78, 2005, 291-300.

152. Varghese, J., Awari, G. K., Singh, M. P., 2007. Experimental analysis of distinct design of a batch solar water heater with integrated collector storage system. Thermal Science, 11, 135-142.

153. Varghese, J., Samsher, Manjunath, K., 2017. A parametric study of a concentrating integral storage solar water heater for domestic uses. Applied Thermal Engineering, 111, 734-744.

154. Varghese, J., Samsher, Manjunath, K., 2017.Techno-economic analysis of an integrated collector storage solar water heater with CPC reflector for households. International Journal of Ambient Energy, https://doi.org/10.1080/01430750.2017.1354327

155. Veeraboina, P., Ratnam, G.Y., 2012. Analysis of the opportunities and challenges of solar water heating system (SWHS) in India: Estimates from the energy audit surveys & review. Renewable and Sustainable Energy Reviews, 16, 668-676.

156. Wang, Z., Yang, W., Qiu, F., Zhang, X., Zhao, X., 2015. Solar water heating: From theory, application, marketing and research. Renewable and Sustainable Energy Reviews, 41, 68-84.

157. Walker, F., 1903. Combined solar and artificial heat water heater. US Patent 735321.

158. Winston, R., 1974. Principles of solar concentrators of a novel design. Solar Energy, 16, 89-95.

159. Wijeysundera, N. E., 1980. Response time of solar collectors. Solar Energy, 18, 65-68.

160. Wong, I.L., Eames, P.C., Perera, R.S., 2007. A review of transparent insulation systems and the evaluation of payback period for building applications. Solar Energy, 81, 1058-1071.

161. Wijeysundera, N. E., 1980. Response time of solar collectors. Solar Energy, 18, 65-68.

162. Xue, H. S., 2016. Experimental investigation of a domestic solar water heater with solar collector coupled phase-change energy storage. Renewable Energy, 86, 257-261.

163. Yadav, P., Tripathi, B., Rathod, S., Kumar, M., 2013. Real-time analysis of low-concentration photovoltaic systems: a review towards development of sustainable energy technology. Renewable and Sustainable Energy Reviews, 28, 812-823.

164. Yan, C., Wang, S., Ma, Z., Shi, W., 2015. A simplified method for optimal design of solar water heating systems based on life-cycle energy analysis. Renewable Energy, 74, 271-278.

165. Yuehong, S., Riffat, S. B., Pei, G., 2012. Comparative study on annual solar energy collection of a novel lens-walled compound parabolic concentrator (lens-walled CPC). Sustainable Cities and Society, 4, 35-40.

166. Zalba, B., Marín, J. M., Cabeza, L. F., Mehling, H., 2003. Review on thermal energy storage with phase change: materials, heat transfer analysis and applications. Applied Thermal Engineering, 23, 251-283.

167. Zambolin, E., Del Col, D., 2010. Experimental analysis of thermal performance of flat plate and evacuated tube solar collectors in stationary standard and daily conditions. Solar Energy, 84, 1382-1396.

168. Zhang, X., Shen, J., Lu, Y., He, W., Xu, P., Zhao, X., Qiu, Z., Zhu, Z., Zhou, J., Dong, X., 2015. Active Solar Thermal Facades (ASTFs): From concept, application to research questions. Renewable and Sustainable Energy Reviews, 50, 32-63.

169. Ziapour, B. M., Aghamiri, A., 2014. Simulation of an enhanced integrated collector-storage solar water heater. Energy Conversion Management, 78, 193-203.

Appendix A

Solar radiation geometry

Latitude angle Ø

Latitude angle Ø of a location is the angle made by the radial line joining the location to the centre of the earth with the projection of the line on the equatorial plane. By convention, the latitude angle Ø is measured as positive for northern hemisphere.

Declination angle δ

Declination angle δ is the angle made by the line joining the centers of the sun and the earth with its projection on the equatorial plane. Cooper has given the following expression for calculating solar declination

$$\delta \text{ (in degrees)} = 23.45 \sin\left[\frac{360}{365}(284 + n)\right] \qquad \text{A.1}$$

Where n is the day of the year.

Solar altitude angle α_a

It is a vertical angle between projection of sun's rays on the horizontal plane and direction of the sun's rays passing through the point.

Zenith angle θ_z

It is complimentary angle of sun's altitude angle. It is a vertical angle between sun's rays and a line perpendicular to the horizontal plane passing through the point. In other words, it is the angle between beam from the sun and the vertical.

Solar surface azimuth angle γ_s

Solar surface azimuth angle γ_s is the angle made in the horizontal plane between the line due south and the projection of the normal to the surface on the horizontal plane. By convention, the angle is taken to be positive if the normal is east of south and negative if west of south.

Hour angle ω

The hour angle ω is an angular measure of time and is equivalent to 15° per hour. It is measured from the noon based on local apparent time (LAT), being positive in the morning and negative in the evening.

Slope β

Slope β is the angle made by the plane surface to the horizontal. It is taken positive for surfaces sloping towards south and negative for surfaces sloping towards north.

Local apparent time (LAT)

The time used for calculating hour angle is the local apparent time. This can be obtained from the standard time observed on a clock by making two corrections. The first correction arises because of the difference between the longitude of the location and the meridian on which the standard time is based. The correction has a magnitude of 4 minutes for every degree difference in longitude. The second correction is called the equation of time correction is due to the fact that the earth's orbit and rate of rotation are subject to small perturbations. Thus local apparent time

LAT = Standard Time ± 4 (Standard time longitude – longitude of location) + equation of time correction. The negative sign in the first correction is applicable for the eastern hemisphere while the positive sign is applicable for the western hemisphere.

Appendix B

Method to determine solar swing angle $\propto_v$ and flux absorbed

$$tan \propto_v = \frac{sin\emptyset sin\delta + cos\emptyset cos\delta}{sin\emptyset cos\delta cos\omega - cos\emptyset sin\delta} \quad \text{B.1}$$

Declination angle $\delta = 23.45\ sin\left[\frac{360}{365}(284+n)\right]$ B.2

ω Angular measurement of time equivalent to15^o per hour measured from noon,

based on local apparent time (LAT)

Day length in hrs. $S_{max} = \frac{2}{15} cos^{-1}[-tan(\emptyset - \beta)tan\delta]$ B.3

For obtaining the parametric Table 1. Values taken are n= 355, ω= 1100 hrs.

and $\propto_v$ obtained is 37.24^o

Half acceptance angle $\theta_a = sin^{-1}\left(\frac{1}{c}\right)$ where C is concentration ratio, C= 2.03 B.4

Average number of reflections

$$m = \frac{1}{2sin\theta_a}(1+C) - \frac{(1-sin\theta_a)(1+2sin\theta_a)}{2sin^2\theta_a} \quad \text{B.5}$$

$\rho_e = \rho^m$ where ρ is the reflectivity value for a single radiation.

Since the slope of the aperture is 28^o, the angle made by the axis of CPC with horizontal is 62^o,

thus the beam radiation having solar elevation angle between the limits $(62^o \pm \theta_a)$

i.e. between 91^o and 33^o would be accepted by collector. In this case the beam radiation is falling

between these limits.

Appendix C

Method to determine overall heat transfer coefficient

Nomenclature:

Material: Suffix: p for plywood, a for air in gap and w for glass wool insulation.

Properties: A_{ap} effective area of absorber surface in m^2, K Thermal conductivity of the material in W/m-K , h_w convective heat transfer coefficient of outside air in W/m^2-K, h_i inside heat transfer coefficient of air in air gap in W/m^2-K, V_∞ velocity of air in m/s, T_{pm} temperature of absorber surface(drum)in K, T_a temperature of ambient air in K , R_{th} thermal resistance in m^2-W/K, U_l overall heat transfer coefficient in W/m^2-K, β in degrees, σ in W/m^2-K^4, q_l heat loss in Watts and L the thickness in metre.

Geometry Suffix: t for top face, f for front face, r for rear face, s for sides and b for the bottom of the SWH

Now

$$q_l = q_t + q_f + q_r + q_s + q_b \qquad \text{C.1}$$

Top face

$$q_t = U_t * A_t\left(T_{pm} - T_a\right) \qquad \text{C.2}$$

Using Klein empirical equation for calculating the top loss coefficient,

$$U_t = \left[\frac{M}{\left(\frac{C}{T_{pm}}\right)\left(\frac{T_{pm}-T_a}{M+f}\right)^{0.33}} + \frac{1}{h_w}\right]^{-1} + \left[\frac{\sigma\left(T_{pm}{}^2 + T_a{}^2\right)\left(T_{pm}+T_a\right)}{\frac{1}{\varepsilon_p+0.05M\left(1-\varepsilon_p\right)} + \frac{(2M+f-1)}{\varepsilon_c} - M}\right] \qquad \text{C.3}$$

where $f = \left(1 - 0.04h_w + 0.0005{h_w}^2\right)(1 + 0.091M)$ C.4

$$C = 365.9(1 - 0.00883\beta + 0.0001298\beta^2)$$ C.5

M = number of glass covers

Front face

$$q_f = R_{thf} * \left(T_{pm} - T_a\right)$$ C.6

$$R_{thf} = \frac{A_{f1}}{\left[\left(\frac{L_p}{K_p} + \frac{L_w}{K_w}\right)\right]} + \frac{A_{f2}}{\left[\left(\frac{L_p}{K_p} + \frac{L_w}{K_w}\right)\right]}$$ C.7

A_{f1}-Area excluding the parabolic section

A_{f2}- Area of the parabolic section"

Rear face

$$q_r = R_{thr} * \left(T_{pm} - T_a\right)$$ C.8

$$R_{thr} = \frac{A_r}{\left(\frac{L_p}{K_p} + \frac{L_w}{K_w}\right)}$$ C.9

Side face (Two sides)

$$q_s = R_{ths}\left(T_{pm} - T_a\right)$$ C.10

$$R_{ths} = \frac{A_s}{\left(\frac{1}{h_i} + \frac{L_p}{K_p} + \frac{L_w}{K_w}\right)}$$ C.11

$$h_i = 1.42 * \left(\frac{\delta T}{L_a}\right)$$ (Holeman [2008]) C.12

Bottom face

$$q_b = R_{thb}\left(T_{pm} - T_a\right)$$ C.13

$$R_{thb} = \frac{A_b}{\left(\frac{L_p}{K_p} + \frac{L_w}{K_w}\right)} \quad \text{C.14}$$

Total heat loss

$$q_l = q_t + q_f + q_r + q_s + q_b \quad \text{C.15}$$

$$U_l = \frac{q_l}{[A_{ap}(T_{pm} - T_a)]} \quad \text{C.16}$$

Appendix D

Technical Specifications of Instrumentation

a) Solar Power meter

Model	TM-207
Display	3½ digits, 2000 readings
Range	2000 W/m2, 634BTU / (ft2xh)
Accuracy	Typically within +/- 10W/m2 [+/-3 BTU/ (ft2xh)] or +/- 5% whichever is greater in sunlight; Additional temperature included error +/- 0.38 W/m2 / º C [+/-0.12 BTU/ (ft2xh)] / º C] from 25 º C
Angular accuracy	Cosine corrected <5% for angles <60º
Over-input	Display "OL"
Sampling time	0.25 second
Operating Temp.	0º C ~ 50 º C below 80% RH

b) Surface Thermocouple for temperature measurement

Model: J Type
Positive leg: Iron
Negative leg: Copper-Nickel
Application range: 200-1400^{0}F (0^0C - 760^0C)
Digital Temperature Display: Make – Themotech
: Model No. TIC 4000 NF
Selector Switch : Make Salzer TIC 4000

c) Glass Tube Thermometer

Thermic fluid: Ethyl alcohol
Temperature range: -10^0c - 110^0c
Least count: 0.1

PUBLICATIONS AND PRESENTATIONS

The present work has partially appeared in the form of following publications:

1) Varghese, J., Samsher, Manjunath, K., 2017. A parametric study of a concentrating integral storage solar water heater for domestic uses, Applied Thermal Engineering 111, 734-744.
2) Varghese, J., Samsher, Manjunath, K., 2017. Techno - economic analysis of an integrated collector storage (ICS) solar water heater with CPC reflector for households, International Journal of Ambient Energy, http://dx.doi.org/10.1080/01430750.2017.1354327.
3) Varghese, J., Samsher, Manjunath, K., 2017. Experimental investigation and comparison between an integrated compound parabolic domestic solar water heater with and without an air gap introduced at the arms of the CPC, International Journal of Advance Research and Innovation, 5, 90 – 93.
4) Varghese, J., Samsher, Manjunath, K., 2015. Current trends in domestic solar water heating - CPC an amicable alternative, a proposed distinct design, International Journal of Science, Technology & Management, 4, 956 - 959.
5) Varghese, J., Samsher, Manjunath, K., 2017. Collector characterization and heat loss tests on a novel Batch Solar Water Heater with CPC reflector for households, communicated to International Journal of Ambient Energy.

Paper Presentations

1) Varghese, J., Samsher, Manjunath, K., 2015. Current trends in domestic solar water heating - CPC an amicable alternative, a proposed distinct design, presented and published in the proceedings of the International conference on "Recent Trends in Engineering Science and

Technology", organized by Jawaharlal Nehru University (JNU, Convention center), New Delhi on 15th March, 2015.

2) Varghese, J., Samsher, Manjunath, K., 2017. Techno- economic analysis of an integrated collector storage (ICS) solar water heater with CPC reflector for households, presented and published in the proceedings of the International Conference of "Advance research and Innovation (ICARI – 2017)", organized by Delhi State Center, Institution of Engineers (India) Bldg., New Delhi, on 29th January, 2017.
3) Varghese, J., Samsher, Manjunath, K., 2017. To study the effect of air gap on the outlet water temperature of a batch solar water heater with CPC reflector using Multi linear regression tool in (SPSS), paper accepted for publication in the proceedings of the International conference on "Mathematics, Modelling and Simulation Technologies and Applications", to be held at Xiamen, China, Dec 24 -25, 2017.

Citations of recent published work: 05

1) Elesheikh, A. H., Sharshir, S.W., Mohamed, E., Essa, F.A., Applications of nanofluids in solar energy: A review of recent advances, 2017. Renewable and Sustainable Energy Reviews, https://doi.org/10.1016/j.rser.2017.10.108.
2) Celine Garnier, Tariq Muneer, John Currie, Renewable Energy, 2018. Numerical and empirical evaluation of a novel building integrated collector storage solar water heater, 126, 281-295.
3) Prakash, D., Thermal analysis of building roof assisted with water heater and insulation material, 2018, Sadhana (Springer), https://doi.org/10.1007/s12046-017-0781-y

4) Varghese, J., Samsher, Manjunath, K., 2017. Techno- economic analysis of an integrated collector storage (ICS) solar water heater with CPC reflector for households, International Journal of Ambient Energy, http://dx.doi.org/10.1080/01430750.2017.1354327.

5) Sanchez, C., Macais, J., Leon, J., 2017. Design, implementation and evaluation of thermal performance of a Thermosyphon flat plate solar collector for water heating in Ecuadorian costal region, ASME 2017 International Mechanical Engineering Congress and Exposition, Volume 6: Energy, Tampa, Florida, USA, November 3–9, 2017, doi: 10.1115/IMECE 2017- 71944.

Brief Bio-Data of the Author

Mr. Jaji Varghese, was born in Nagpur, Maharashtra, India, and native of Venmony, in Kerala. He did his B.E in Mechanical Engineering from Nagpur University and M.Tech from School of Energy and Environmental Studies (S.E.E.S), DAAV, Indore. His field of interest is solar energy and was privileged to learn and work under Prof. R.L Sawhney, renowned expert in the field of solar energy. He has 22 years of teaching experience and during the course has guided projects with an eye on saving energy. He fabricated a water energy saver air cooler which was well appreciated, having received a letter of consent from Ministry of Power, Govt. of India. He was also instrumental in the installation of a wind mill for pumping water at S.S.G.M college of Engineering, Shegaon, Maharashtra. He has presented papers in National and International conferences and has publications in International Journals of repute. His work has been cited in journals like Thermal Science, International journal of Energy and, Renewable & Sustainable Energy Reviews-Journal. Presently he is working as Lecturer at Aryabhat Institute of Technology, Govt. of NCT of Delhi since August 2000.